Development and Optimization of Methodology Towards Pyrrolic Frameworks

by

Mmasinachi Ijeoma Atansi

Submitted in partial fulfilment of the requirements
for the degree of Master of Science

at

Dalhousie University
Halifax, Nova Scotia
December 2021

To my family and every woman in STEM.

Table of Contents

List of Tables

List of Figures

List of Schemes

Abstract

This thesis focuses on the development and optimization of synthetic methodology towards pyrrolic frameworks. Two projects are discussed herein: the synthesis of azobispyrroles and attempts towards the synthesis of *F*-BODIPYs using a stoichiometric amount of dipyrrin and $BF_3{\cdot}OEt_2$ in a continuous flow operation.

Chapter 2 explores the synthesis and optimization of the unreported group of azo dyes azobispyrroles using both the traditional approach via diazonium chemistry and through the reaction of a nitrobutanone with ammonium acetate in an acidic medium.

Chapter 3 explores attempts towards the synthesis of *F*-BODIPYs using a stoichiometric amount of dipyrrin and $BF_3{\cdot}OEt_2$ in a continuous flow operation. The flow system aimed to avert the effects of the by-product fluoride which reacts with unreacted $BF_3{\cdot}OEt_2$ leading to the formation of the BF_4^- anion, and consequently HBF_4 dipyrrin salt, rather than enabling both free dipyrrin and $BF_3{\cdot}OEt_2$ to remain in solution for subsequent reaction. The use of inorganic bases as potential HF scavengers was also evaluated.

List of Abbreviations Used

abs	absorbance
app	apparent
Ar	aryl
bs	broad singlet
br	broad
calc	calculated
CI	Conical intersection
d	doublet
dd	doublet of doublet
DMSO	dimethyl sulfoxide
DBU	1,8-diazabicyclo[5.4.0]undec-7-ene
eq.	equivalent
F-BODIPY	4,4-difluoro-4-bora-3a,4a-diaza-s-indacene
GP	general procedure
h	hour
IUPAC	International Union of Pure and Applied Chemistry
J	coupling constant
min	minute
mmol	millimole
m	multiplet
Mes	mesityl
m/z	mass/charge
NMR	nuclear magnetic resonance
PET	photo-induced electron transfer
Ph	phenyl
ppm	parts per million
q	quartet

quin	quintet
RBF	round-bottom flask
R_f	retention factor
r.t.	room temperature
s	singlet
t	triplet
TOF	time-of-flight
THF	tetrahydrofuran
Uv-Vis	ultraviolet and visible
α	alpha
β	beta
δ	chemical shift
°C	degrees Celsius
λabs	absorption wavelength
ε	extinction coefficient
M.W.	microwave
μM	micromole
Δ	heat

Acknowledgment

First and foremost, I would like to express my sincerest gratitude to my supervisor, Dr. Alison Thompson, for her love, guidance, support, and patience throughout my degree. You believed in my abilities even when I never did, and you helped me to grow both personally and professionally and even when I gave up on myself, you never did. I would also like to acknowledge my committee members: Dr. Alex Speed, Dr. Norman Schepp, and Dr. Saurabh Chitins. Thank you for providing feedback and advice throughout my degree.

I would like to thank Dr. Mike Lumsden for help with NMR experiments and training pertaining to NMR, and Xiao Feng for acquiring and processing mass spectra for all my compounds, as well as all the support staff from the Department of Chemistry.

I am forever grateful for the financial support provided by Dr. Thompson, the Dalhousie University Faculty of Graduate Studies, the Dalhousie University Department of Chemistry, and the National Science and Engineering Research Council of Canada without which I would not be here today.

I would also like to acknowledge both past and present members of the Thompson group: Dr. Sarah Greening, Dr. Adil Alkas, Dr. Jim Hilborn, Dr. Michael Beh, Dr. Craig Smith, Liandrah Gapare, Nazanin Omidvar, Roberto Diaz-Rodriguez, Steve Sequeira, Breanna Taylor, Jacob Campbell, Luke Freguson, Mike Cotnam, Victoria Williams, and Bry Crabbe, each one of you have helped me throughout this journey.

I would like to thank my husband Barr Ikenna Aniedo, for being there for me throughout my entire degree and helping me through the toughest parts. Thank you for being so patient with me and for every sacrifice you've had to make for me to be here, and the happiness you've brought along the way.

I would like to acknowledge my sister from another mother Pastor Patricia Oko-Basil, your prayers and sacrifices can never be overlooked and to all my friends, of whom there are too many to name, but who are all so important.

Last but not the least, I would like to thank my family the Atansi's - words can not express what you all mean to me. Thank you for your unconditional love and support, indeed there is nothing compared to family.

Chapter 1 Introduction

The pyrrole heterocycle is a prominent chemical motif and is found widely in natural products, drugs, catalysts, and advanced materials. This thesis deals specifically with compounds which have the pyrrole moiety incorporated within. This thesis discusses the synthesis of dipyrrin, its coordinating complexes (*F*-BODIPYs) and the synthesis of azo dyes containing pyrrole units.

1.1. Pyrrole

Runge in 1834 discovered pyrrole when working with Dippel on the destructive distillation of bone.[1] Pyrrole is a planar, five-membered aromatic heterocycle containing a nitrogen atom (Figure 1.1) The 1-position is referred to as the "N-position," the 2- and 5- positions are called the α-positions, and the 3- and 4- positions are called the β-positions.

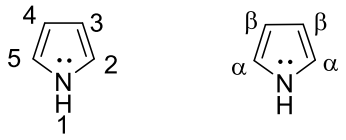

Figure 1.1. Structure and numbering of pyrrole

The aromaticity of pyrrole is due to the conjugation of 6 π (pi) electrons within a planar cyclic structure. The lone pair of electrons of the nitrogen atom in pyrrole is a component of the aromatic system, unlike in pyridine, thus fulfilling the Hückel aromatic system (4n + 2). Pyrrole is an electron-rich heterocycle as it is considered to bear six π electrons spread over five atoms. Pyrrole exhibits high reactivity towards electrophilic reactions at the α- and β-positions. However, reactions at the α-positions are typically favorable compared to those at the β-position, and this is because of resonance stability of intermediates (Figure 1.2).

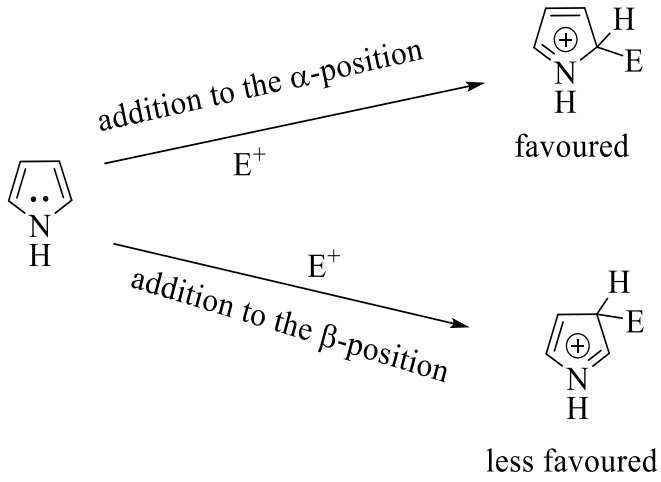

Figure 1.2. Electrophilic addition on pyrrole at α- and β-positions

As can be seen in Figure 1.2, electrophilic addition to the α-position provides a fully conjugated intermediate which is thus better stabilized than the cross-conjugated intermediate resulting from the electrophilic addition to the β-position. In both cases, the intermediate features a full octet of electrons at each atom, according to the Lewis bonding model, and thus electrophilic addition to pyrrole is more favorable (highly reactive) than electrophilic addition to benzene.

The chemistry of pyrrole and pyrrole-containing species is the focus in the Thompson group. Knorr,[2,3,4,5] Paal-Knorr,[6,7] and Van Leusen[8,9] have provided well-known robust synthetic schemes to pyrroles (Scheme 1.1). These synthetic approaches, particularly that of Knorr, utilizes readily available starting materials. However, these approaches are somewhat limited in terms of the extent that substitution can be incorporated onto the pyrrole. The Knorr pyrrole synthesis is discussed in Chapter 3 of this thesis.

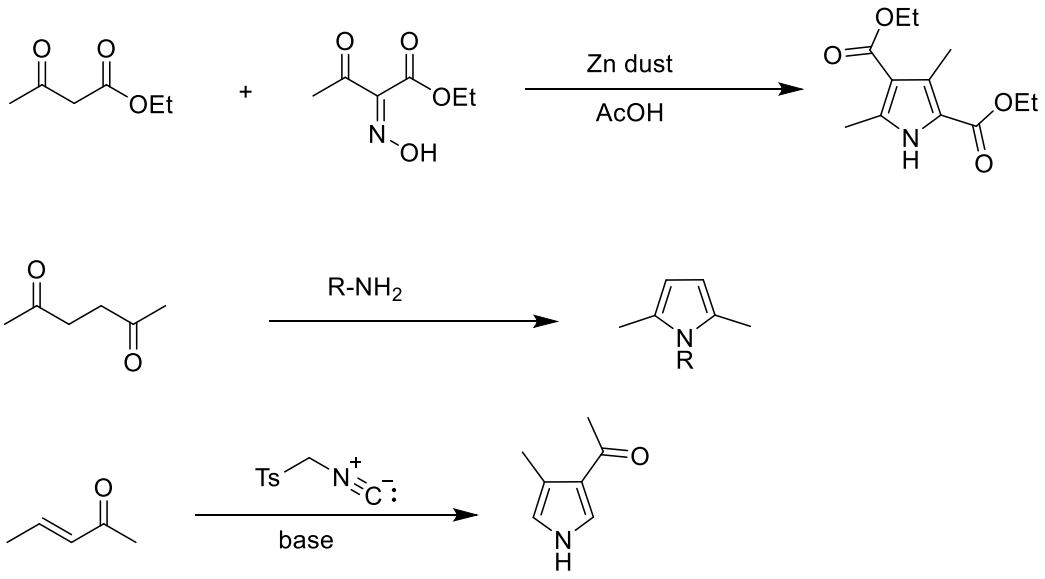

Scheme 1.1. Some common pyrrole syntheses (top: Knorr synthesis, middle: Paal-Knorr synthesis, bottom: Van-Leusen synthesis)

1.2. Azo Dyes

Peter Griess first discovered diazonium salts in 1858 and the chemistry of the diazonium moiety has since led to the synthesis of many azo dyes with a vast range applications. Azobenzene (ArNNAr) is the most studied of the azo dyes.[10,11] Modification of structure allows for the synthesis of a wide range of pigments (dyes), for example from Yellow 12 to Trypan blue (used in the textile industries).[12] Azo dyes have found application in the textile, food and plastic industries because of an ability to absorb light at different wavelengths. In the 1930s, the azo compound sulfonamidochrysoïdine, also called Prontosil, was discovered and was the first commercial azo-containing antibiotic which revolutionized the medical field.[13] Highly fluorescent dyes emitting in the far-red or near-infrared (NIR) region are preferred for biological imaging because they offer maximum light penetration through skin and tissue, with minimum scattering,[14] and have found important applications in materials and medical sciences, for example, as biological sensing and imaging agents.

Azo compounds are characterised by the presence of one or more azo bridges (-N=N-), which connect organic units. At least one of the organic units is typically aromatic. The traditional way through which azo compounds are synthesized involves coupling diazonium salts with phenols, naphthols, arylamines, pyrazolones or other suitable components to give hydroxyazo or aminoazo compounds or their tautomeric equivalents. In the resulting dyes, the azo group is the chromophore, and the hydroxyl or amino group serves as an auxochrome.[15]

Interestingly, it was only around the 1930s, after the discovery of Prontosil, that chemists learned that azo compounds could exist in *E* and *Z* isomeric forms, of which the former is typically more stable (Figure 1.3) on steric grounds. These isomers can often be interconverted using light, and it is in this way that the first photochemical switches (photo switches) were accessed.[16,17,18,19] For example, azobenzenes can be switched from a trans (*E*) to a cis isomer (*Z*), and vice versa, by external stimuli such as light and/or temperature. This switch is accompanied by a large geometrical transformation from the extended, flat trans form to the more compact cis isomer.

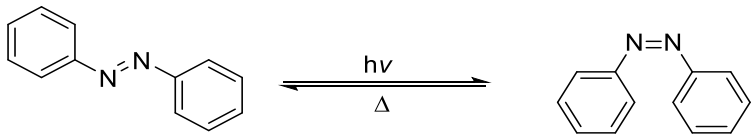

Figure 1.3. Isomerization of azobenzene

Azo dyes are often made from the simple diazotization reaction of an aromatic amine. This is then followed by coupling with an electron-rich nucleophile such as those containing amino and hydroxy groups. The literature is dominated by azo dyes featuring phenyl rings, naphthalenes, aromatic heterocycles or with enolizable aliphatic groups bound to the central azo unit.[20] These aromatic units are essential to give the color of the dye, with their shades and different intensities. In general, the chemical structure of an azo dye is represented by a backbone, the auxochrome groups, and the chromophoric groups.[21,22,23] The chromophores and auxochromes determine the color of each azo dye.[24,25]

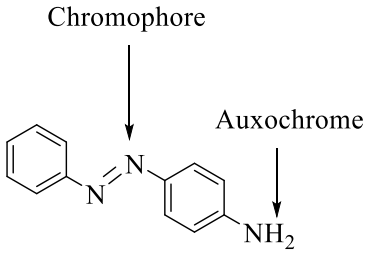

Figure 1.4. Structure of an azo dye indicating chromophore and auxochrome

Azo dyes are classified according to the number of azo linkages found in each molecule such as mono, disazo, trisazo, polyazo and azoic. In the Color Index (CI) System, azo dyes are assigned with numbers ranging from 11,000 to 39,999 according to the chemical structure (Table 1.1). The Color Index Number, developed by the Society of Dyers and Colorists, is used for dye classification.[26] The reactive functional group (auxochrome) makes the dye capable of forming covalent bonds with textile substrates. The energy needed to break this bond between dye and textile is almost the same as the energy needed to degrade the compound itself, thus meaning that the dye-textile interaction is very strong, as would be necessary for a robust and useful dye. Azo dyes are the most used dyes and account for almost 70% of the dyes used in the textile, painting and paper manufacturing industries, cosmetics, lasers, electronics, optics material science etc.[27]

Chemical class	CI Numbers
MONOZO	11000–19999
DISAZO	20000–29999
TRISAZO	30000–34999
POLYAZO	35000–36999
AZOIC	37000–39999

Table 1.1. Classification of azo dyes in the Colour Index

Azo dyes are also used as an indicator to measure the utility of photocatalytic solar disinfection.[28] This is based on the solar dose (i.e. a treatment light) needed for optimal inactivation of *Ascaris ova*, *E. coli* and *Pseudomonas aeruginosa*. These waterborne pathogens are resistant to many other anti-microbial treatments and are frequently found in surface water sources in developing countries (Africa, Latin America, and the Caribbean). Azo dyes (e.g., acid orange 24) were explored to indicate the extent to which photocatalytic solar disinfection against waterborne pathogens was achieved.

Heteroaryl-azophenol dyes have also been shown to have antibacterial activities against microorganisms (*Pseudomonas aeruginosa, Escherichia coli, Bacillus subtilis* and *Micrococcus luteus*) *in vitro*.[29] In general, these azo dyes showed antibacterial activity of a comparable level to those exhibited by tetracycline and penicillin. In another applications, these types of dyes were also applied to polyester fiber dyeing and afforded red-orange shades with excellent wash fastness properties. Azo dyes have also been used as drug carriers, either by acting as a 'carrier' that entraps therapeutic agents, or as a prodrug. The drug is released by internal or external stimuli in the region of interest, as observed in colon-targeted drug delivery.[30] In another example, 5-aminosalicylic acid (5ASA) has been incorporated into an azo-containing pro-drug and used as an anti-inflammatory agent used for the treatment of inflammatory bowel disease (IBD).[30]

1.3. Dipyrrins and their Coordination Complexes

Dipyrrins were traditionally used as intermediates for the synthesis of porphyrins. More recent work has led to the development of fluorescent markers and coordination compounds containing the dipyrrin framework. Dipyrrins are often prepared from the oxidation of dipyromathanes. The synthesis of dipyrromethanes is usually achieved via an acid-catalysed condensation of pyrrole with aldehydes in an organic solvent. Careful control over the condensation reaction is necessary to stop it when the dipyrrin concentration is at its maximum, i.e., to minimize polymerisation of pyrrole to tri, tetra, and oligo pyrrolic species. Functionalized dipyrrins are attractive for the development of optical anion sensors, in biological systems and the remediation of challenges and/or pollution as regards environmental problems.[31]

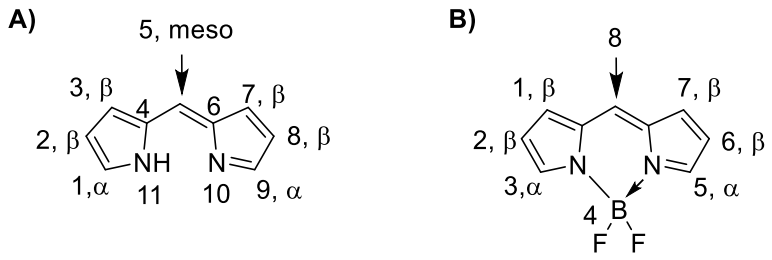

Figure 1.5. **A**) Numbering of the dipyrrin skeleton **B**) Numbering of the *F*-BODIPY

Dipyrrins are the precursors for the synthesis of *F*-BODIPY dyes (4,4-difluoro-4-bora-*3a*,*4a*-diaza-*s*-indacenes). Just like in pyrrole (Figure 1.1) the α/β naming system is usually used for the carbon atoms that make up each pyrrolic unit of a dipyrrin (Figure 1.5). As such, the 1- and 9-positions are the α-positions, and 2-, 3-, 7-, and 8-positions are the β-positions. The carbon of the methine bridge, the 5-position, is usually referred to as the *meso*-position. The numbering of dipyrrins is different to the numbering of *F*-BODIPYs, with the latter originating with the system used for indacene. The photophysical properties of *F*-BODIPYs make them ideal fluorescent frameworks for use as electron traps and position probes in dual positron emission tomography (PET)/optical imaging techniques in disease processes such as cancers because of their photochemical properties and physiologically stable chemical structure.[32,33] *F*-BODIPY complexes are dipyrrinato ligands coordinated to a $–BF_2$ unit. These complexes are fully conjugated and rigid structures with absorption and emission wavelength typically centered around 530 nm.[32] The desirable stability, tunable high quantum yield of fluorescence, intense absorption, and solubility have made these dyes of interest for several decades. *F*-BODIPYs can be derivatized by the incorporation of different substituents at the pyrrole,[34] meso, [35]and N-positions.[36] The dipyrrin (Figure 1.5) stability can be modified through alkyl substitution at the 1-, 2-, 3-, 7-, 8-, and 9- positions or via aryl substitution at the 5-positions (meso). Incorporation of the ^{18}F isotope at the boron atom of *F*-BODIPYs provides radioactive variants of this fluorescent motif. ^{18}F-probes, among others, have been shown useful for monitoring the delivery of drugs to desired organs or location in the body courtesy of the half-life (t1/2 = 109.8 mins) of ^{18}F.[37,38,39] Imaging

using fluorescent probes such as those of *F*-BODIPYs has been used for intraoperative tumor detection[40,41] and the examination of open surgical wounds during surgery.[41,42] Optimization of BODIPY properties can be done by functionalizing the core structure, thus tuning its fluorescence and photophysical properties for a variety of applications such as indicators for metal ions, reactive oxygen species and fluorescent sensing.[32,43] The BODIPY motif has been incorporated into pharmacologically active molecules such as peptides for drug discovery.[44,45]

1.4. Thesis Overview

This thesis focuses on the synthesis of pyrrolic compounds, specifically *F*-BODIPYs and azobispyrroles, i.e., azo compounds featuring two pyrrolic units. As such, a chapter has been dedicated to each framework, including an experimental section for all synthesized compounds. A conclusion section follows. In Chapter 2, progress towards the synthesis and characterization of azobispyrroles is discussed. Chapter 3 features attempts towards the synthesis of *F*-BODIPYs using a stoichiometric amount of dipyrrin and $BF_3 \cdot OEt_2$ in a continuous flow operation.

Chapter 2

2.1. Introduction

Work on azo dyes started in 1858 when Peter Griess discovered diazonium salts (Figure 2.1**A**).[46] These salts were made by reacting aniline with nitrous acid (nitrous acid is a weak and monoprotic acid known only in solution; it is prepared from its conjugate base $NaNO_2$).

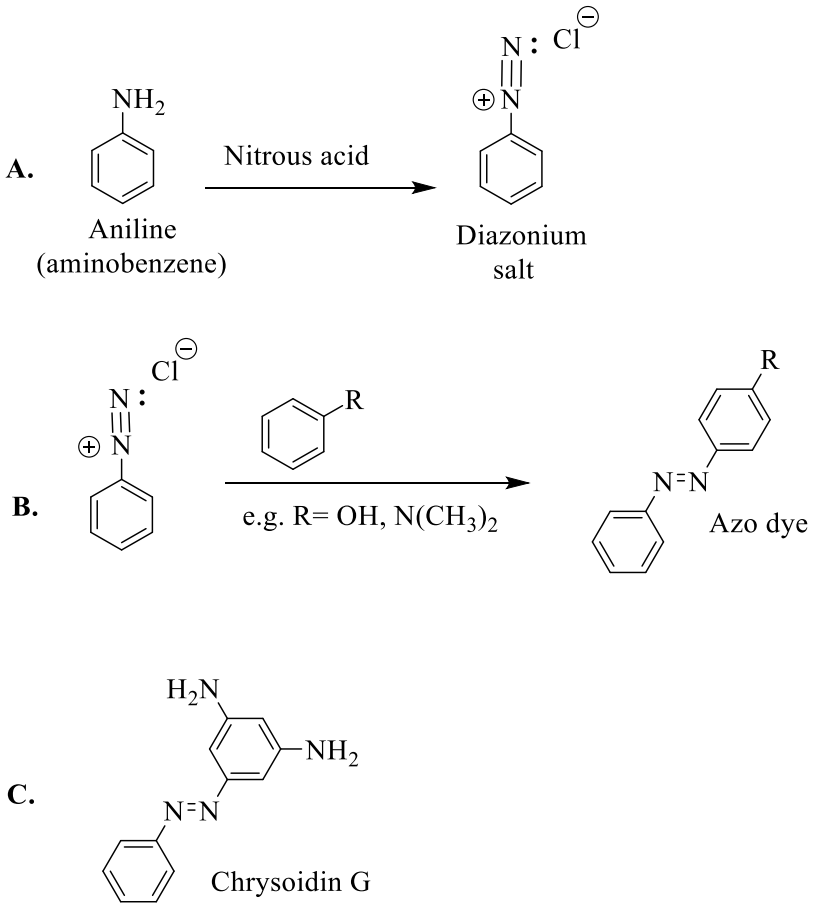

Figure 2.1. (**A**) The reaction of aniline with nitrous acid to form a diazonium salt. (**B**) Reaction of a diazonium salt with aromatic derivatives, including amines and phenols, to produce stable azo dyes. (**C**) The azo dye Chrysoidin G (chrysoidine).

Nitrous acid is commonly used to make diazonium salts from amines, thereby constituting the most popular way through which azo dyes are made (Figure 2.1**B**). Modification of the substituent pattern of the diazonium salt allows for azo dyes to exhibit different physical and optical properties.[47] Azo dyes are generally made through a coupling reaction of a diazonium salt (which acts as an electrophile) with an electron-rich coupling component (a phenol or an amine) or an arene (aromatic hydrocarbons). The reaction proceeds via an electrophilic aromatic substitution mechanism where the hydroxyl or amine group directs the aryl diazonium ion to the para site, if this site is not occupied, otherwise attachment occurs at the ortho position. The interesting photophysical properties displayed by azo dyes are commonly exploited when such dyes are used in textile, food, rubber, and plastic industries. Azo dyes are the largest group of synthetic dyes, courtesy of widely substituted ring structures,[48] the range of colours, and the stability.

Prontosil was the first azo-containing antibiotic to be commercialized.[49] Prontosil was identified as an anti-infective agent against *Streptococcal* infection in mice and demonstrated its efficacy via *in vivo* mouse infection models. Prontosil in the body is reductively metabolized into the active component sulfanilamide, which has a broad effect against gram-positive bacteria. Sulfanilamide is generated upon the reductive cleavage of the azo bond of Prontosil by the gut bacteria. With the finding of Prontosil as a pro-drug, that is converted to an active metabolite by the gut bacteria, the azo linkage has since been used in developing colon-specific pro-drugs that are activated by gut bacteria.

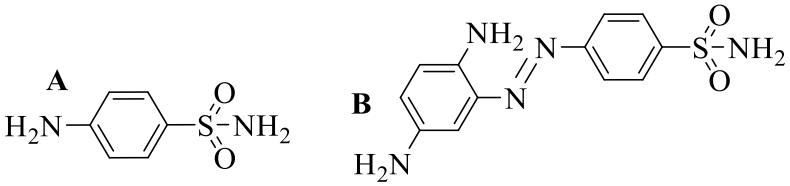

Figure 2.2. Structures of sulfanilamide (**A**) and Prontosil (**B**)

Azo dyes can exist in *E* and *Z* isomeric forms, of which the *E* isomer of most compounds is more stable and thus, the *Z* isomer rapidly converts to the *E* form.[50] One interesting property of these *E* and *Z* isomers of azo dye is their ability to interconvert (photo switch) when irradiated with light[51]

(Figure 2.3). This property renders azo dyes of potential use as photo switches. This *E* - *Z* interconversion results in changes in molecular geometry and polarity and has led to a wealth of research into azo compounds. Azobenzene is the most studied azo compound.[52] Use of alternative aryl groups, in place of one or both of the phenyl groups, has led to the large amount of research that constitutes this field.

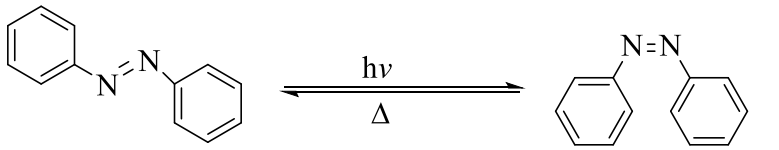

E, or trans, isomer

Z, or cis, isomer

Figure 2.3. Isomerization of azobenzene

Isomerization of azobenzene (*E* - *Z*) can be triggered photochemically by irradiating azobenzene with light of appropriate wavelength. The reverse *Z* - *E* isomerisation can often be induced both photochemically and thermally.[53] Exceptions include molecules in which the ArNNAr moiety is part of a macrocycle (Figure 2.4) for which the *Z* isomer is more stable and thus the opposite behaviour is possible.[54,53]

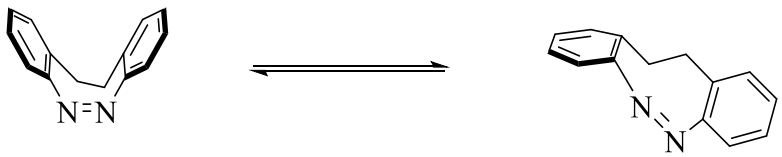

Figure 2.4. Structure of an azobenzene where the ArNNAr moiety is part of a macrocycle

According to Crespi, S. *et al*.,[55] the isomerisation of azobenzene can take place via three mechanistic routes i.e., inversion,[56] rotation,[56] and a combination of both. The *Z* - *E* isomerization of azobenzene proceeds by inversion at nitrogen, whereby the N=N-C angle opens along the molecular plane of around 180℃ in the transition state and an intact N=N double bond. This is often energetically more favorable compared to the *Z* - *E* isomerism along the rotation angle. Inversion is a relatively slow process which is typical of azobenzene and a vast majority of substituted derivatives.[56] *Z* - *E* isomerisation can also proceed by rotation along the rotation angle in which the C-N=N-C dihedral angle describes a rotation around the central N=N-C bond (with loss of π character) of about 90℃ at the transition state.[56] An example of such is an ArNNAr species with an electron-donating substituent in a polar solvent. For some azobenzenes isomerization is neither pure rotation or pure inversion but instead represents a combination of both. These mechanistic routes are substituent, solvent and polarity influenced. Figure 2.5 is similar to that reported in the literature.[60]

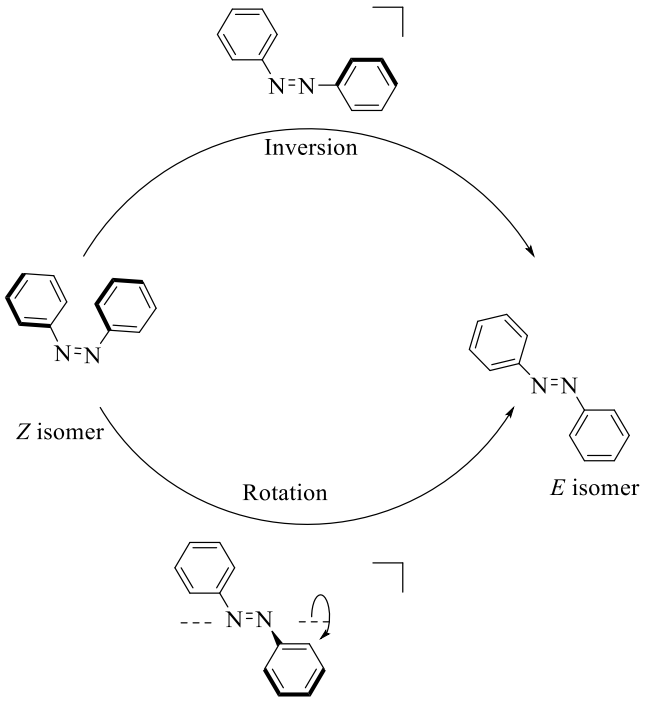

Figure 2.5. Inversion and rotation of azobenzene (PhNNPh)

According to Crespi, S. *et al*.[55], excitation of *E*-PhNNPh from its S_0 ground electronic state to its first singlet excited state S_1 is representation of a weakly allowed n→π transition in the visible region ($\lambda \approx 450$ nm).[57] The PhNNPh primary photochemical function involves the isomerization of the azo function group (N=N)[57] i.e. the conversion of *E*-PhNNPh into the *Z*-PhNNPh. Isomerization occurs at the S_1 state, with its own quantum yield (the number of isomerization per photon absorbed by the compound). This effect is promoted by the $S_1 \rightarrow S_0$ conical intersection (CI) that is energetically accessible leading to funnelling through a CI that connects S_1 and S_0 and promotes isomerization (Figure 2.6). Photoisomerization of PhNNPh generally proceeds by an inversion pathway.[58,59] Figure 2.6 is a simplified version of one reported in the literature.[60]

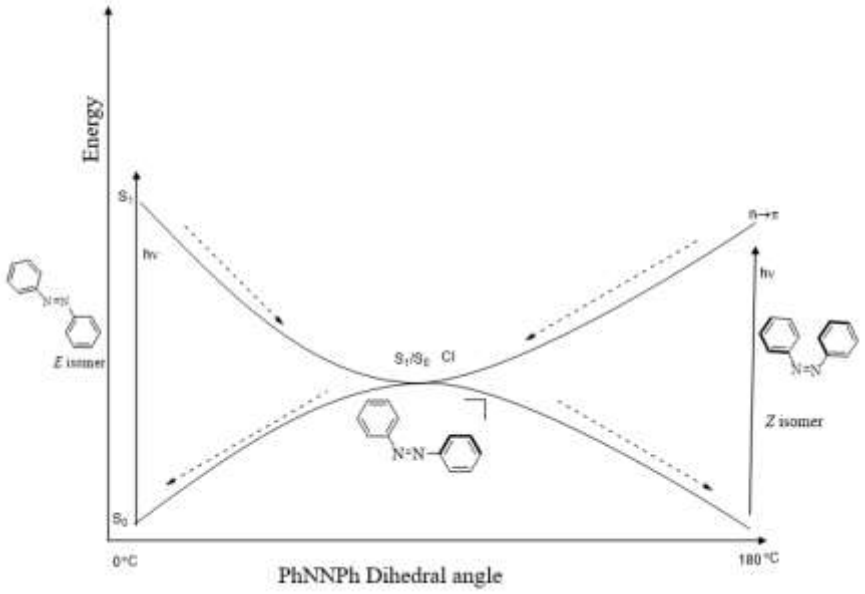

Figure 2.6. An energy diagram showing the isomerization of azobenzene (PhNNPh)

There are three characteristic parameters through which photo switching (or photoisomerization) can be investigated, the first being the relative thermal stability of the isomers. Thermal stability, or thermal isomerization, is greatly dependent on the polarity and nature of solvent used for the investigation.[50,60] The second parameter is the steady-state relative abundance of *E* and Z isomers

when the photo switch is exposed to a given source of light (or kept in the dark).[55] The third parameter is the wavelength of maximum light absorption and the quantum yield of the ensuing isomerization (the extent of isomerization per photon absorbed by the system).[53]

Photo switches also exist in the form of heteroaryl azo compounds featuring aryl groups other than those of azobenzenes or substituted benzenes. The study of pyrrole-containing azo compounds is a new and emerging field[52] within heteroaryl azo compounds, many of which contain nitrogen within the heterocycle. The electron rich nature of pyrrole offers a broader variety of photophysical and chemical properties differing from those involving azobenzene provides a new area of interest. Replacing one heteroaryl (Figure 2.7**A**) can perturb photophysical properties and add opportunity for hydrogen-bonding or metal coordination. These interactions modify the azo chromophore and present opportunities for sensing pH or detecting the presence of metal ions. Arylazo pyrroles (Figure 2.7.**B**) have been shown to be effective photo switches. The *Z* isomer persists for hours/days provided that substituents do not result in severe steric strain, in which case the lifetime can be seconds.[52,61]

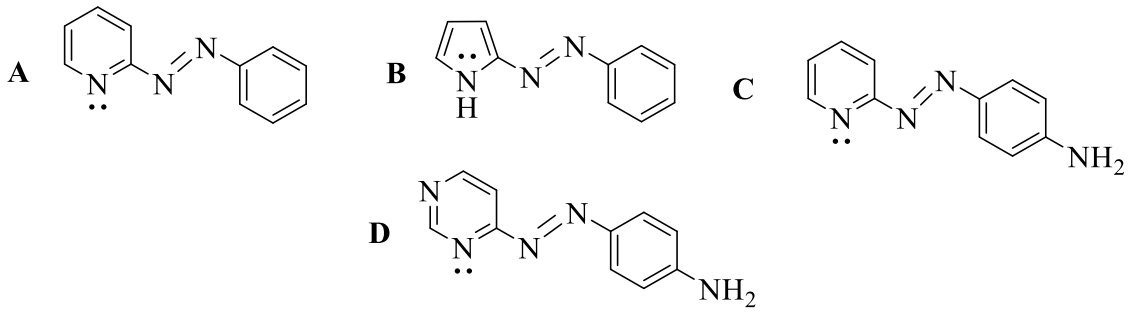

Figure 2.7. Structures of phenyl azopyridine (**A**), arylazopyrrole (**B**), 4-aminophenyl azo pyridine (**C**) and phenylpyrimidine (**D**)

In the case where one of the aryls in azobenzene is replaced with an electron poor pyridine or pyrimidine at one of the sides of the -N=N- group (Figure 2.7. **C**), plus the presence of -OR or -NR_2 electron-donating group, a push-pull effect can be observed (Figure 2.8).[62,60] This can lead to

tautomerization, in addition to the *E* - Z isomerization. As shown in Figure 2.8, this tautomerization results in a sigma N-N interaction that facilitates rotation and thus the interconversion of the *E* and Z isomer. Figure 2.8 is similar to that reported in the literature.[60]

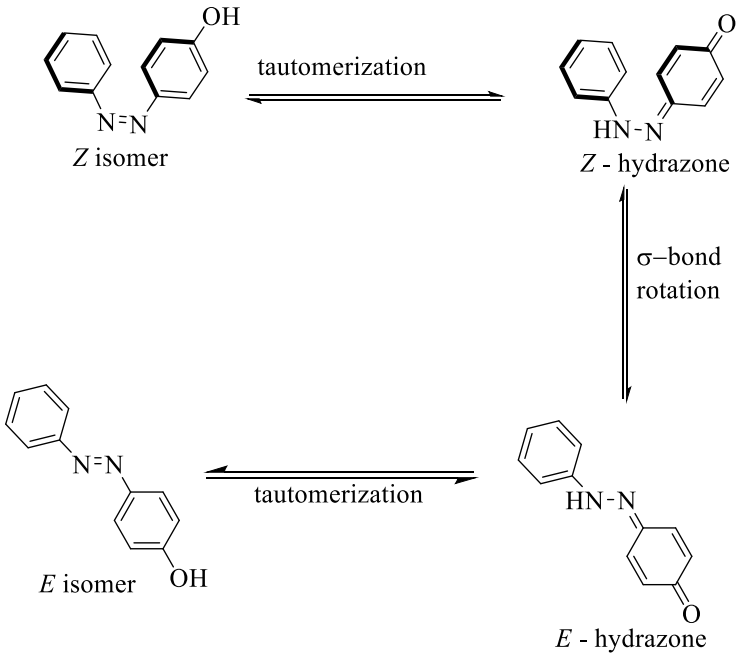

Figure 2.8. Push - pull effect of an azobenzene bearing an electron-donating substituent

Thus *E* - *Z* isomerization goes through the rotation mechanism with loss of the N-N double bond character. In this case the *Z* isomer has a long lifetime and is more stable than the *E* isomer. This *Z* isomer converts to the *E* form via an inversion mechanism, and *Z* isomer isomerization is slower than that of PhNNPh.[52] Pyrimidines in azopyrimidines (Figure 2.7.**D**) are more electron deficient than would be pyridine and as such a suitable substituent in the azo push-pull system. The thermal stability of the *Z* isomer in azo compounds, where aryl equals pyrazole or indazole, is dependant upon steric strain, solvent, and concentration. The push-pull effect can thus be influenced by the presence of an electron-donating substituent on the aryl ring. Very few reports describe azo compounds with heteroatoms other than N in the aromatic ring.[55]

Azo compounds bearing pyrroles on both sides of the -N=N- azo moiety were first discovered by a former Master student Roberto Diaz-Rodriguez during his work in the Thompson group.[63] This route involves the reaction of nitrobutanones with ammonium acetate as shown in Figure 2.9**A**. This reaction is typically used for the preparation of aza-dipyrrins, but incorporation of aryl groups with significant substitution led instead to formation of the previously unobserved azobispyrroles as shown (Figure 2.9**B**).

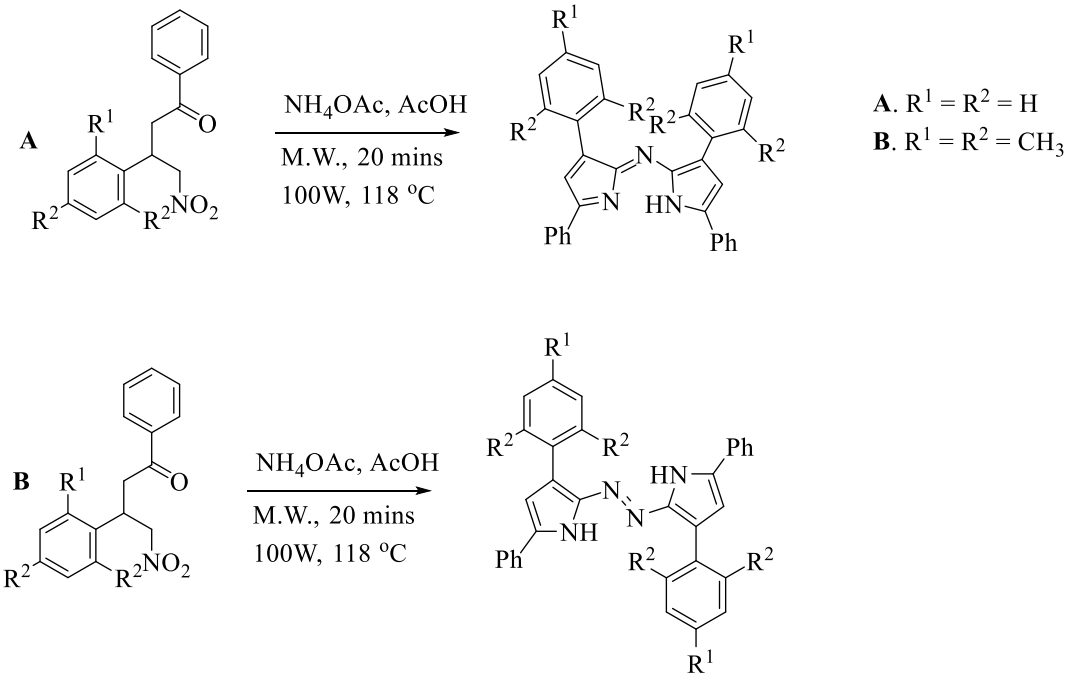

Figure 2.9. Synthesis of aza-dipyrrins (**A**) and synthesis of azobispyrrole (**B**)

This work was restricted to the incorporation of pyrroles substituted with large aryl groups, such as mesityl. The complexity of the mechanism for the generation of an azobispyrrole under the reaction shown in Figure 2.9, when the nitrobutanone has large aryl groups instead of the expected azadipyrrin, is not yet well understood. Presumably, the steric bulk provided by the mesityl group disfavours attack at the electrophilic imine at carbon as would be required for dipyrrin formation. Instead, the pathways favour formation of azo compounds. Nitrobutanones with small aryl groups

provide the azadipyrrin, whereas those with bulky aryl groups provide the azobispyrrole as a competitive outcome over the azadipyrrin.

2.2. Project Goal

The goals of this part of this MSc project were to demonstrate reproducibility of the azobispyrrole formation and to develop an improved methodology for the synthesis of a series of azobispyrroles with varying substituents. Improved yields were also sought. Ideally, improving the methodology would provide sufficient material to enable investigation of the respective photophysical properties of these compounds.

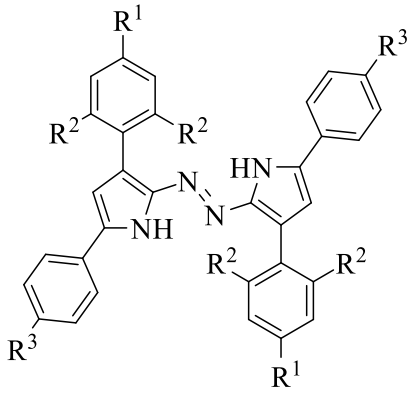

B23 $R^1 = R^2 = CH_3$, $R^3 = H$

B24 $R^1 = R^3 = H$, $R^2 = Cl$

B25 $R^2 = R^1 = CH_3$, $R^3 = OCH_3$

B26 $R^1 = H$, $R^2 = Cl$, $R^3 = Cl$

Figure 2.10. Structures of azobispyrroles with different substituents

Initial work would focus on assessing reproducibility. A subsequent goal would involve the incorporation of electron-donating substituents on the aryl rings, so as to enable exploration of the push-pull tautomerization effect.

2.3. Results and Discussion

The discovery of azobispyrroles from nitrobutanones by Roberto Diaz-Rodriguez[63] was met with a poor yield for **B23** and **B24**. With that, this current thesis work originally focused on developing a methodology to afford azobispyrroles with improved yield, following the traditional way through which azo dyes are made i.e., via diazonium salts.

In order to make the azobispyrroles following the traditional strategy, there was the need to synthesize **B5** (2,4-diphenylpyrrole). This pyrrole was required as starting material (Scheme 2.2) to enable for the synthesis of the diphenylpyrrole diazonium salt **B8**. In order to synthesize 2,4-diphenyl pyrrole (**B5**), the reaction sequence shown in Scheme 2.1 was followed. This reaction scheme has some modifications from the published procedure.[64,65] These modifications include a different purification process for **B4** and **B5** and variation of the base from dimethylamine to DBU in the conversion of chalcone **B3** to nitrobutanone **B4.**

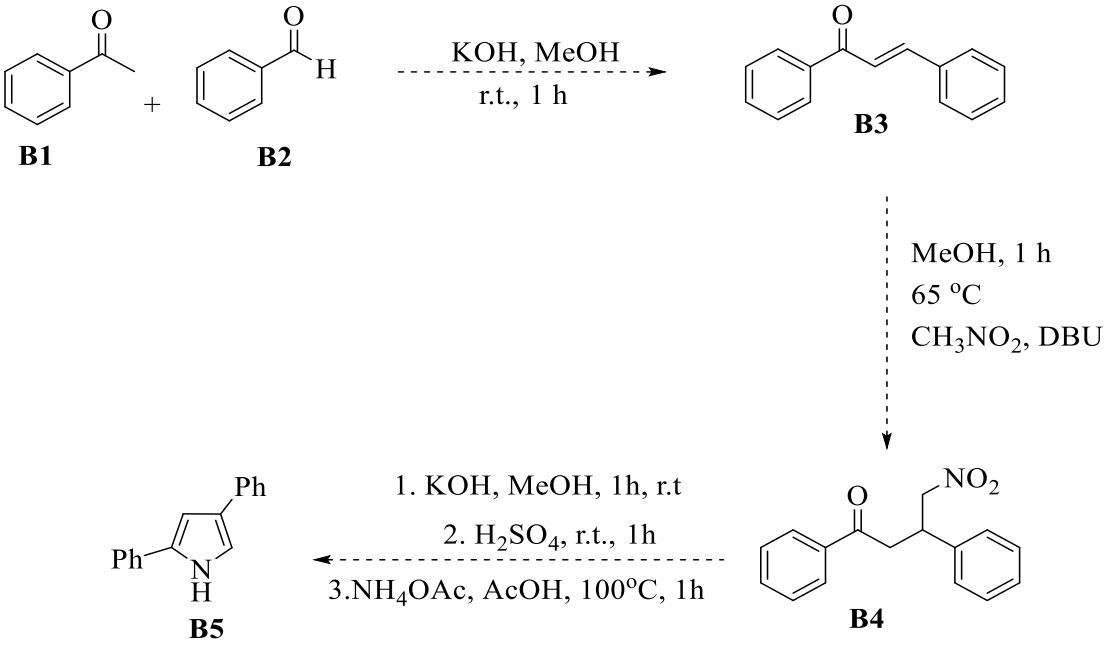

Scheme 2.1. Synthesis of 2,4-diphenylpyrrole (**B5**)

Following a published procedure,[65] acetophenone (**B1)** and benzaldehyde (**B2**) were reacted under basic conditions as shown (Figure 2.11) to result in the formation of trans chalcone **B3** in 85% isolated yield. **B3** is also commercially available.

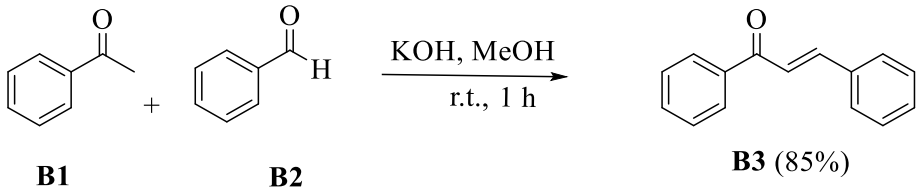

Figure 2.11. Synthesis of trans chalcone (**B3**)

Chalcone **B3** was reacted with nitromethane under basic conditions and the reaction mixture stirred at reflux temperature for 1h (Figure 2.11). The reaction mixture was then quenched via the addition of 1M HCl until pH 2 was achieved. At pH 2, the product precipitated as a white solid and was then isolated via filtration. In order to purify the white solid, it was dissolved in minimal dichloromethane and excess 20% ethyl acetate/hexane was added, and the resulting mixture allowed to stand until a precipitate formed. The precipitate was then isolated via filtration and dried to afford the nitrobutanone **B4** as a white powdery solid in 87% yield. Although a literature procedure was used as a template for this synthesis,[66] DBU was identified as a superior alternative to diethylamine which was the reported base for this Michael addition of nitromethane to the enone **B3**.

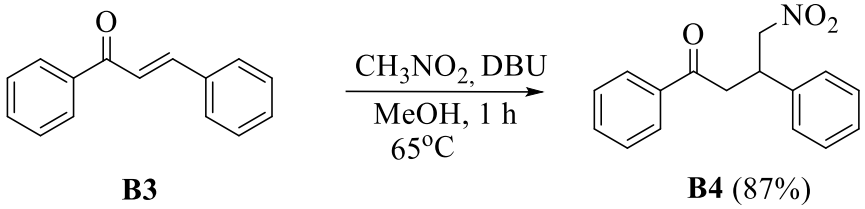

Figure 2.12. Synthesis of nitro butanone (**B4**)

With 2,4-diphenyl pyrrole as the target compound, nitrobutanone **B4** was treated with KOH in anhydrous MeOH. The reaction mixture was stirred at room temperature for 1h and then the colorless solution was added dropwise into a solution of concentrated H_2SO_4 in anhydrous MeOH at 0°C. The reaction mixture was then allowed to slowly warm up to room temperature and further stirred for 1h (Figure 2.13). The reaction was quenched by the addition of water and ice, then neutralized to pH7 with 4M NaOH. The mixture was then filtered, and the white solid thus obtained was dissolved in acetic acid and NH_4OAc was then added. The mixture was stirred at reflux temperature (100°C) for 1h. The mixture was cooled, poured over ice, and neutralized to pH7 with 4M NaOH. The resulting precipitate was isolated via filtration, and then dried. The pale pink solid was dissolved in minimal dichloromethane, through heating the solution, and then cooled to room temperature. Upon the addition of excess cold pentane, a white solid precipitated. This was isolated via filtration and washed with cold pentane and dried to afford **B5** as a free flowing-solid in 50% yield. This was lower than the reported yield,[64] although it is of note that the published work reported **B5** to be pink solid.

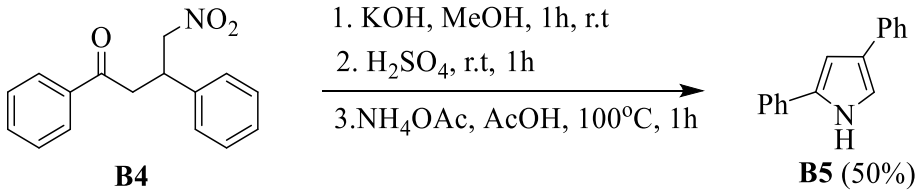

B4 **B5** (50%)

Figure 2.13. Synthesis of diphenyl pyrrole (**B5**)

With the desired 2,4-diphenyl pyrrole (**B5**) in hand, this pyrrole was subjected to the typical reaction sequence used for the preparation of symmetrical azobisaryls (Scheme 2.2). This was to involve formation of the known nitroso-pyrrole **B6**, followed by reduction to provide amino diphenylpyrrole **B7**. Although **B7** has been reported, the described synthesis is accompanied by caution as regards the need to protect the material from decomposition. Our goal was to achieve conversion to **B7**, and then diazonium salt **B8**, followed by reaction with **B5** to form the desired **B9**. When approaching this work, we were fully aware of the electron-rich nature of the pyrrole

and thus the need to investigate strategies by which to discourage oxidation. Nevertheless, given that this is the traditional route to azodiaryls, we wished to explore feasibility.

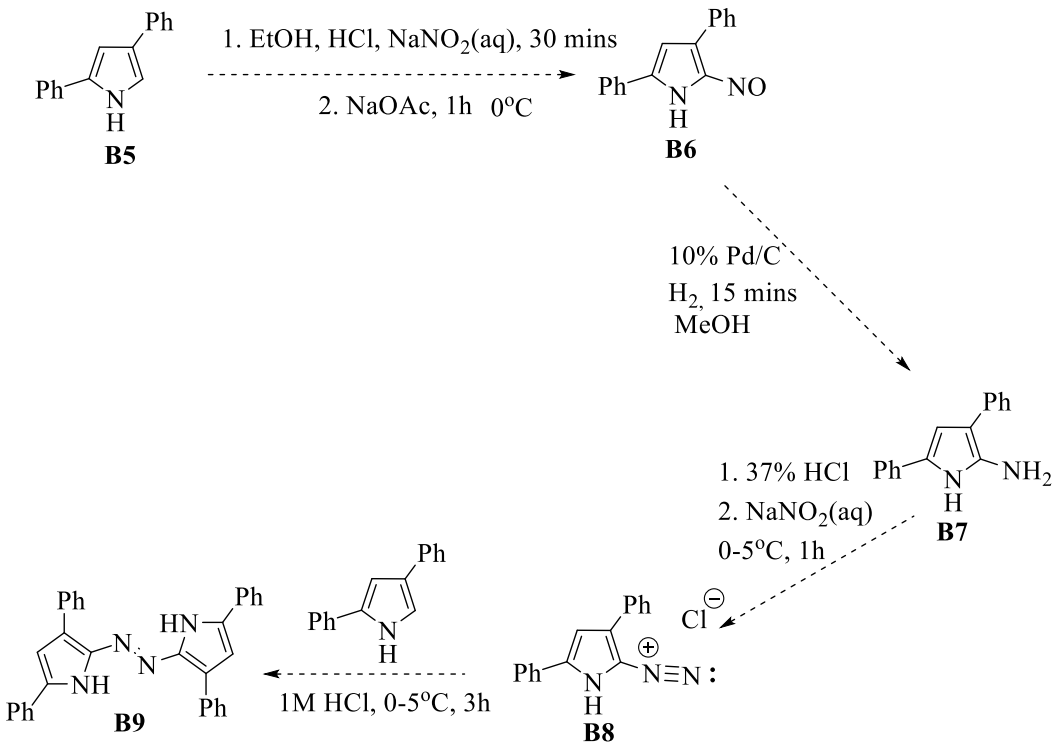

Scheme 2.2. A proposed scheme for the synthesis of azobispyrrole (**B9**)

Following a published procedure,[64] a solution of 2,4-diphenyl pyrrole (**B5**) in EtOH was treated with aq $NaNO_2$ and the reaction mixture stirred for 30 mins, followed by the addition of 1 eq. of HCl at 0°C. The reaction mixture was then stirred for 1 h (Scheme 2.2). The resulting red solid was collected via filtration and washed with Et_2O. The red solid, the hydrochloride salt of **B6**, was then dissolved in minimal EtOH and excess aq NaOAc and ice were added, and the mixture stirred for 1h. The resulting green solid was collected via filtration, washed with water, and then dried. In order to purify the green solid, it was dissolved in minimal dichloromethane and precipitated upon the addition of cold pentane to afford **B6** as a green solid in 80% isolated yield.

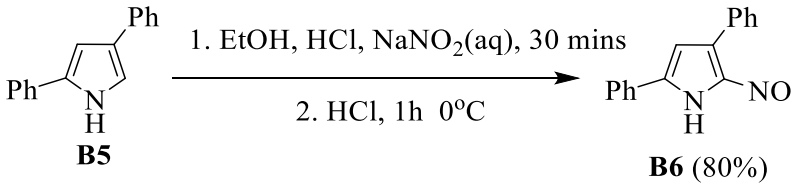

B5 **B6** (80%)

Figure 2.14. Synthesis of nitroso pyrrole (**B6**)

The 2-amino pyrrole (**B7**) is reported to be relatively unstable at temperatures above 25 ℃ and can rapidly convert into an azadipyrrin when exposed to oxygen.[66] To enable preparation of the 2-amino diphenylpyrrole (**B7**), a published procedure[64] was adopted with some modifications whereby nitroso pyrrole (**B6)** was placed in a two-neck RBF, and purged with nitrogen (3 times). Anhydrous MeOH and Pd/C were added (Scheme 2.2), and three further rounds of nitrogen purge were completed. A balloon filled with hydrogen was then fixed onto the RBF and the reaction atmosphere was gradually changed to hydrogen (nitrogen-vacuum-hydrogen). The reaction mixture, now under 1 atm. hydrogen was stirred for 15 mins to reduce the nitroso functionality to the amino functionality. After 15 mins the reaction atmosphere was changed to nitrogen and the reaction mixture was taken to the nitrogen-filled glove box where it was filtered over a thick pad of celite. The solvent was then removed to yield the amino diphenyl pyrrole **B7** as a grey solid in 80% yield. Analysis of the ^{1}H NMR spectrum of **B7** revealed a singlet at 3.63 ppm characteristic of the protons of NH_2, integrating to 2H and in accordance with literature.[64]

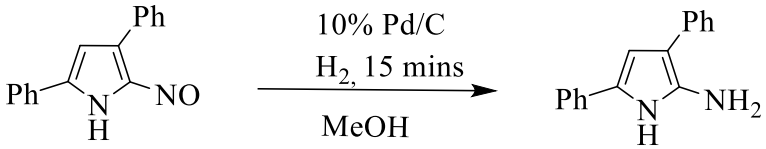

B6 **B7** (80%)

Figure 2.15. Synthesis of amino pyrrole (**B7**)

Following a published procedure,[66] amino diphenyl pyrrole (**B7**) was placed in a RBF, purged with nitrogen (3 times) and treated with aq $NaNO_2$ and 37% HCl then stirred for 1h in an attempt to form the diazonium salt solution. A change in colour from brown to bight blue was observed. Diazotization reactions are often accompanied by a colour change. The diazonium salts from this kind of reaction are typically prepared *in situ* as they are unstable and can be explosive when dry. The diazonium salt solution was then slowly added to the coupling solution, in this case **B5** at 0 - 5°C and the resulting mixture was stirred (Scheme 2.3) for three hours. The final solution was then slowly added to a 1M NH_3 solution in an attempt to yield the desired azobispyrrole **B9**.

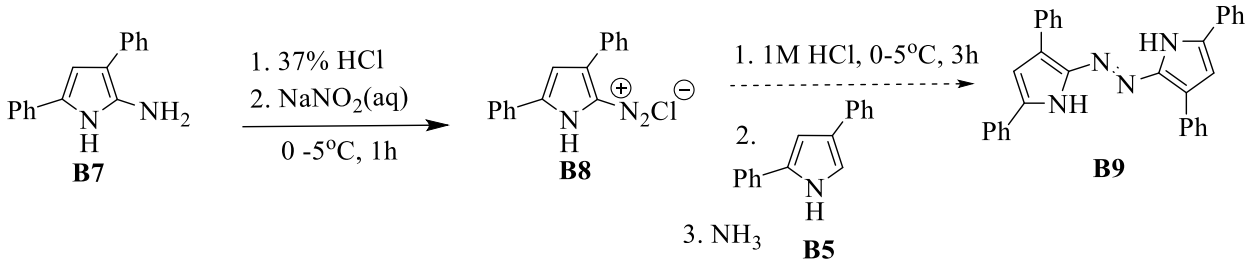

Scheme 2.3. Attempted synthesis of azobispyrrole **B9**

Analysis of the final product revealed that the desired product azobispyrole (**B9**) was not synthesized from the above reaction sequence (Scheme 2.3). The reaction was repeated a couple of times making sure to carefully follow published procedure (i.e., literature procedures for the synthesis of 4-amino azobenzene),[66] but **B9** was not made in any of these trials. To evaluate what the challenge could be the method was probed by using phenyl-based aryls in place of each of the two pyrrole moieties (Scheme 2.4).

Given that the amino diphenyl pyrrole (**B7**) is reported as unstable above 25°C and rapidly converts to an azadipyrrin when exposed to oxygen,[66] aniline (**B10**) was used to explore the integrity of the reaction conditions used. Aniline has been previously used in the synthesis of azobisaryls.[66]

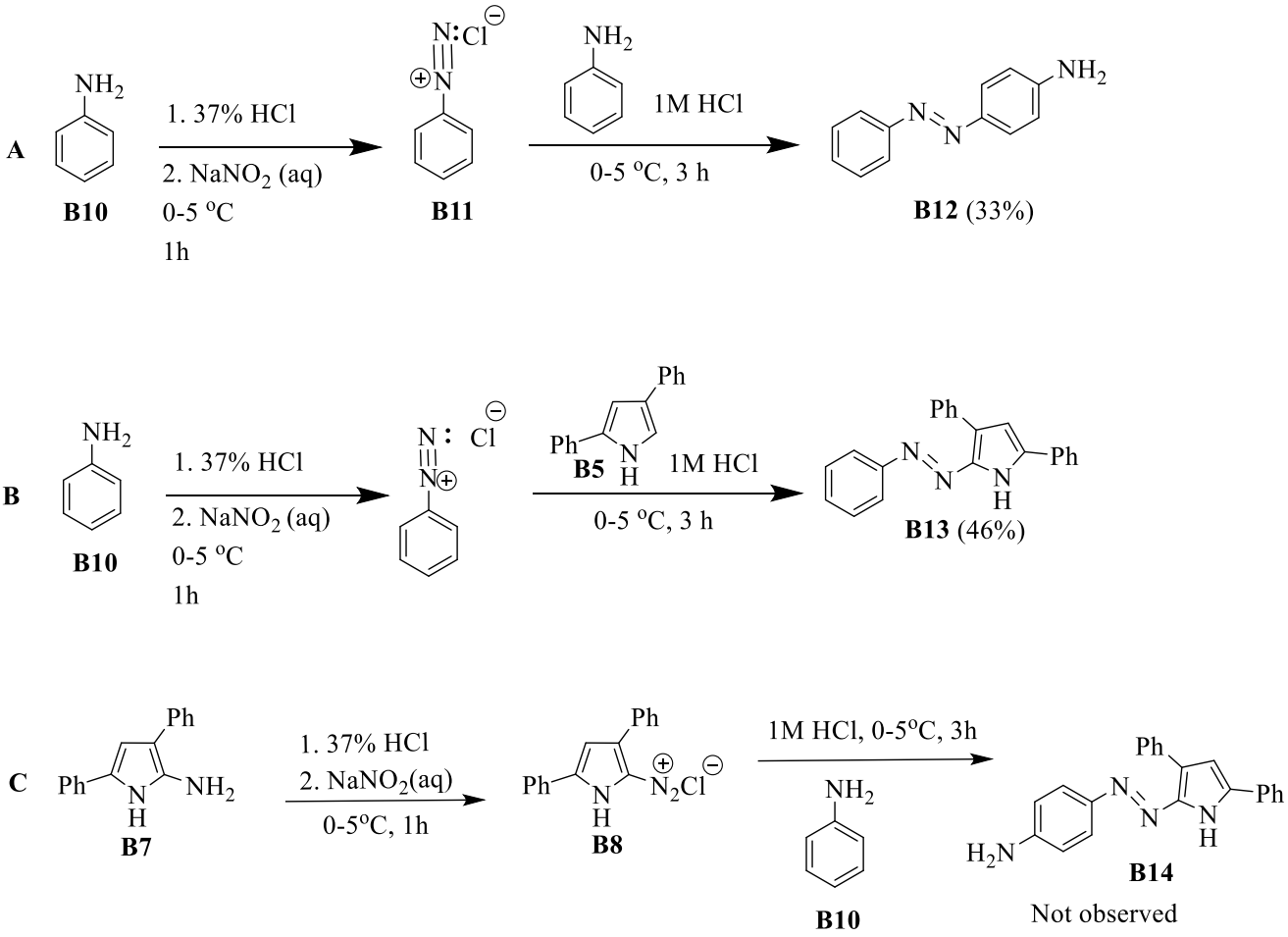

Scheme 2.4. (**A**) Synthesis of azo dye **B12** using aniline as an amine species and the coupling partner, (**B**) Synthesis of azo dye **B13** using aniline as an amine species and diphenyl pyrrole as the coupling partner, (**C**) Attempted synthesis of azo dye using amino diphenyl pyrrole as an amine species and aniline as the coupling partner.

To investigate why the reaction according to Scheme 2.3 was unsuccessful, Scheme 2.4**A** was followed. This proceeded in the same fashion as followed previously (Scheme 2.3) but using aniline (**B10**) in place of both the amino diphenyl pyrrole (**B7**) and the diphenyl pyrrole (**B5**). The azo dye 4-amino azobenzene (**B12**) was isolated in 33% yield (Scheme 2.4**A**) thus demonstrating a successful reaction sequence although in lower yield than that reported.[67] Given that the method was successful for the synthesis of azobisaryl (**B12**), the coupling was varied though use of the desired coupling partner diphenyl pyrrole (**B5**), as shown in Scheme 2.4**B**. The coupling sequence

was varied in this manner so as to investigate the ability of diphenyl pyrrole (**B5)** to act as a coupling partner with diazonium salts. Scheme 2.4**B** proceeded in the same fashion as Scheme 2.3 and phenylazopyrrole (**B13**), a novel compound, was isolated in 46% yield as an orange solid. Analysis of the corresponding ^{1}H NMR spectrum suggested that a mixture of both cis (*Z*) and trans (*E*) isomers of phenylazopyrrole (Scheme 2.4**B**) were formed. Having shown that diphenylpyrrole (**B5**) has the ability to couple to a diazonium salt (Scheme 2.4**B**), it was time to investigate the ability of amino diphenyl pyrrole (**B7)** to undergo the diazotization reaction by attempting the coupling with aniline (**B10**) as shown in (Scheme 2.4**C**). This investigation (Scheme 2.4**C**) again proceeded as shown in Scheme 2.3 to hopefully synthesize 4-amino phenylazopyrrole **(B14**) as shown in Scheme 2.4**C**. However, analysis of the product mixture revealed that **B14** was not synthesized (Scheme 2.4**C**). This could be because the amino diphenyl pyrrole **B7** failed to undergo the diazotization reaction and thus **B8** was unavailable to couple to the aniline **B10**. This is supported by the recovery of **B10** after work up.

To further investigate Scheme 2.4C, **B7** needed to be synthesized again. Upon reaction of **B6** to form **B7** (Figure 2.15) a bright blue solid was surprisingly obtained, unlike the grey solid which was previously isolated as **B7** (Figure 2.15). Upon analysis using ^{1}H NMR spectroscopy, it was discovered that the blue solid was an azadipyrrin. This means that the target amino diphenyl pyrrole (**B7**) was converted to an azadipyrrin as would be expected upon exposure to air. Presumably the high humidity level experienced in the Thompson lab during the summer season was thwarting isolation of **B7**. Every further attempt to synthesize **B7** was abortive. Thus, the intended goal of this project could not be achieved. As such, the goal herein became the synthesis of azobispyrroles (Scheme 2.5) via the original route involving nitrobutanones.

In order to synthesize new azobispyrroles with varying substituent patterns (Scheme 2.5), the synthetic route through which **B23** and **B24** were initially made was adopted.[65]

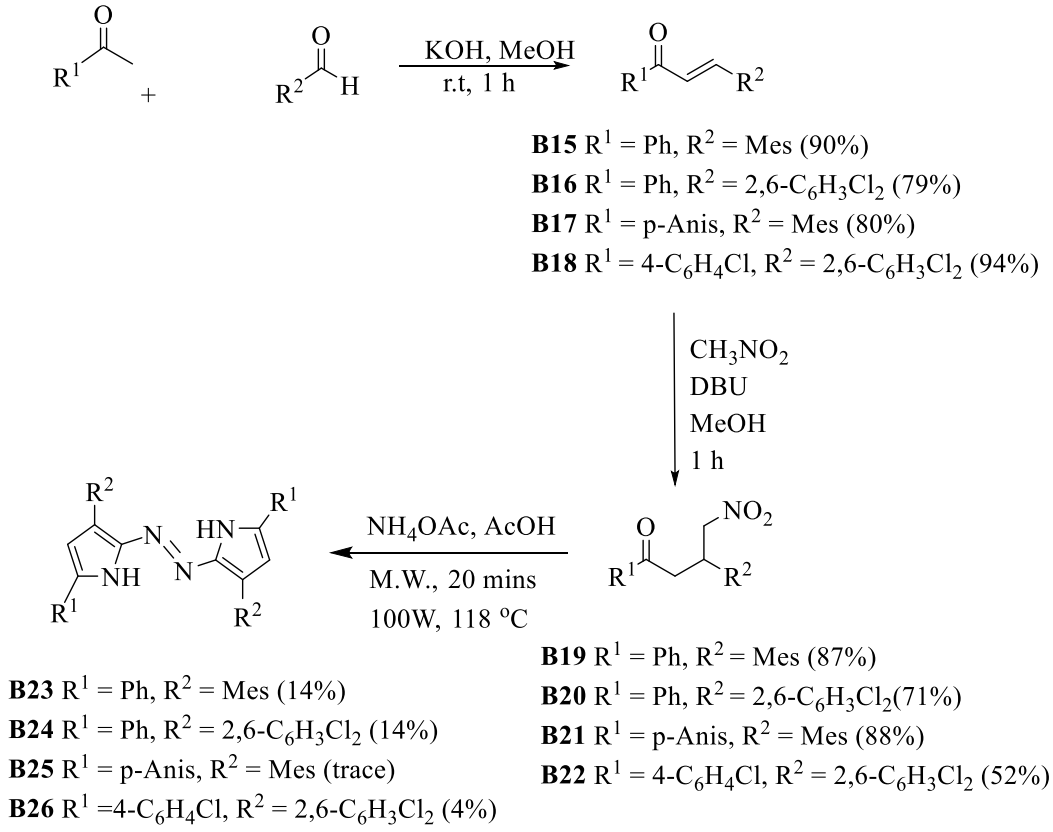

Scheme 2.5. Synthetic strategy for the preparation of azobispyrroles with varied substitution

In order to synthesize the azobispyrroles with varying substituents, the chalcones **B15** - **B18**, as shown in Scheme 2.5, were prepared and isolated. These reactions were repeated several times with good yields obtained in each case. These chalcones were each treated with nitromethane under basic conditions to provide the four nitrobutanones **B19** - **B22**. The derivative **B22** is a novel compound.

With **B19** - **B22** in hand, it was time to synthesize the corresponding azobispyrroles (**B23**- **B26**). To make the desired azobispyrrole **B23**, a solution of **B19** in AcOH was placed in a microwave (M.W.) vial, with NH_4OAc, and then treated with microwave irradiation (20 mins, 118°C, 100 W). After 20 mins the reaction mixture had changed from a colorless mixture to a deep purple. The reaction mixture was quenched with water and then extracted with dichloromethane. The crude product (now deep pink/red in color) was purified over silica eluting with 40%

dichloromethane/hexane to provide **B23** as a bright red solid in 14% yield. Flash column chromatography of the crude material was quite challenging, as the desired product has a very close R_f value to those of other by-products formed during this reaction. The chromatographic process was repeated at least two times to get clean product. This contributed to the poor isolated yield of the desired product **B23**. The synthesis of azobispyrrole **B24**, proceeded in a similar manner to provide 14% isolated yield. These yields are very similar to those obtained previously, thus demonstrating reproducibility of the methodology described in the thesis of Roberto Diaz-rodriguez.[63] With the synthesis of **B24** and **B25** in hand, nitrobutanone **B22** was reacted with NH_4OAc as shown in Scheme 2.5. Although successful, the novel azobispyrrole **B26** was isolated in only 4% yield after an extensive purification. Similarly, attempts to prepare azobispyrrole **B25** using nitrobutanone **B21** resulted in only in trace amounts of the described product.

Upon analysis of the ^{1}H NMR spectra of **B23**, **B24** and **B26**, these showed a broad singlet ^{1}H peak typical to those of ^{1}H atoms bound to the N-position of pyrrole (11.60 ppm for **B26**, 9.39 ppm for **B24** and 9.36 ppm for **B23**). These peaks each integrated to 2 protons, assuming two equivalent phenyl rings, indicating symmetry. Singlets were also seen at 6.49 ppm for **B23**, 6.67 ppm for **B24** and 6.71 ppm for **B26**. These also are typical of protons at unsubstituted positions of a pyrrole ring. Each of these also integrated to 2 protons: this again indicates symmetry, each proton belonging to the pyrrole on either side of the N=N functionality. The mass spectrometry data confirm the presence of the *m/z* peaks of **B23**, **B24**, **B25** and **B26** at 571, 602, 608, and 672, respectively, with each confirmed via accurate mass measurements.

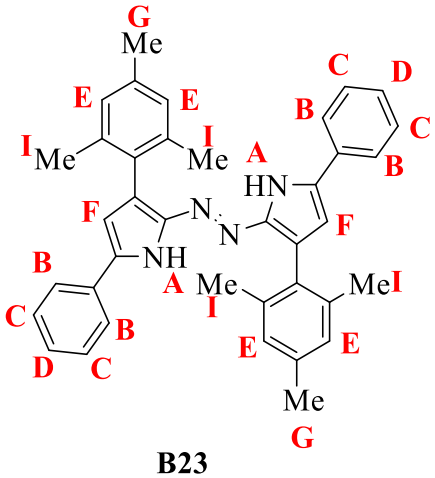

B23

Figure 2.16. Structure of the azobispyrrole **B23**

To further understand the characterization of **B23** and looking at the structure of **B23** (Figure 2.16) and relating it to its ^{1}H NMR spectrum (attached in appendix), starting from the most deshielded peak to the least deshielded or most shielded, the multiplicity and integration values of the different peaks indicates the presence of symmetry i.e., a symmetrical compound (where one half of the compound matches to the other half). Starting with the broad weak singlet at 9.36 ppm, this is indicative of a pyrrolic N - H and integrates to 2H (**A**) indicating the presence of two pyrrole rings within a symmetrical environment. Moving on to the next peak a doublet is observed at 7.53 ppm (4H, **B**). These peaks are within the chemical shift region expected for aryl groups and the most deshielded of all the aryl protons. These are the 4H (2H each ring) at the ortho position of the α-phenyl pyrrole rings. Next is a triplet (7.37 ppm, 4H, **C**) corresponding to the meta protons of the α-phenyl pyrrole rings i.e., 2H each on each ring. Next is another triplet (7.26 ppm, 2H, **D** partially obscured by the $CDCl_3$ signal). These are the para protons on the α-phenyl pyrrole rings. Then we have a singlet (7.00 ppm, 4H, **E**), due to the unsubstituted positions of the β - mesityl rings. These protons experience a shielding effect from the adjacent -CH_3 group and are thus the least deshielded of all the non-pyrrolic aryl protons. Next is another singlet (6.49 ppm, 2H, **H**), indicative of pyrrolic protons. Lastly, we have 2 singlets at 2.38 ppm and 2.21 ppm (6H and 12H, respectively), due to the protons of the -CH_3 groups on the β - mesityl pyrrole rings (**G** and **F** respectively). The multiplicity and integration present in the spectrum of **B23** are common with those of the **B24** and **B26** ^{1}H NMR spectra.

All these azobispyrroles **B23**, **B24**, **B25**, and **B26** are bright red in color. Looking at the optical absorbance spectrum of **B23** (Figure 2.17), reveals two maxima at 322 nm and 345 nm in dichloromethane solution at room temperature, with the most intense having an extinction coefficient of 20,700 $M^{-1}cm^{-1}$ (Figure 2.18). The absorbance spectrum of **B24** reveals three maxima at 509 nm, 534 nm, and 668 nm (Figure 2.19). Azobispyrrole **B26** has absorbance maxima at 510 nm, 539 nm, and 662 nm (Figure 2.21). The extinction coefficients of **B24** and **B26** were calculated to be 4,500 $M^{-1}cm^{-1}$ (Figure 2.20) and 2,800 $M^{-1}cm^{-1}$ (Figure 2.22), respectively, using Beer's Law. All three azobispyrroles (**B23**, **B24** and **B26**) exhibited little to no fluorescence.

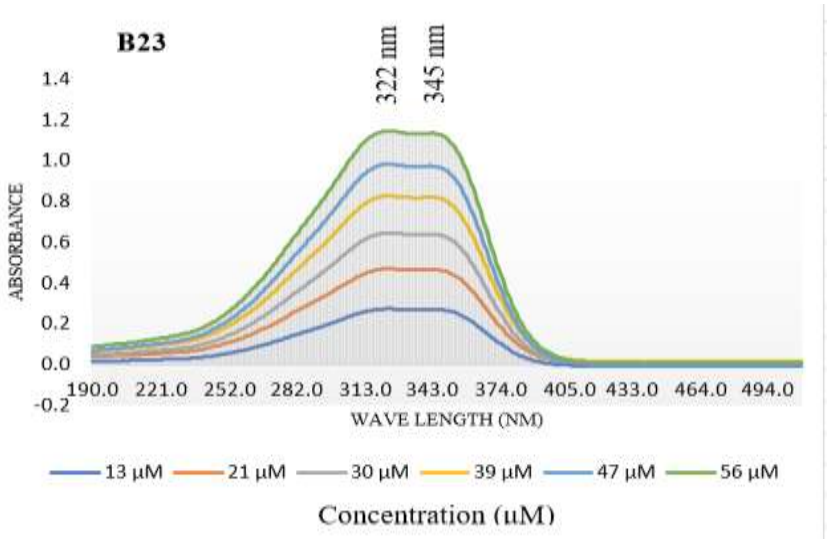

Figure 2.17. UV-Vis absorbance spectra of **B23** in dichloromethane at various concentrations

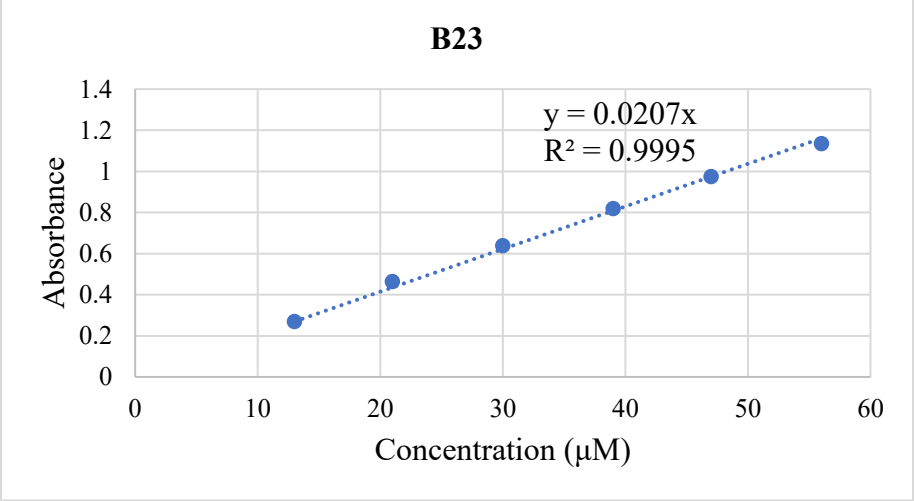

Figure 2.18. Plot of absorbance versus concentration of a solution of **B23** in dichloromethane

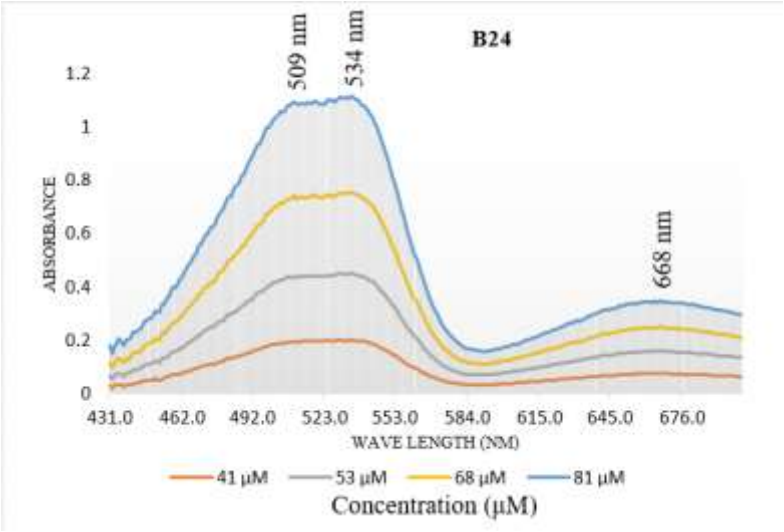

Figure 2.19. UV-Vis Absorbance of **B24** in dichloromethane at various concentrations

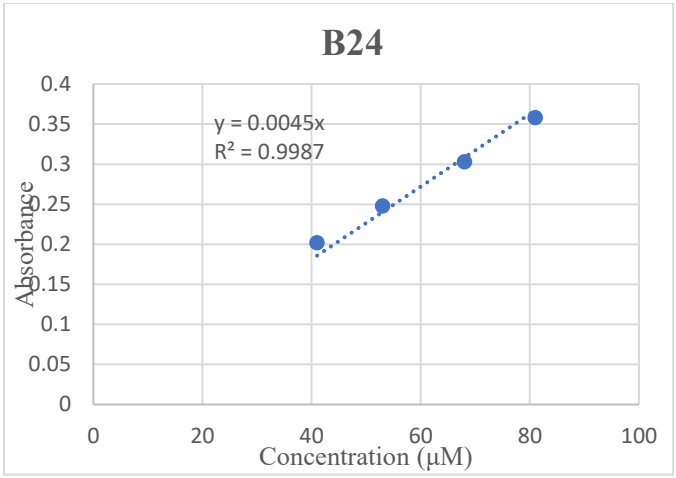

Figure 2.20. Plot of absorbance versus concentration of a solution of **B24** in dichloromethane

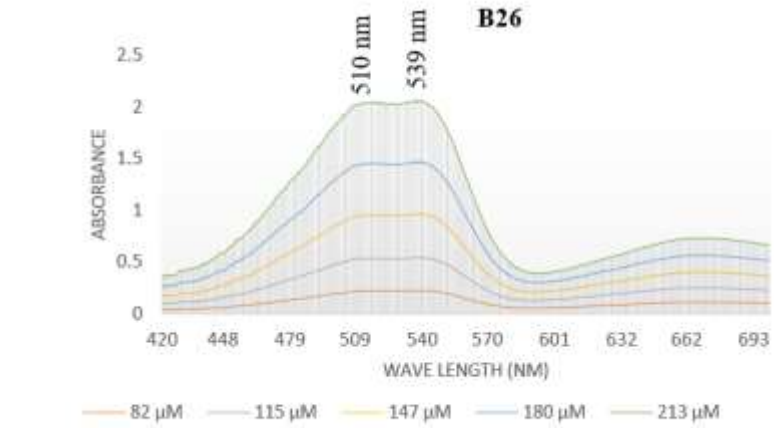

Figure 2.21. UV-Vis absorbance of **B26** in dichloromethane at various concentrations

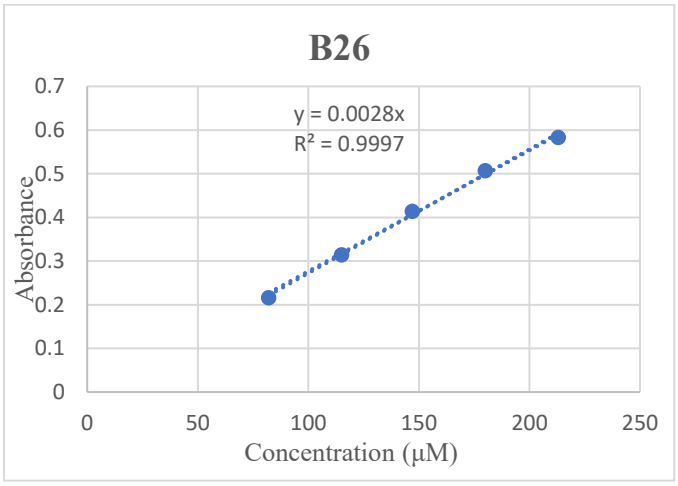

Figure 2.22. Plot of absorbance versus concentration of a solution of **B26** in dichloromethane

2.4. Conclusion

This study reports the synthesis of the two new azobispyrroles **B25** and **B26**. These two new azobispyrroles complement the synthesis of **B23** and **B24** reported previously,[68] albeit in trace amounts for **B25**. This achievement demonstrates the reproducibility of the synthetic route to azobispyrrole from 4-nitrobutanones. Azobispyrrole, **B26** was fully characterized, and **B25** was identified through mass spectrometry supported by characteristic physical properties of polarity and colour.

Future work should focus on obtaining larger amounts of **B23** - **B26** so that a full photochemical evaluation can be completed alongside an evaluation of *E* - *Z* switching behaviors. The synthesis of the methoxy-containing **B25** should be repeated, so that an assessment of the effect of this electron-donating group can be completed alongside potential push-pull effects.

Given that the synthesis of amino diphenylpyrrole (**B7**) was unreliable, future focus should attempt to convert this compound directly into the diazonium salt, enroute to azobispyrroles using the same synthetic strategy as is used for preparation of many bisarylazo compounds. This route (Scheme 2.2) could potentially afford improved yields and a less challenging purification of the desired azo dye contrary to Scheme 2.5 where challenging purification of the azo dyes was faced (**B23**, **B24** and **B26**).

2.5. Experimental

NMR spectra were obtained using a 500 MHz spectrometer or a 300 MHz spectrometer. ^{1}H chemical shifts are reported in ppm relative to tetramethyl silane (0 ppm) using the solvent residuals of $CHCl_3$ (δ = 7.26 ppm) or $CHDCl_2$ (δ = 5.32 ppm) as an internal standard. ^{13}C NMR spectra were recorded using the proton decoupled UDEFT pulse sequence, and chemical shifts are reported in ppm referenced to the $CHCl_3$ (δ = 77.2 ppm) or $CHDCl_2$ (δ = 53.84 ppm) as solvent residuals. Mass spectrometry was performed using a TOF spectrometer operating in ESI+ or APCI mode, as indicated. All chemicals were used as received. Thin layer chromatography was

performed on silica. Experimental parameters for structures reported herein are included in the Appendix.

General procedure 1 (GP1) for B15 – B18

Following a published procedure[65] for the synthesis of aza-BODIPYs, to synthesize the chalcones **B15 - B18**, KOH (84 mmol, 2.5 eq.) was added to a stirring solution of a benzaldehyde (34 mmol, 1 eq.) and acetophenone (34 mmol, 1 eq.) in anhydrous MeOH (25 mL). The reaction mixture was stirred at r.t. for 1 h. The precipitate formed was isolated via filtration, washed with MeOH and cold pentane and then dried under vacuum to afford the desired chalcone.

(E)-1-Phenyl-3-prop-2-en-1-one (B15)

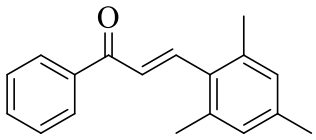

B15

B15 was synthesized by reacting 2,4,6-trimethyl benzaldehyde (5.0 mL, 34 mmol) with acetophenone (4.0 mL, 34 mmol) following GP1 to give **B15** as a light-yellow solid (90% yield, 7.68 g). ^{1}H NMR (500 MHz, DMSO): δ = 8.09 - 8.06 (m, 2H), 7.85 (d, *J* = 15 Hz, 1H), 7.70 - 7.67 (m, 1H), 7.60 - 7.56 (m, 2H), 7.37 (d, *J* = 15 Hz, 1H), 6.98 (s, 2H), 2.37 (s, 6H), 2.27 ppm (s, 3H). Data in accordance with published literature,[65] though a different solvent was used for ^{1}H NMR analysis (DMSO in place of $CDCl_3$)

1-Phenyl-3-(2,6-dichlorophenyl)-prop-2-en-1-one (B16)

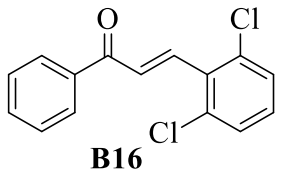

B16

B16 was synthesized by reacting 2,6-dichlorobenzaldehyde (5.0 g, 29 mmol) with acetophenone (3.3 g, 29 mmol) following GP1 to give **B16** as a light-yellow solid (79% yield, 6.35 g). ^{1}H NMR (500 MHz, $CDCl_3$): δ = 8.04 - 8.03 (m, 2H), 7.86 (d, *J* = 16 Hz, 1H), 7.67 (d, *J* = 16 Hz, 1H), 7.61 - 7.59 (m, 1H), 7.52 (t, *J* = 5 Hz, 2H), 7.39 (d, *J* = 10 Hz, 2H) 7.22 - 7.19 ppm (m, 1H). Data in accordance with published literature.[65]

(2E)-3-(4-Methoxyphenyl)-1-phenyl-3-mesityl-prop-2-en-1-one (B17)

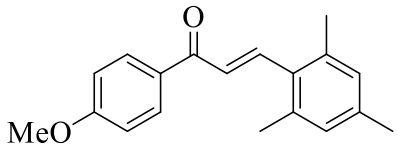

B17

B17 was synthesized by reacting 2,4,6-trimethyl benzaldehyde (3.0 g, 20 mmol) with 4-methoxyacetophenone (3.0 g, 20 mmol) following GP1 to give **B17** as a light-yellow solid (80% yield, 4.49 g). ^{1}H NMR (500 MHz, $CDCl_3$): δ = 8.04 - 8.01 (m, 2H), 7.98 (d, *J* = 15 Hz, 1H), 7.19 (d, *J* = 15 Hz, 1H), 7.00 - 6.97 (m, 2H), 6.93 (s, 2H), 3.88 (s, 3H), 2.41 (s, 6H), 2.31 ppm (s, 3H), data in accordance with published literature.[65]

4-Chloro-1-phenyl-3-(2,6-dichlorophenyl)-prop-2-en-1-one (B18)

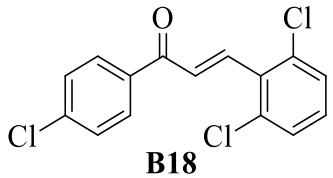

B18

B18 was synthesized by reacting 2,6-dichlorobenzaldehyde (3.0 g, 20 mmol) with 4-chloroacetophenone (3.4 g, 19 mmol) to give **B18** (a novel compound) as a light-yellow-solid (94% yield, 5.56 g). ^{1}H NMR (500 MHz, $CDCl_3$): δ = 7.95 (d, *J* = 5 Hz, 2H), 7.85 (d, *J* = 16 Hz, 1H), 7.61 (d, *J* = 16 Hz, 1H), 7.47 (d, *J* = 10 Hz, 2H), 7.38 (d, *J* = 10 Hz, 2H), 7.21 ppm (t, *J* = 5 Hz, 1H); ^{13}C NMR (125 MHz, $CDCl_3$): δ =196.9, 188.9, 139.6, 138.3, 136.0, 135.2, 132.4, 130.1, 130.0, 129.5, 129.0, 128.8 ppm; HRMS-ESI^{+} (*m/z*); [M + Na^{+}]: calc-d for $C_{15}H_9Cl_3ONa$: 332.9617, found at 332.9609.

General procedure 2 (GP2) for B4 and B19 – B22

Following a published procedure[65] for the synthesis of aza-BODIPYs, with some modifications, to synthesize the nitrobutanone **B4** and **B19** - **B22**, 1,8-diazabicyclo [5.4.0] undec-7-ene (DBU), (99.5 mmol, 5 eq.) and nitromethane (99.5 mmol, 5 eq.) were added to a chalcone (20 mmol, 1 eq.) in anhydrous MeOH (75 mL). The resulting solution was heated at reflux temperature for 1 h, then concentrated under vacuum and purified.

4-Nitro-3-phenyl-1-phenylbutanone (B4)

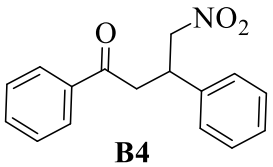

B4

To synthesize **B4**, DBU (18.3 mL, 100 mmol) and nitromethane (7.3 mL, 120 mmol) were added to a methanolic solution of **B3** (5.0 g, 24 mmol) according to GP2. The crude product was purified over silica eluting with 40% dichloromethane/hexane to afford the title compound as a pale-orange solid (87%, 5.6 g). ^{1}H NMR (300 MHz, $CDCl_3$): δ = 7.93 - 7.90 (m, 2H), 7.60 - 7.56 (m, 2H), 7.46 (t, *J* = 3 Hz, 2H), 7.34 (t, *J* =3 Hz, 2H), 7.29 - 7.27 (m, 2H, partially obscured by solvent residual), 4.83 (dd, *J* = 6 Hz, *J* = 3 Hz, 1H), 4.70 (dd, *J* = 3 Hz, *J* = 6 Hz, 1H), 4.23 (quin, *J* = 3 Hz, 1H), 3.51 - 3.41 ppm (m, 2H). Data in accordance with published literature.[65]

4-Nitro-3-mesityl-1-phenylbutanone (B19)

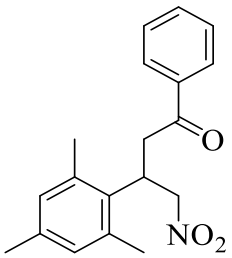

B19

To synthesize **B19**, DBU (15.1 mL, 100 mmol) and nitromethane (6 mL, 100 mmol) were added to a methanolic solution of **B15** (5.0 g, 20 mmol) according to GP2. The crude product was purified over silica column eluting with 40% dichloromethane/hexane to afford **B19** as a pale-orange solid (87%, 5.4 g). ^{1}H NMR (300 MHz, $CDCl_3$): δ = 7.93 - 7.91 (m, 2H), 7.60 - 7.56 (m, 1H), 7.48 - 7.45 (m, 2H), 6.88 (s, 1H), 6.83 (s, 1H), 4.91 - 4.85 (m, 2H), 4.79 - 4.73 (m, 1H), 3.57 - 3.48 (m, *J* = 3 Hz, 2H), 2.45 (s, 6H), 2.24 ppm (s, 3H). Data in accordance to published procedure.[65]

4-Nitro-3-(2,6-dichlorophenyl)-1-phenylbutanone (B20)

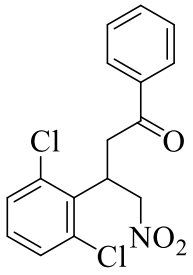

B20

To synthesize **B20**, DBU (13.5 mL, 90 mmol) and nitromethane (4.8 mL, 90 mmol) were added to a methanolic solution of **B16** (5.0 g, 18 mmol) according to GP2. The crude product was purified over silica eluting with 100% chloroform to afford **B20** as a pale-yellow solid (71% yield, 4.3 g). ^{1}H NMR (500 MHz, $CDCl_3$) δ = 7.95 - 7.93 (m, 2H), 7.59 - 7.55 (m, 1H), 7.45 (t, *J* = 5 Hz, 2H), 7.37 (d, *J* = 10 Hz, 1H), 7.28 (d, *J* = 10 Hz, 1H), 7.14 (t, *J* = 5 Hz, 1H), 5.34 - 5.28 (m, 1H), 5.07 (dd, *J* = 10 Hz, *J* = 10 Hz, 1H), 4.98 (dd, *J* = 5 Hz, *J* = 10 Hz, 1H), 3.76 - 3.65 ppm (m, 2H). Data in accordance to published data.[65]

4-Nitro-3-mesityl-1-(4-methoxyphenyl) butanone (B21)

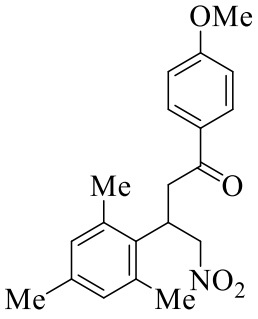

B21

To synthesize **B21**, DBU (7.9 mL, 52 mmol) and nitromethane (3.2 mL, 52 mmol) were added to a methanolic solution of **B17** (3.0 g, 10 mmol) according to GP2. The crude product was purified over silica eluting with 100% ethyl ether to afford **B21** as a dark orange oil (88% yield, 3.0 g). ^{1}H NMR (300 MHz, $CDCl_3$): δ = 7.92 - 7.87 (m, 2H), 6.95 - 6.90 (m, 2H), 6.84 (s, 1H), 6.82 (s, 1H), 4.93 - 4.73 (m, 3H), 3.87 (s, 3H), 3.47 - 3.43 (m, 2H), 2.44 (s, 6H), 2.23 ppm (s, 3H). Data in accordance to published procedure.[65]

4-Nitro-3-(2,6-dichlorophenyl)-4-chloro--1-phenylbutanone (B22)

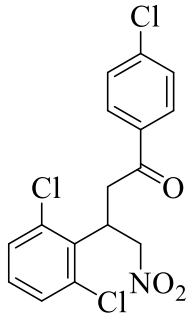

B22

To synthesize **B22**, DBU (12 mL, 80 mmol) and nitromethane (5 mL, 80 mmol) were added to a methanolic solution of **B18** (5.0 g, 16 mmol) according to GP2. The crude product was purified over silica eluting with 100% chloroform to afford **B22**, a novel compound, as a yellow oil (52% yield, 3.1 g). ^{1}H NMR (300 MHz, $CDCl_3$) δ = 7.87 - 7.81 (m, 2H), 7.42 - 7.37 (m, 2H), 7.34 (d, J = 9 Hz, 1H), 7.22 (d, J = 6 Hz, 1H), 7.12 (t, J = 6 Hz, 1H), 5.25 (quin, J = 6 Hz, 1H), 5.03 - 4.89 (m, 2H), 3.64 ppm (d, J = 9 Hz, 2H).^{13}C NMR (300 MHz, $CDCl_3$) δ = 195.4, 140.2, 137.1, 134.5, 134.2, 130.1, 129.5, 129.4, 129.4, 129.1, 76.36, 39.0, 35.4 ppm, missing 1 carbon signal in the aliphatic region. HRMS-ESI^{+} (m/z): [M + Na^{+}] calc-d for $C_{16}H_{12}Cl_3NO_3Na$: 393.9781; found 393.9774.

General synthetic procedure 3 (GP3) for B23 -B26

Following a published procedure[65] for the synthesis of aza-BODIPYs, with some modifications, to synthesize compound **B23** - **B26**, the requisite nitro butanone (0.79 mmol, 1 eq.) and ammonium acetate (33.4 mmol, 42 eq.) were dissolved in glacial acetic acid (5 mL) and the resulting solution pre-stirred at room temperature and then heated under microwave irradiation (20 mins, 118℃, 100 W). The reaction mixture was transferred into a separatory flask, water (100 mL) was added, and the mixture extracted into dichloromethane (3 x 50 mL). The organic layers were combined and washed with brine (50 mL), and the organic phase dried over anhydrous sodium sulfate. Solvent was removed in vacuo and the crude product purified on silica.

Bis(3(1,3,5-trimethylphenyl))-5-diphenylpyrrole-2-azo (B23)

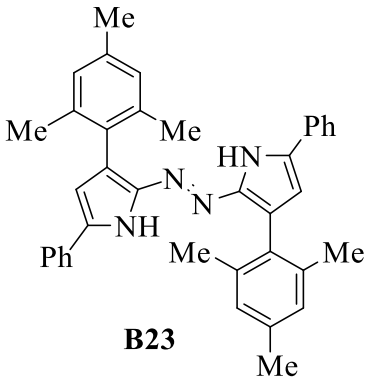

B23

To synthesize **B23**, **B19** (250 mg, 0.80 mmol) and ammonium acetate (2.6 g, 33 mmol) were dissolved in glacial acetic acid (5 mL). The crude product was purified eluting with a gradient of dichloromethane/hexanes (40% - 80% dichloromethane) to give **B23** as a bright red solid. The solid was again dissolved in minimal dichloromethane and cold pentane at 0℃ was added to form a precipitate. This was allowed to rest in the fridge overnight and then the solid was isolated via filtration to yield **B23** as bright red crystals (31 mg, 14%). ^{1}H NMR (500 MHz, $CDCl_3$) δ = 9.36 (br s, 2H), 7.52 (d, *J* = 10 Hz, 4H), 7.37 (t, *J* = 5 Hz, 4H), 7.28 - 7.23 (m, 2H partially obscured by solvent residual), 7.00 (s, 4H), 6.50 (s, 2H), 2.39 (s, 6H), 2.22 ppm (s, 12H). ^{13}C NMR (125 MHz, $CDCl_3$) δ = 142.9, 137.8, 136.7, 133.5, 131.3, 131.3, 128.9, 128.0, 127.6, 127.4, 124.4, 110.7,

21.2, 21.1 ppm. HRMS-ESI$^+$ (*m/z*): [M + Na$^+$] calc-d for $C_{38}H_{36}N_4Na$: 571.2832; found 571.2855. λabs (Dichloromethane) 322 nm, 345 nm, ε = 20,700 $M^{-1}cm^{-1}$, λ = 530 nm

Bis(3(2,6-dichlorophenyl))-5-diphenylpyrrole-2-azo (B24)

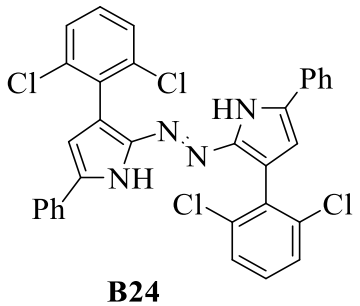

B24

To synthesize **B24**, **B20** (250 mg, 0.74 mmol) and ammonium acetate (2.4 g, 31 mmol) were dissolved in glacial acetic acid (5 mL) according to GP3. The crude product was purified eluting with ethyl acetate/hexanes (10% ethyl acetate) to give **B24** as a bright red solid. The solid was again dissolved in minimal dichloromethane and cold pentane at 0°C was added to form a precipitate. **B24** was isolated as a bright red crystal (31 mg, 14% yield). ^{1}H NMR (500 MHz, $CDCl_3$) δ = 9.40 (br s, 2H), 7.54 (d, *J* = 10 Hz, 4H), 7.46 - 7.36 (m, 8H), 7.28 - 7.23 (m, 4H), 6.67 ppm (br s, 2H). ^{13}C NMR (125 MHz, $CDCl_3$) δ = 142.8, 136.4, 133.7, 133.1, 131.0, 129.1, 129.0, 128.0, 127.7, 124.5, 123.3, 110.9 ppm. HRMS-ESI+ (*m/z*): [M +H]$^+$ calc-d for $C_{32}H_{20}Cl_4N_4$: 601.0515; found 601.0500. λabs (Dichloromethane) 509 nm, 534 nm, 668 nm, ε = 4,500 $M^{-1}cm^{-1}$, λ = 530 nm.

Bis(3(4-methoxyphenyl)-5-(1,3,5-trimethylphenyl)-diphenylpyrrole-2-azo (B25)

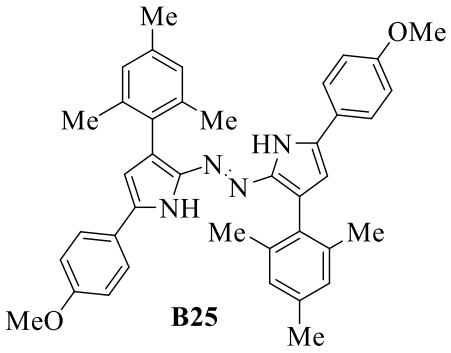

B25

To synthesize **B25**, **B21** (250 mg, 0.80 mmol) and ammonium acetate (2.6 g, 35 mmol) were dissolved in glacial acetic acid (5 mL). The crude product was purified eluting with a gradient of dichloromethane/hexanes (40% dichloromethane) to give **B25** as a bright red solid. The solid was again dissolved in minimal dichloromethane and cold pentane at 0°C was added to form a precipitate. **B25** was obtained as a pale red solid (trace amount). LRMS-ESI+ (*m/z*): [M +H] found 608.3.

Bis(3(4-chlorophenyl))-5-(2,6-dichlorophenyl)-diphenylpyrrole-2-azo (B26)

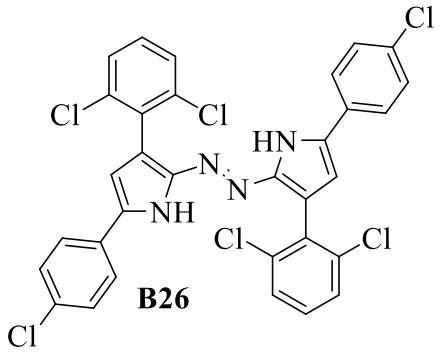

B26

To synthesize **B26**, **B22** (250 mg, 0.67 mmol) and ammonium acetate (2.2 g, 28 mmol) were dissolved in glacial acetic acid (5 mL). The crude product was purified eluting with a gradient of ethyl acetate/hexanes (10% dichloromethane) to give **B26** as a bright red solid. The solid was again dissolved in minimal dichloromethane and cold pentane at 0°C was added to form a precipitate. **B26** was obtained as a bright red crystal (10 mg, 4%). ^{1}H NMR (500 MHz, DMSO) δ = 11.00 (br

s, 2H), 7.81 (d, J = 10 Hz, 4H), 7.45 (d, J = 10 Hz, 4H), 7.35 - 7.32 (m, 4H), 7.30 - 7.28 (m, 2H), 6.73 ppm (app d, J = 5 Hz, 2H). ^{13}C NMR (125 MHz, $(CD_3)_2CO$) δ = 143.9, 135.7, 133.5, 132.8, 132.3, 130.3, 129.2, 128.9, 127.6, 126.1, 110.9 ppm (one signal not observed). HRMS-ESI+ (*m/z*): $[M+H]^+$ calc-d for $C_{32}H_{18}Cl_6N_4$: 668.9735; found 668.9727. λabs (Dichloromethane) 510 nm, 539 nm, 662 nm, ε = 2,800 $M^{-1}cm^{-1}$, λ = 530 nm

2,4-Diphenyl pyrrole (B5)

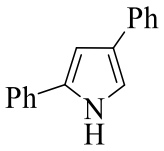

B5

B5 was synthesized following a published procedure[64] with some modification as regards the purification method used. A stirred suspension of **B4** (2.0 g, 7.2 mmol) in MeOH (20 mL) was treated at rt with a solution of KOH (2.1 g, 37 mmol) in MeOH (20 mL). After 1 h, the colourless solution was added dropwise to a solution of concentrated H_2SO_4 (15.2 mL) in MeOH (80 mL) at 0 °C, following which the solution was allowed to warm to rt and stirred for a further 1 h. Water (180 mL) and ice (180 g) were added, and the mixture was neutralized to pH 7 with aqueous 4 M NaOH. The stirred mixture produced a white solid which was isolated via filtration. The solid was washed with water, dried, and used for the following step without further purification. The solid was dissolved in acetic acid (36 mL), and NH_4OAc (1.4 g) was added. The mixture was heated at 100 °C for 1 h, cooled to rt, poured into ice (400 g), and neutralized to pH 7 with 4 M NaOH. The precipitate was isolated via filtration, then washed with water, and dried to give a pink solid. To purify the pink solid, it was dissolved in minimal dichloromethane and cold pentane at 0°C was added to form a precipitate which was isolated via filtration to yield **B5** as a white solid (0.79 g, 50%): ^{1}H NMR (500 MHz, $CDCl_3$) δ = 8.44 (br s, 1H), 7.59 - 7.57 (m, 2H), 7.54 - 7.51 (m, 2H), 7.38 (app quin, J = 5 Hz, 4H), 7.24 - 7.19 (m, 2H), 7.15 (s, 1H), 6.84 - 6.83 ppm (m, 1H). Data in accordance with literature.[64]

2-Nitroso-3,5-diphenyl pyrrole (B6)

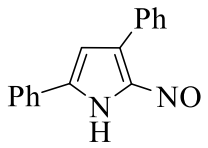

B6

B6 was synthesized following a published procedure,[64] with some modification with regards to the purification method used. To a stirred solution of **B5** (300 mg, 1.36 mmol) in EtOH (14 mL) was added concentrated HCl (260 µL), followed by a dropwise addition of aq $NaNO_2$ (1.15 eq., 1.56 mmol, 108 mg, in 2.6 mL of H_2O). The solution was stirred for 30 min and then cooled to 0 °C, and another portion of concentrated HCl (1.34 mL) was added. The solution was stirred for 1 h, and the resulting red solid was collected by filtration and washed with Et_2O. The solid was dissolved in minimal EtOH, an excess of aq NaOAc and ice was added, and the solution was stirred for 1 h. The resulting solid was collected by filtration, washed with water, and dried. To purify the green solid, it was dissolved in minimal dichloromethane. Cold pentane was then added to form a precipitate which was isolated vis filtration to yield **B6** as a green solid (270 mg, 80%): ^{1}H NMR (500 MHz, $CDCl_3$) δ = 8.20 - 8.17 (m, 2H), 7.85 - 7.80 (m, 2H), 7.52 - 7.45 (m, 6H), 7.15 ppm (s, 1H), N-H peak not observed for this compound. Data in accordance with literature.[64]

4-Amino-3,5-diphenyl pyrrole (B7)

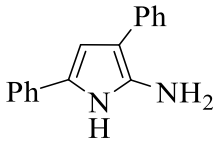

B7

B7 was synthesized following a modified procedure, **B6** (150 mg, 0.6 mmol) was placed in a two-neck RBF, then purged with nitrogen (3 times). Anhydrous MeOH (17 mL) and Pd/C (3 mg, 0.03 mmol) were added, and three rounds of vacuum/nitrogen purge cycles were done. A balloon filled

with hydrogen was then fixed onto the RBF and the reaction atmosphere was gradually changed to 1 atm hydrogen via three nitrogen/vacuum-hydrogen cycles. The reaction mixture was stirred for 15 mins. After 15 mins the reaction atmosphere was changed to nitrogen and the reaction mixture was taken to the glove box and filtered over a thick pad of celite. The solvent was then removed to yield **B7** as a grey-like solid (112 mg, 80%). M.P.: 144 - 145 °C (decomp). ^{1}H NMR (500 MHz, $CDCl_3$) δ = 8.12 (br s, 1H, NH), 7.75 - 7.00 (m, 10H), 6.57 (s, 1H), 3.56 ppm (s, 2H, NH_2 partially obscured with residual methanol). Data in accordance with literature.[64]

4-Aminoazobenzene (B12)

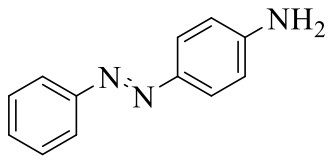

B12

B12 was synthesized following a published procedure,[67] **B10** (0.92 g, 10 mmol) was added dropwise to a solution of concentrated HCl (37%, 3 mL) in distilled water (30 mL). The mixture was stirred in an ice bath to keep the reaction temperature at 0 ~ 5 °C. Then a solution of sodium nitrite (0.70 g, 10 mmol) in water (5 mL) was added slowly over 10 min. The mixture was stirred at 0 ~ 5 °C for a further 60 min. A blue diazonium salt solution was obtained. A coupling solution was prepared as follows: **B10** (0.92 g, 10 mmol) and HCl (1 M, 10 mL) was dissolved in 30 mL of water under vigorous stirring at 0 ~ 5 °C. Then the diazonium salt solution was added dropwise to the coupling solution at 0 ~ 5 °C, and the mixture then stirred at this for 3 h. Then the final solution was added slowly to 1M NH_3 (30 mL) to form a brown precipitate. The precipitate was isolated via filtration and washed with a small amount of aq sodium hydrogen carbonate (pH = 8). The precipitate was collected by filtration, washed with distilled water (X 3), and dried under vacuum to yield **B12** as a burnt orange solid (0.69 g, 33%). ^{1}H NMR (500 MHz, $CDCl_3$) δ = 7.85 - 7.50 (m, 4H), 7.49 (t, *J* = 5 Hz, 2H), 7.41 (t, *J* = 5 Hz, 1H), 6.74 (d, *J* = 10 Hz, 2H), 4.03 ppm (s, 2H). Data in accordance with literature.[67]

Phenylazodiphenylpyrrole (B13)

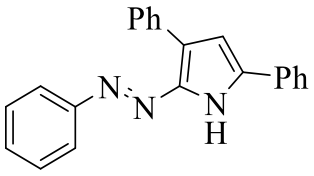

B13

B13 was synthesized following a published procedure,[67] **B10** (0.31 mg, 3.33 mmol) was added dropwise to a solution of concentrated HCl (37%, 1 mL) in distilled water (3 mL). The mixture was stirred in an ice bath to keep the reaction temperature at 0 ~ 5 °C. Then a solution of sodium nitrite (21 mg, 3.33 mmol) in water (1.67 mL) was added slowly over 10 min. The mixture was stirred at 0 ~ 5 °C for further 60 min. A blue transparent diazonium salt solution was obtained. A coupling solution was prepared as follows: **B5** (0.73, 3.33 mmol) and HCl (1 M, 3.3 mL) was dissolved in 3 mL of water under vigorous stirring at 0 ~ 5 °C. Then the diazonium salt solution was added dropwise to the coupling solution at 0 ~ 5 °C, then stirred at 0 ~ 5 °C for 3 h. Then the final solution was added slowly to 1M NH_3 (3.3 mL) to form a brown precipitate. The precipitate was isolated via filtration and washed with a small amount of aq sodium hydrogen carbonate (pH = 8). The precipitate was collected by filtration, washed with distilled water three times, and dried under vacuum to yield **B13** as a bright orange solid (50 mg, 46%). ^{1}H NMR (500 MHz, $CDCl_3$) δ = 9.56 (br s, 1H, isomer **A**), 8.45 (br s, 1H, isomer **B**), 8.04 - 8.00 (m, 2H, isomer **A**), 7.89 - 7.85 (m, 2H, isomer **A**), 7.73 - 7.67 (m, 2H, isomer **A**), 7.60 - 7.13 (m, 9H for isomer **A** plus 15H for isomer **B**), 6.97 (s, 1H, isomer **A**), 6.84 (s, 1H, isomer **B**) with isomers **A** and **B** being present in an approximate 2:1 ratio in this isolated mixture ppm. HRMS-ESI$^+$ (*m/z*) calcd for $C_{17}H_{18}N_3$ $[M]^+$ 323.1413, found 324.1418. Analysis of the corresponding ^{1}H NMR spectrum indicate an inseparable mixture of both the cis (*Z*) and trans (*E*) isomer of phenylazopyrrole and these *Z* and *E* isomers could either be isomer **A** or **B**.

Chapter 3 Attempts towards the synthesis of *F*-BODIPYs using a stoichiometric amount of dipyrrin and $BF_3{\cdot}OEt_2$ in a continuous flow operation.

3.1. Introduction

Dipyrrins formally consist of two pyrrolic units which are connected through a methine, *CH*, bridge. Coordination of dipyrrins to a variety of metals has been reported, with the most prominent type of dipyrrinato complex featuring coordination of the ligand framework to a $-BF_2$ unit to create a 4,4-difluoro-4-bora-3*a*,4*a*-diaza-*s*-indacene (*F*-BODIPY, Figure 3.1).[68,69]

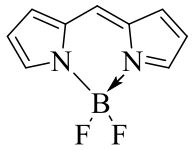

Figure 3.1. Structure of the *F*-BODIPY core

F-BODIPYs are generally chemically robust, as well as thermally, photochemically and physiologically stable. Structural variations to the pyrrolic and methine (meso) positions have enabled fine-tuning of photophysical and electrochemical properties.[70] This has supported their utility as dyes for fluorescence imaging of natural macromolecules such as proteins and DNA.[71] Furthermore *F*-BODIPYs have shown utility as charge transporting units in electronic devices, such as transistors and solar cells, and as light-triggered catalysts for the synthesis and degradation of polymers.[72]

The synthesis of *F*-BODIPYs is traditionally performed by reacting a dipyrrin with an excess amount of a base (typically NEt_3) and excess $BF_3{\cdot}OEt_2$. These reagents have been used for several decades, including in the first reported synthesis of an *F*-BODIPY by Treibs and Krauzer in 1968.[73] Treatment of a dipyrrin with 6 eq. of NEt_3 and 9 eq. of $BF_3{\cdot}OEt_2$ in an anhydrous solvent gives *F*-BODIPYs in yields generally greater than 70%.[74] However, the use of these large excesses of reactants gives rise to the formation of the unwanted $BF_3{\cdot}NEt_3$ by-product. The presence of this

by-product often makes isolation and purification difficult and can result in significant reduction in yields of the desired BODIPY product. This observation is particularly seen when working on a large scale (Scheme 3.1, method **A**). Other approaches such as those shown in **B, C** and **D** (Scheme 3.1) have been reported but these require either the use of excess amounts of reactants or the use of strictly anhydrous conditions, thus making all approaches environmentally and economically undesirable, as well as sometimes challenging in terms of product isolation and purification.

Indeed, one method uses 1 eq. LiHMDS and 1 eq. of $BF_3{\cdot}OEt_2$ under anhydrous conditions (Scheme 3.1**B**).[75] Recent work has shown that the requirement for anhydrous conditions can be averted via the addition of a second aliquot of excess amine and $BF_3{\cdot}OEt_2$ (Scheme 3.1**C**).

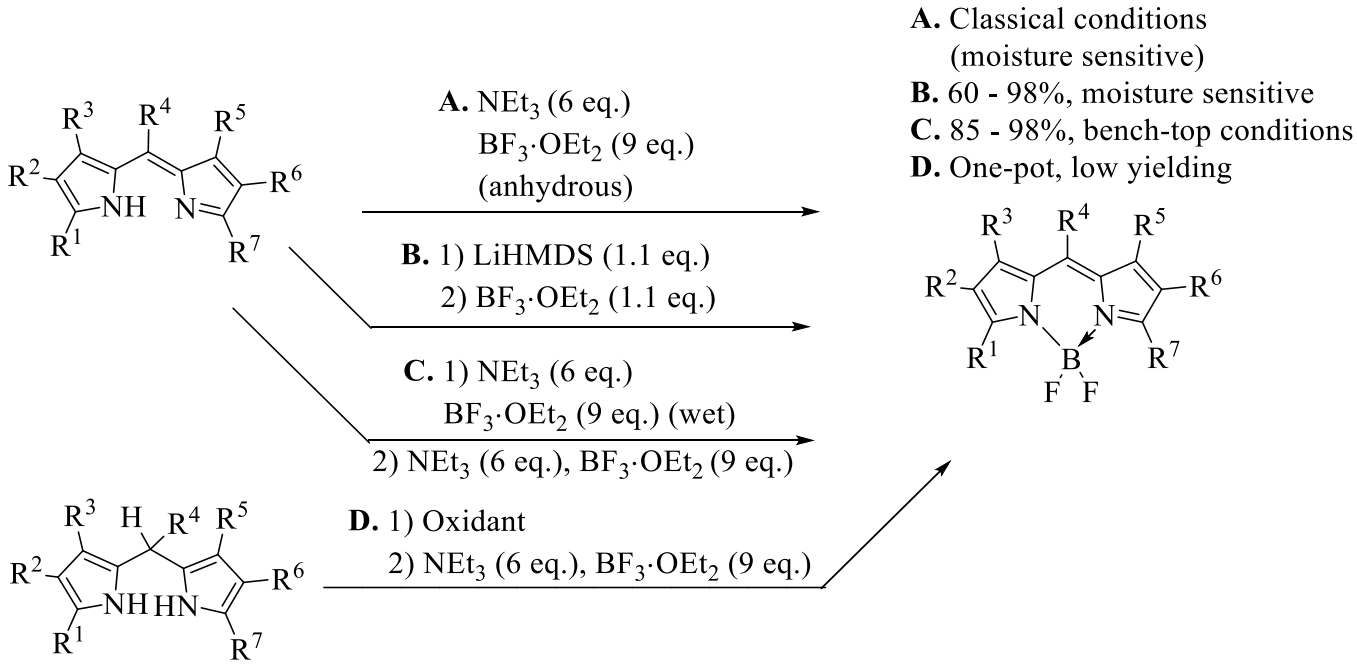

Scheme 3.1. Approaches to the synthesis of *F*-BODIPYs

F-BODIPYs can also be generated via the one-pot conversion of dipyrromethanes (Scheme 3.1.**D**).[76] This method involves the one-pot oxidation of dipyrromethanes to generate the dipyrrin,

followed by the addition of $BF_3{\cdot}OEt_2$. This in situ oxidation and complexation avoids the need to purify synthetic intermediates, although can be low yielding in terms of trapping dipyrrins as their boron complex.

These challenges, including difficult purification procedures and often low yields for the one-pot approaches, showcase the need to develop a new synthetic approach to *F*-BODIPYs that is high yielding and equally environmentally acceptable through minimized use of reagents. Work reported by Dr. Groves in his PhD[77] work with the Thompson group explored the addition of just 1 eq. of $BF_3{\cdot}OEt_2$ to free-base dipyrrin, in the absence of the base, and reported the formation of the desired *F*-BODIPY and the HBF_4 salt of dipyrrin in 49% and 42% isolated yields, respectively (Figure 3.2).

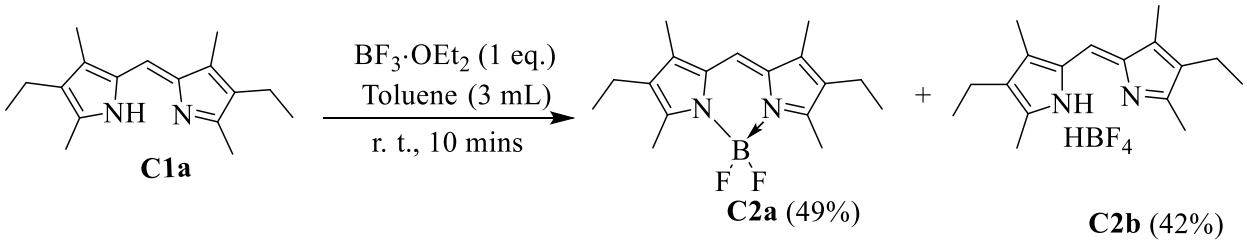

Figure 3.2. Addition of $BF_3{\cdot}OEt_2$ (1 eq.) to free-base **C1a** in toluene

The formation of *F*-BODIPYs through the use of 1 eq. of $BF_3{\cdot}OEt_2$, in the absence of a base is appealing. Although the yield of the *F*-BODIPY is lower than that achieved using some other approaches, these preliminary investigations offer a rationale for the synthetic work described in this chapter. While this new methodology represents a highly atom economic use of the $BF_3{\cdot}OEt_2$, ,the formation of the unwanted HBF_4 salt needs to be addressed in order for higher yields of the desired *F*-BODIPY to be attained (Figure 3.2).

In the synthesis of *F*-BODIPYs as shown in Figure 3.2, the ligation of the free-base dipyrrin to $BF_3{\cdot}OEt_2$ formally liberates fluoride ion (F^-). This anion readily binds with the unreacted $BF_3{\cdot}OEt_2$, generating anionic BF_4^-, and thus enabling the HBF_4 dipyrrin salts to form. This results from the greater affinity of BF_3 for fluoride ion than for the free-base dipyrrin, and it makes

$BF_3{\cdot}OEt_2$ unavailable to react with the remaining free-base dipyrrin. Instead, the unwanted dipyrrin HBF_4 salt is formed and *F*-BODIPY yield is capped at a maximum of 50%.

There is, therefore, a need to minimize interaction between the HF (H^+ and fluoride) formally produced and the unreacted $BF_3{\cdot}OEt_2$. This need encouraged us to explore the use of a continuous flow process for this transformation, with the goal of minimizing dipyrrin HBF_4 salt formation and thus maximizing *F*-BODIPY formation. The essential goal was to prevent the produced fluoride from interacting with the as-yet unreacted $BF_3{\cdot}OEt_2$.

3.2. Flow Chemistry

Bench, or conventional, conditions are used in classical organic transformations. These reaction system set-ups typically include the use of round-bottom flasks, stir bars, and oil or sand baths for heating. Reactions performed in this fashion might lack uniform mixing and efficient heat transfer and therefore suffer from sub-optimal yields. Undesired by-products can often form from this one-pot set-up because of possible interaction between by-product, starting materials and/or reagent. As a result, the organic synthesis community has sought viable alternatives to classical methodologies that improve in these areas of focus. Continuous flow chemistry has been investigated over the past few decades as a potential solution. "Continuous flow"[78] or "flow chemistry" involves performing chemical reactions in a tube or a pipe. In continuous chemistry, reagents are continuously pumped through different streams, combined, the resulting mixture passed through a reactor coil, i.e., tube or pipe, and the product continuously collected downstream (Figure 3.3). There is, therefore, no interaction between the incoming reagents and the products formed downstream.

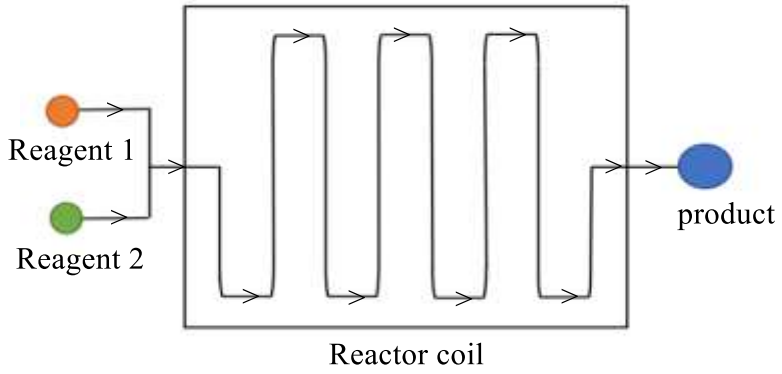

Figure 3.3. A schematic of a simple continuous flow set-up

Flow chemistry enables control of reaction parameters such as heat transfer, mass transfer, mixing and residence times, all with the potential to lead to improved efficiency compared with equivalent reactions performed via batch method. The residence time refers to the duration between mixing of reagent and quenching downstream. Residence time is dependant upon the flow rate applied and the volume of the reactor tubing.

Residence time (tR) is calculated using the following equation, where a 30 cm reactor tube of diameter 0.05 cm is used.

$$\text{Residence time} = \text{Reactor Volume/Flow Rate}$$

$$\text{Reactor volume} = \text{Cross section X Length of tubing} = \pi r^2 L$$

$$= 3.1416\ (0.05\ \text{cm})^2 \text{ X } 30\ \text{cm}$$

$$= 0.236\ \text{cm}^3$$

3.3. Project Goals

This project aims to develop a new method for the synthesis of *F*-BODIPYs using a continuous flow process that uses 1 eq. of $BF_3{\cdot}OEt_2$ and ideally minimizes the use of a base. This method will ideally increase the availability of $BF_3{\cdot}OEt_2$ for reaction with the free-base dipyrrin, thus potentially increasing the yield of the desired *F*-BODIPY product. The use of 1 eq. $BF_3{\cdot}OEt_2$ in the absence of NEt_3 will avert the production of Lewis adducts such as $BF_3.NEt_3$, thereby enhancing purification procedures and product yields. The hypothesis was that the use of flow chemistry i.e., pumping the dipyrrin and the $BF_3{\cdot}OEt_2$ into the reaction tube through different streams, would lead to mixing at the common point and formation of the *F*-BODIPY instantly. Therefore, the fluoride and proton (HF) by-products formally produced would be continuously pumped downstream of the incoming $BF_3{\cdot}OEt_2$ and thus dipyrrin HBF_4 salt production will be minimized. Protonation of the free-base dipyrrin inhibits reaction of the dipyrrin with the $BF_3{\cdot}OEt_2$. Furthermore, BF_4^- anion formation removes $BF_3{\cdot}OEt_2$ from the reaction mixture. Both processes are detrimental to *F*-BODIPY yield greater than 50% and so both should be restricted. Exploring methods by which to restrict these processes are at the heart of this part of this Master thesis.

3.4. Results and Discussion

In the Thompson group we have access to an extensive library of free-base dipyrrins and their HBr salts. Since the goal of this current work was to develop a new method for the synthesis of *F*-BODIPYs, using a continuous flow process, this library provided a wide substrate scope via which to approach this goal. Prior to performing the synthesis of an *F*-BODIPY using flow chemistry, there was need to understand the synthesis using the batch method (Figure 3.4). To do this, compound **C1a** was selected as substrate, and to serve as a reference for comparison for the reaction in flow chemistry. In order to have a good stock of **C1a** for the different series of reactions there was need to synthesize more, and this is discussed herein.

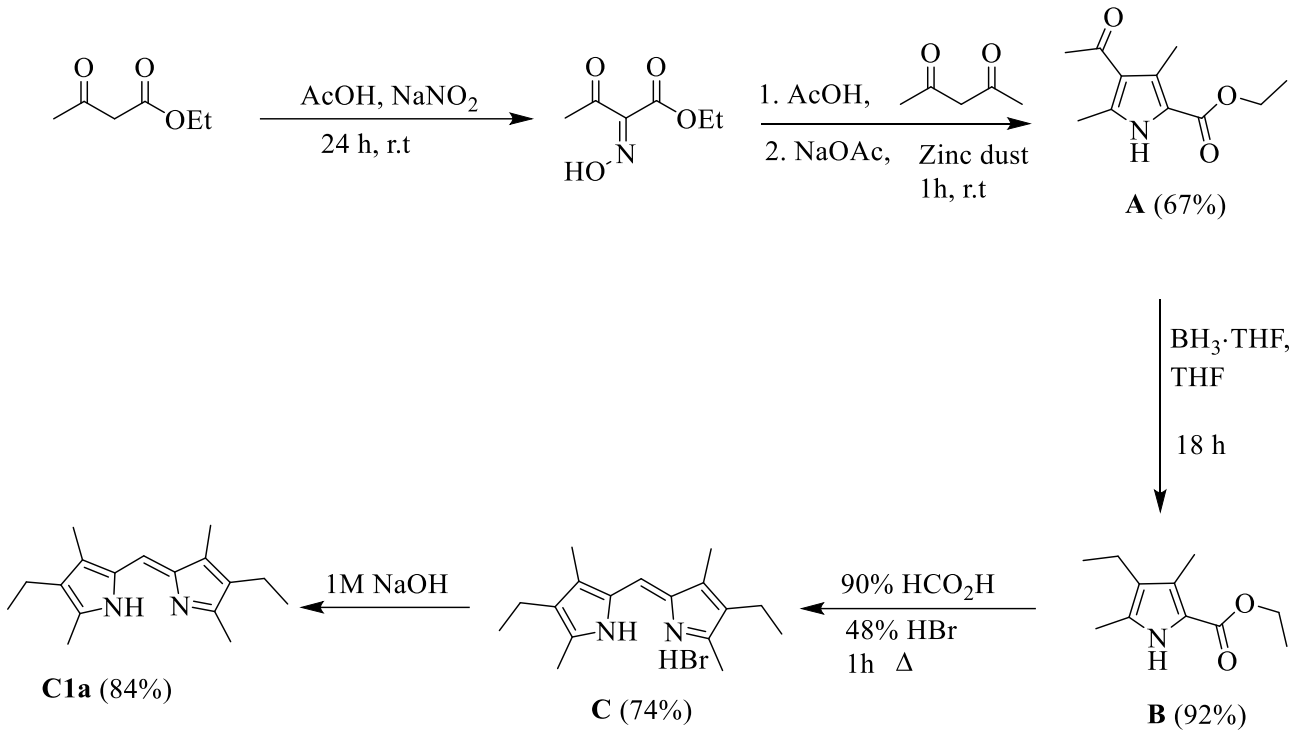

Scheme 3.2. A scheme for the synthesis of 3-ethy1-5-[(4-ethy1-3,5-dimethyl-2H-pyrrol-2-ylidene) methyl]-2,4-dimethyl-1H-pyrrole **C1a**

Following a published procedure[72] for the synthesis of ethyl ester 4-acetyl-3,5-dimethy1-1H-pyrrole-2-carboxylic acid (**A**) (Scheme 3.2), ethyl acetoacetate was treated with aq sodium nitrite at 0℃ in an acidic medium. This reaction mixture was allowed to slowly warm up to room temperature and stirred for 24 h. After 24 h, the reaction mixture containing the oxime was transferred to a dropping funnel. In another 3-neck flask, to a solution of pentane-2,4-dione in acetic acid was added anhydrous sodium carbonate with stirring. The dropping funnel containing the oxime was placed on the left-most neck of the 3-necked flask and its contents (oxime) added dropwise, with stirring, while zinc dust was also slowly added via the right-most neck of the flask, making sure that all zinc dust became miscible before the next amount was added. Th central neck of the 3-necked flask was used for an overhead stirrer, given that this reaction was conducted on 55 mmol scale. After this time, the mixture was allowed to cool to room temperature, diluted with H_2O and then allowed to stand at room temperature overnight. The following morning, the reaction

mixture was filtered. The isolated white solid was washed with excess water to remove all possible acetic acid, followed by an excess of hexane to remove all hexane-soluble impurities. The white solid was then dissolved in CH_2Cl_2, and the solution filtered (this removes any remaining zinc dust from the white solid). The filtrate was then dried over Na_2SO_4, and the resulting solution concentrated in vacuo to give the final compound (**A**) as a white solid in 67% in accordance with literature.[72]

Following a published procedure[79] for the synthesis of ethyl ester 4-ethyl-3,5-dimethyl-1H-pyrrole-2-carboxylic acid (**B**) (Scheme 3.2), ethyl-4-acetyl-3,5-dimethy1-1H-pyrrole-2-carboxylic acid (**A**) was treated with BH_3·THF in a drop-wise manner with stirring for 18 h under a nitrogen environment. The reaction mixture was then quenched by slowly adding water and 5% aqueous HCl, with stirring at room temperature for 30 mins. A basic workup was then carried out on the reaction mixture which was then extracted with EtOAc three times. The combined organic fractions were washed with saturated aqueous $NaHCO_3$ and brine, dried over Na_2SO_4, then concentrated in vacuo to give as a white solid (**B**), 92% in accordance with literature.[79] Following a published procedure[79] for the synthesis of the dipyrrin salt 3-ethy1-5-[(4-ethy1-3,5-dimethyl-2H-pyrrol-2-ylidene) methyl]-2,4-dimethyl-1H-pyrrole monohydrobromide (**C**) (Scheme 3.2), ethyl ester 4-ethyl-3,5-dimethyl-1H-pyrrole-2-carboxylic acid was treated with 48% HBr with stirring at reflux temperature for 1 h. The reaction mixture was then allowed to cool to room temperature and then refrigerated for 2h. The resulting precipitate was isolated via filtration, washed with ether and then dried at room temperature in air to give **C** as a dark-red crystalline solid in 74% in accordance with literature.[79]

Following a published procedure[77] for the synthesis of 3-ethy1-5-[(4-ethy1-3,5-dimethyl-2H-pyrrol-2-ylidene)methyl]-2,4-dimethyl-1H-pyrrole (**C1a**) (Scheme 3.2), the hydrobromide salt 3-ethy1-5-[(4-ethy1-3,5-dimethyl-2H-pyrrol-2-ylidene)methyl]-2,4-dimethyl-1H-pyrrole monohydrobromide was dissolved in CH_2Cl_2 and washed with aqueous 1M NaOH three times. The organic layer was then dried over anhydrous Na_2SO_4, and the solvent removed to yield dipyrrin **C1a** as a brown, crystalline solid 84%.[77]

With **C1a** in hand it was time the carry out the reaction as shown in Figure 3.4. For this reaction, 50 mg of dipyrrin **C1a** was dissolved in 3 mL of anhydrous toluene under a nitrogen atmosphere, and 1 eq. of BF_3·$OEt_2$was added with stirring. A rapid yellow-to-red colour change was observed,

as was the formation of a precipitate as the reaction was stirred for 10 mins. The reaction was quenched in the usual way for *F*-BODIPYs,[80] i.e., the crude reaction mixture was quenched by the addition of H_2O followed by extraction with CH_2Cl_2 (3 times). The combined organic fractions were then washed with aqueous $NaHCO_3$ (3 times), resulting in dissolution of the precipitate in the organic layer which was then dried over Na_2SO_4. Following purification over basic alumina, *F*-BODIPY **C2a** was afforded in a 44% yield as a red solid, and the dipyrrin HBF_4 salt was isolated in 38% yield as a bright orange solid. The yields recorded for this reaction aligned with those reported by Dr. Groves during his PhD studies with the Thompson Group.[77]

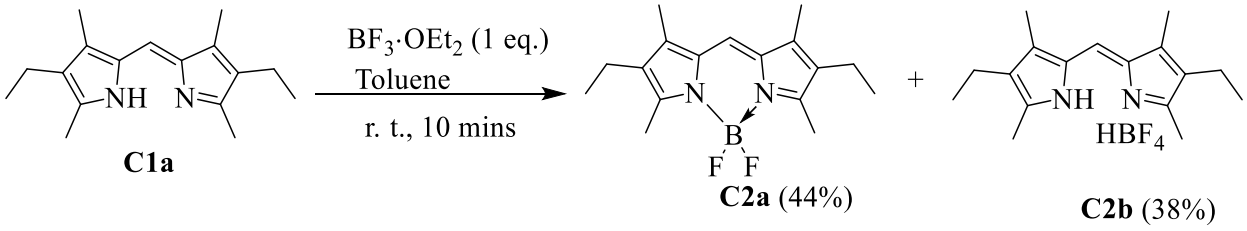

Figure 3.4. Addition of $BF_3{\cdot}OEt_2$ (1 eq.) to free-base **C1a** in toluene

With the results for this synthesis using the traditional batch method in hand, focus moved to developing the flow chemistry method. Firstly, to maximize efficiency, a facile and accurate method for determining yields was adopted. This analytical method was developed by Dr. Michael Beh during his PhD studies with the Thompson group.[81] Dr Beh's method involves using ^{1}H NMR spectroscopic analysis of the crude reaction mixture, thus avoiding the need to isolate the *F*-BODIPY resulting from each trial.[82] Given the practicality of this method, it was adopted for the work described herein. Avoiding the need for work-up and isolation of the *F*-BODIPY after each trial helped save time and allowed for simultaneous reactions to be conducted, thus maximizing the number of trials completed in a short amount of time.

As a reference and as preparation for comparison to the reaction in flow chemistry, the above batch (Figure 3.4) reaction was repeated three times and monitored. To a toluene solution of **C1a** in a round-bottom flask was added $BF_3{\cdot}OEt_2$ and the reaction mixture then stirred at room temperature

for 10 mins. The reaction mixture was then quenched/washed with aq $NaHCO_3$ resulting in dissolution of the precipitate in the organic layer. The organic layer was dried over Na_2SO_4 followed by removal of the solvent in vacuo. To determine the yields of the different components within the crude product mixture, ^{1}HNMR spectroscopy was employed. To identify and/or quantify all the components of a given mixture, the amount of specific (known) components may be determined using an internal standard. The internal standard must be present in a known amount and its spectrum must have at least one peak that does not overlap with other peaks in the spectrum.[82] Benzene was chosen for this investigation, as explored by Dr. Beh.[81] To determine the yields this way, once the reaction had run for the allocated amount of time, the reaction mixture was quenched as described above, solvent was removed in vacuo, and the crude product was dissolved in a known volume of $CDCl_3$. A known amount of benzene was added as an internal standard and a known aliquot of the solution in $CDCl_3$ and containing benzene, was added to an NMR tube, and then diluted with $CDCl_3$ to reach a volume suitable for ^{1}H NMR analysis. Once the reproductivity of the batch method was confirmed, there was need to also validate the analytical method involving ^{1}H NMR spectroscopy.

To determine and analyse the reaction components and yields, the crude reaction product from the batch method (Figure 3.4) was dissolved in 4.0 mL of $CDCl_3$ (added using a 5 mL/5000 µL syringe) to which 4 µL of benzene were added using a 10 µL syringe. Cognizant of the number of moles of benzene in the 4 mL solution (4.49×10^{-5} mol), the molar concentration of benzene in this solution was calculated (Mbenz = 0.0224 mol/L). A 200 µL aliquot of this solution (volume NMR, VNMR) was added to an NMR sample tube and the solution diluted to 600 µL of $CDCl_3$ volume for analysis, all achieved using a 500 µL syringe. Using Mbenz, the moles of benzene present in this aliquot, (nbenz aliquot) could be calculated. The integral value for the unique *meso*-H signal of the desired *F*-BODIPY product **C2a** (∫**C2**a) was calculated when the integration of benzene was set to 6. Multiplying nbenz aliquot by ∫**C2**a allowed the moles of **C2a** in the 200 µL aliquot (nBF aliquot) to be calculated. The concentration of **C2a** in the original 4 mL solution (MBF) could be calculated as follows:

$$nbenz\ aliquot = Mbenz*VNMR = 2.24 \times 10^{-6} \text{ mol}$$

$$nBF\ aliquot = nbenz\ aliquot * \int C\mathbf{2}a = 6.75 \times 10^{-6} \text{ mol}$$

$$MBF = nBF\ aliquot / VNMR = 0.0338 \text{ mol/L}$$

In this way, the moles of **C2a** produced during the reaction (nBF) was calculated:

$$nBF = MBF * VCDCl_3 = 1.35 \times 10^{-4} \text{ mol}$$

Figure 3.5 shows a comparison of the ^{1}H NMR spectra for the isolated *F*-BODIPY (**C2a**, middle), the isolated HBF_4 salt (**C2b**, top) and the crude reaction mixture containing both prepared via the batch method. Analysis of the ^{1}H NMR spectrum of the crude mixture reveals non-overlapping signals corresponding to those of the *meso*-H of the *F*-BODIPY **C2a**[74,80] and the HBF_4 **C2b**[75] salt at around 6.94 ppm and 7.06 ppm, respectively, alongside a proton signal for the benzene ring resonating at around 7.30 ppm. As expected, these signals also correspond with the ones in their individual spectra.

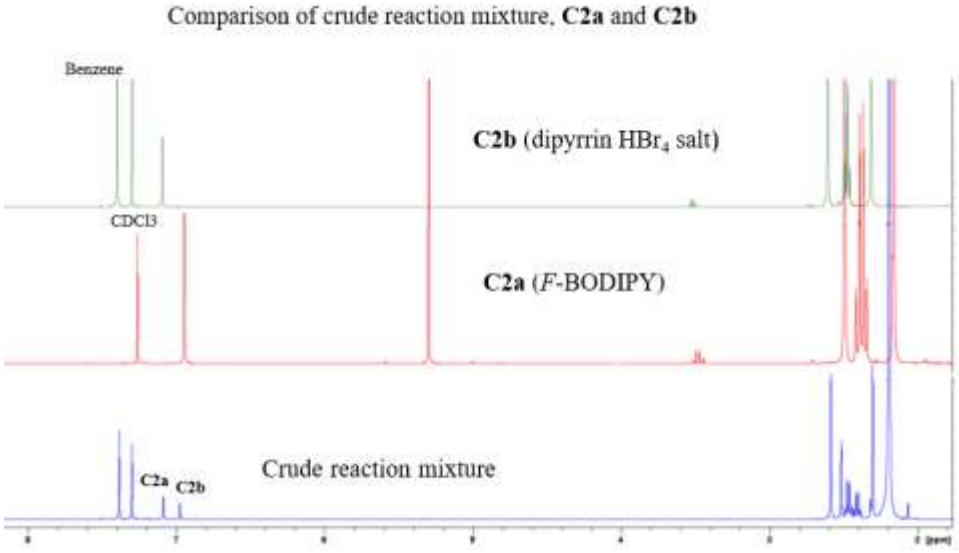

Figure 3.5. ^{1}HNMR spectra of **C2a**, **C2b**, and batch **C2a** and **C2b** in a crude mixture with benzene as an internal standard

By setting the integral of benzene to 6, the integrals for the *meso*-H of the *F*-BODIPY and the HBF_4 salt were each determined. Since a known amount of benzene had been added, the number of moles of benzene could, therefore, be calculated. The number of moles of each component present in the crude reaction mixture was then calculated from the molar amount of internal standard.

The mass of the sample does not factor into the calculation because the method relies solely on the molar ratio of the internal standard to the compound to be determined. Once the number of moles of the products present at the end of the reaction was known, the percentage yield of each product could be calculated using the initial number of moles of the dipyrrin **C2b** used. As a reference for the results from the flow chemistry reaction, the batch method was again conducted three times (Figure 3.4) and the crude product material analysed using the NMR method as described above. The results are shown in (Table 3.1)

Entry	**$BF_3{\cdot}OEt_2$ eq.**	**C2a (%)**	**C2b (%)**
1	1.0	34	49
2	1.0	34	49
3	1.0	34	49

Table 3.1. Results from the addition of $BF_3{\cdot}OEt_2$ (1 eq.) to free-base **C1a** in toluene batch method (using ^1H NMR spectroscopy analytical method)

These results, and the reproducibility, demonstrate that this ^{1}H NMR spectroscopic method is suitable for the analysis of the reaction shown in Figure 3.4, without need to isolate or purify the product *F*-BODIPY.

3.5. Reaction Optimization in Flow Operation

To begin the study for the synthesis of *F*-BODIPY **C2a**, using a flow method, the equivalents previously investigated using the batch method were used in a continuous flow reactor setup as shown in (Figure 3.6). This work was a team project with another graduate student Liandrah Gapare in the Thompson group. For that reason, the following work involves the use of dichloromethane as solvent (Figure 3.7), complementing other work involving toluene.

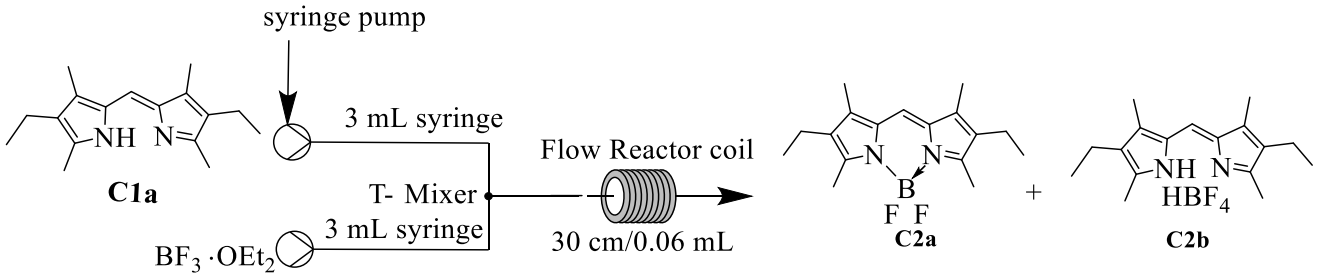

Figure 3.6. Continuous flow setup for the synthesis of *F*-BODIPY **C2a**

Accordingly, 50 mg of **C1a** was placed in a pear-shaped flask. This was purged with nitrogen three times and then 3 mL of anhydrous CH_2Cl_2 was added into the flask. In another pear-shaped flask, $BF_3{\cdot}OEt_2$, was treated in the same manner. Each solution was loaded under nitrogen, into a gas tight syringe. Both syringes were then filled up with nitrogen to keep the reaction anhydrous and ensure that the nitrogen gas pushes the reaction mixture through the flow reactor and thus no solution is left in the tubing. The solutions were then each pumped by a syringe pump through a 0.05 cm internal diameter tee mixer into perfluoroalkoxyalkane (PFA) tubing, also of 0.05 cm internal diameter. The length of the PFA flow reactor coil was short and kept constant at 30 cm

(as the reaction takes place at the T-mixer). To test the hypothesis that formation of HBF_4 dipyrrin salt could be decreased by use of a flow method, the flow rate was varied to adjust the residence time. When the two streams came in contact at the T-mixer, an immediate colour change from yellow to deep red was observed, indicating at least some formation of the desired *F*-BODIPY immediately upon mixing. The reaction mixture was collected in a vial downstream, and quenched in the usual way for *F*-BODIPYs.[80] To determine and analyse the reaction components using the ^{1}H NMR spectroscopy method the crude reaction product was treated just like in the batch method.

The calculation of the number of moles of **C2a** formed could now be used to calculate the percentage conversion of **C1a** to **C2a**. A total of four different experiments were performed and the results are shown in (Table 3.2) according to Figure 3.7. Again, each experiment was performed in triplicate and the average results are reported.

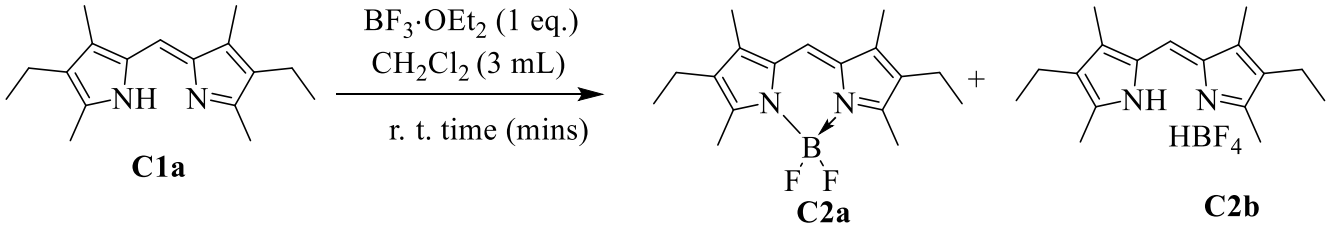

Figure 3.7. Addition of $BF_3{\cdot}OEt_2$ (1 eq.) to dipyrrin **C1a** in CH_2Cl_2 using the flow chemistry setup

Entry	Flow rate (mL/min)	Residence time (mins)	$BF_3{\cdot}OEt_2$ eq.	C2a (%)	C2b (%)
1	0.2	18.3	1.0	14	40
2	0.2	18.3	1.5	27	42
3	0.5	7.3	1.0	31	47
4	0.5	7.3	1.5	36	56

Table 3.2. Attempts to optimize the continuous flow process with a flow reactor coil of 30 cm and 0.05 cm internal diameter tubing (Each of the entries were run 3 times and an average was recorded)

For example, the results for entry 1 using the ^{1}H NMR spectroscopy method were as follows:

First run = **C2a** (12%), **C2b** (40%)

Second run = **C2a** (14%) **C2b** (42%)

Third run = **C2a** (16%) **C2b** (38%)

The first, second and third runs each gave similar results. An average of the three runs is recorded. An identical approach was taken for the experiments reported in the entries 2 - 4 (Table 3.2). The reactor volume was constant for the entire investigation, while stoichiometry of $BF_3{\cdot}OEt_2$ and flow rate were varied, with the residence time calculated accordingly. For entries 1 and 2, the flow rate was constant while the stoichiometry of $BF_3{\cdot}OEt_2$ was varied. Although the stoichiometry of $BF_3{\cdot}OEt_2$ increases, the HBF_4 salt was formed in similar amounts. This indicates that the $BF_3{\cdot}OEt_2$

might have a greater affinity for the HF formally produced *in situ* than for the dipyrrin coming from a different stream. The presence of starting material and impurities in the crude mixture accounts for why the sum of **C2a** and **C2b** does not amount to 100%. Bearing in mind that the hypothesis is that the reaction occurs in the T-mixer (backed up by the immediate colour change from yellow to deep red observed when the two streams come in contact at the T-mixer, i.e. indicating formation of the *F*-BODIPY), the effects of increasing flow rate were investigated in entries 3 and 4 (Table 3.2). Increasing the flow rate (0.5 mL/min) and varying the stoichiometry of $BF_3{\cdot}OEt_2$ was explored (entries 3 and 4), and resulted in slight increase in percentage yield of *F*-BODIPY yet a direct increase in production of the dipyrrin HBr_4 salt too. The NMR spectrum of the reaction mixture also shows the presence of starting material and some impurities.

Since we were met with little success with this system (flow chemistry), we decided to return to a batch set-up and employ scavengers to attempt to mop up the proton and fluoride ions formally produced *in situ* (Figure 3.8).

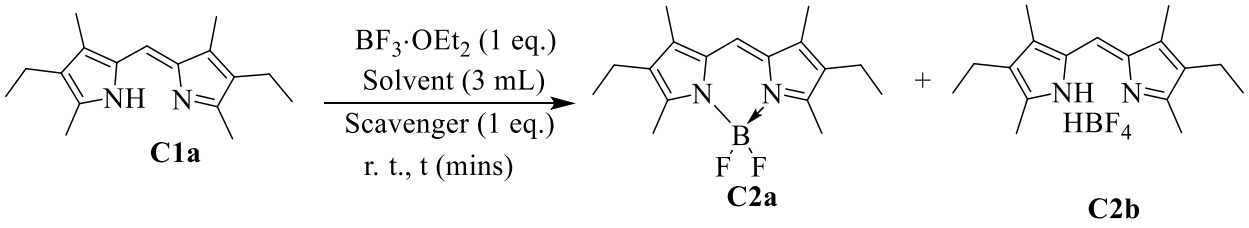

Figure 3.8. Addition of $BF_3{\cdot}OEt_2$ (1 eq.) to free-base **C1a** in the presence of an HF scavenger for the synthesis of *F*-BODIPY **C2a**

HF scavengers such as Na_2CO_3, K_2CO_3 and $CaCO_3$ have been reported to be effective in mopping up HF in reactions where the presence of HF could potentially interfere with the formation of the desired product. Furthermore, mopping up (sequestering) the HF product could serve to drive reaction equilibrium towards product, and thus increase yields. An example is seen in a study[83] (Figure 3.9) by researchers at Johnson & Johnson Pharmaceutical Research & Development aiming to form the difluoro boron product shown. Various HF scavengers (>1.0 eq.) were

evaluated as part of the reaction mixture to neutralize HF such as to drive the equilibrium toward the desired product. Treatment of 1-cyclopropyl-6,7-difluoro-8-methoxy-4-oxo-1,4-dihydroquinoline3-carboxylic acid with $BF_3 \cdot OEt_2$ in THF solution at reflux temperature in the presence of HF scavengers (Na_2CO_3, K_2CO_3 and $CaCO_3$) produced (1-cyclopropyl-6,7-difluoro-1,4-dihydro-8-methoxy-4-(oxo-κ0)-3-quinolinecarb-oxylato-κ03) difluoro-boron in almost quantitative yield (>97%) with excellent chemical purity.[83]

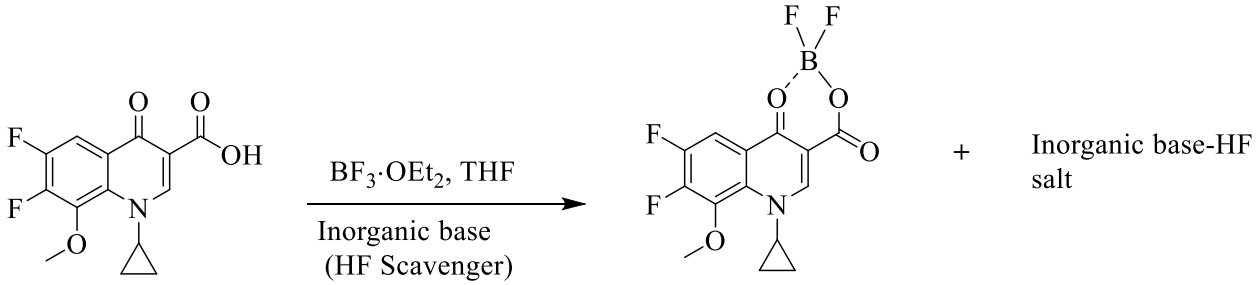

Figure 3.9. Synthesis of difluoro-boron complex using HF scavengers

Building upon this work and that of others seeking to scavenge HF, various HF scavengers were investigated as regards their utility in the promoting *F*-BODIPY formation. The effectiveness of these scavengers in the reaction of **C1a** with $BF_3 \cdot OEt_2$ was thus investigated. To investigate this reaction (Figure 3.8), **C1a** was again selected. This reaction was explored using CH_2Cl_2 and tetrahydrofuran (THF) as solvents and Na_2CO_3, K_2CO_3, $CaCO_3$ and diethylamino trimethylsilane (DEATMS)[14] as scavengers (again this work was done as a team thus results using CH_2Cl_2 and THF are reported herein).

Entry	Scavenger	THF (For 10 mins)		CH_2Cl_2 (For 10 mins)		CH_2Cl_2 (For 90 mins)	
		C2a (%)	**C2b** (%)	**C2a** (%)	**C2b** (%)	**C2a** (%)	**C2b** (%)
1	Na_2CO_3	Trace	81	23	56	16	73
2	K_2CO_3	Trace	81	31	47	19	70
3	$CaCO_3$	7	72	31	56	14	74
4	DEATMS	0	81	09	79	-	-

Table 3.3. Effect of using 1.5 eq. of four potential HF scavengers on the synthesis of *F*-BODIPY **C2b** from dipyrrin **C1a** (Batch method, all reactions were repeated 3 times and an average was recorded)

For this investigation, to a stirring solution of **C1a** was suspended the scavenger. The mixture was then treated with 1 eq. $BF_3{\cdot}OEt_2$ in a dropwise manner. The reaction mixture was stirred for the allocated time (see Table 3.3). The reaction was quenched in the usual way for *F*-BODIPYs,[80] resulting in dissolution of the precipitate in the organic layer. Percentage conversion was determined using ^{1}H NMR spectroscopy, as previously described herein for the flow operation.

For entry 1, Na_2CO_3 was suspended in the reaction mixture (THF as solvent) with **C1a**, and the mixture then treated with 1 eq. of $BF_3{\cdot}OEt_2$. A faint red color (deep red color typical with *F*-BODIPYs) was initially observed, which quickly disappeared (this observation was common with K_2CO_3, $CaCO_3$ and DEATMS in THF as solvent stirring for 10 mins). Results from this reaction shows that the production of **C2b** was favored compared to **C2a**. This shows that the scavengers were not effective at mopping up the HF produced during the reaction. To further investigate the effects of these scavengers, the reaction was repeated using CH_2Cl_2 as solvent. Just like in batch (in the absence of scavenger) a deep red color associated with *F*-BODIPYs was observed, which again quickly disappeared. The reaction was quenched in the usual way for *F*-BODIPYs.[80] This

investigation was also met with no significant increase in the yields of **C2a** compared to those previously reported for batch set-ups in the absence of scavenger. In a bid to further investigate the effect of time on this reaction, a solution of **C1a**, scavenger and 1 eq. of $BF_3{\cdot}OEt_2$ in CH_2Cl_2 were stirred for 90 mins. Upon analysis using ^1H NMR spectroscopy, it was apparent that **C2b** was formed more abundantly than the *F*-BODIPY, again suggesting that less of the $BF_3{\cdot}OEt_2$ was available to react with **C1a** furthermore. These results suggest that the scavengers did not sequester fluoride or HF. Stirring the reaction mixture in CH_2Cl_2 for 90 mins resulted in a higher salt: *F*-BODIPY ratio, and thus did not favor increased yield of the desired *F*-BODIPY.

3.6. Conclusion

The synthesis of *F*-BODIPY using a continuous flow operation has been investigated in a preliminary manner. The results confirmed that the reaction between a free-base dipyrrin and $BF_3{\cdot}OEt_2$ is rapid, despite the absence of base. However, comparison of results obtained in batch to those obtained using a crude flow operation shows that there was no significant change in the yields obtained. The results obtained suggest that the continuous flow operation failed to eliminate the interaction between the HF (formally) produced *in situ* with the unreacted $BF_3{\cdot}OEt_2$. Rather, the BF_4^- anion is formed which acts as a counter ion to the protonated dipyrrin and thus leads to the formation of the dipyrrin HBF_4 salt in high amounts. Adding further complexity, and not promoting formation of the desired *F*-BODIPY, the HBF_4 salt of the dipyrrin precipitated upon formation, thus removing both the dipyrrin and the BF_3 from the solution phase. Le Chatelier's Principle would predict such that precipitation significantly reduces success of the desired reaction.

Furthermore, no significant increase was observed with the use of several HF scavengers. In short, there remains the need to develop a methodology which affords better yields of *F*-BODIPY using stoichiometric amounts of $BF_3{\cdot}OEt_2$ and free-base dipyrrin. This may include the use of alternative HF and/or fluoride scavengers.[83] It is important to note that a screen of alternative bases has already been conducted.[80] Another potential solution involves a flow system where mixing and flow rate are increased such as to match the rate of reaction between dipyrrin and $BF_3{\cdot}OEt_2$. Nevertheless, the use of 1 eq. $BF_3{\cdot}OEt_2$ may be used to synthesize up to 50% yield of *F*-BODIPY, where the remaining 50% of the material is readily recovered as the re-useable and recyclable HBF_4 salt.

3.7. Experimental

General Experimental

All chemicals were purchased and used as received unless otherwise indicated. Hexanes and CH_2C1_2 used for chromatography were obtained crude and purified via distillation under atmospheric conditions before use. Anhydrous solvents were used as received. TLC was performed using glass-backed silica gel plates or plastic-backed neutral alumina plates. Visualization of TLC plates was performed using UV light. Air-and moisture-sensitive compounds were introduced via syringe. NMR spectra were obtained using a 500 MHz or 300 MHz instrument using the solvent signal of $CDC1_3$ (^{1}H 7.26 ppm and ^{13}C 77.16 ppm) as an internal reference for ^{1}H and ^{13}C chemical shifts. ^{11}B and ^{19}F NMR spectra were referenced using the absolute referencing procedure standard for Bruker digital spectrometers, with $BF_3{\cdot}OEt_2$ (15% in $CDC1_3$) and $CC1_3F$ defining the 0 ppm position, respectively. All continuous flow reactions were performed using Dupont 0.05 cm inner diameter PFA tubing, utilizing a T-mixer and pumped using a KD Scientific syringe pump model no. 780210V.

General Procedure for the synthesis of *F*-BODIPY with 1 eq. of $BF_3{\cdot}OEt_2$ in a batch process (GP4)

The free-base dipyrrin **C1a** (50 mg, 0.20 mmol) was dissolved in anhydrous toluene (3 mL) under a nitrogen atmosphere and $BF_3{\cdot}OEt_2$ (100%, 25 μL, 0.20 mmol) was added to the solution. The reaction mixture was then stirred for 10 mins at room temperature. The crude reaction mixture was quenched by the addition of H_2O, followed with an extraction with CH_2Cl_2 (30 mL, 3 times). The combined organic fractions were then washed with aqueous $NaHCO_3$ (3 times), resulting in dissolution of the crude product in the organic layer which was then dried over Na_2SO_4 and concentrated in vacuo. Hexane was added to the concentrated crude product to form a suspension which was then filtered over a pad of celite. Rinsing with excess hexanes and concentration of the

resulting fraction in vacuo afforded the *F*-BODIPY **C2a** as a deep red solid with a green fluorescence. The celite pad was re-washed with excess CH_2Cl_2 and the resulting fraction was concentrated in vacuo to isolate the HBF_4 dipyrrin salt **C2b** as a bright orange solid.

General Procedure for the synthesis of *F*-BODIPY with 1 eq. of $BF_3{\cdot}OEt_2$ in a continuous flow process (GP5)

The free-base dipyrrin **C1a** (50 mg, 0.20 mmol) was dissolved in anhydrous CH_2Cl_2 (1.5 mL) under a nitrogen atmosphere in a pear-shaped bottom flask. In another pear-shaped flask, $BF_3{\cdot}OEt_2$ (100%, 25 µL, 0.20 mmol) was dissolved in anhydrous CH_2Cl_2 (1.5 mL) under a nitrogen atmosphere. The solutions were each loaded into 3 mL syringes and nitrogen gas was then used to fill the extra volume of the syringe to keep the mixture under a nitrogen gas environment. This was done by pulling some of the nitrogen gas from the bottle of anhydrous solvent which was placed under a nitrogen gas environment. Both reagents were then pumped, at the same flow rate, and combined at a T-piece mixer. The combined stream was directed to a 30 cm (0.06 mL) PFA flow reactor coil at room temperature. The crude reaction mixture was quenched in H_2O followed by an extraction with CH_2Cl_2 (30 mL, 3 times). The combined organic fractions were then washed with aqueous $NaHCO_3$ (3 times), resulting in dissolution of the crude product in the organic layer which was then dried over Na_2SO_4 and concentrated in vacuo. The resulting residue was dissolved in $CDC1_3$ (4 mL), and benzene (4 mL) was added, with stirring. An aliquot (200 µL) of this solution was added to an NMR sample tube and then diluted with $CDC1_3$ (400 µL). A ^1H NMR spectrum of the sample was collected, and the NMR-based yield was determined.

General Procedure for the synthesis of *F*-BODIPY with 1 eq. of $BF_3{\cdot}OEt_2$ in a continuous flow process while using a HF scavenger (Na_2CO_3, K_2CO_3, $CaCO_3$ and DEATMS (GP6)

The free-base dipyrrin **C1a** (50 mg, 0.20 mmol) was dissolved in anhydrous CH_2Cl_2 (3 mL) under a nitrogen atmosphere, followed by the addition scavenger (0.30 mmol) and $BF_3{\cdot}OEt_2$ (25 µL, 0.20 mmol) which was then added dropwise into the solution. The reaction mixture was stirred for the allocated time at room temperature. The crude reaction mixture was quenched by the addition of H_2O, followed by an extraction with CH_2Cl_2 (30 mL, 3 times). The combined organic fractions were then washed with aqueous $NaHCO_3$ (3 times), resulting in dissolution of the crude product in the organic layer which was then dried over Na_2SO_4 and concentrated in vacuo. The resulting residue was dissolved in benzene (4 mL). An aliquot (200 µL) of this solution was added to an NMR sample tube and then diluted with $CDC1_3$ (400 µL). A ^1H NMR spectrum of the sample was collected, and the NMR-based yield was determined as desired.

Synthesis of compounds

Ethyl Ester 4-Acetyl-3,5-dimethy1-1H-pyrrole-2-carboxylic Acid (A)

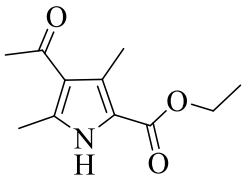

The title compound was synthesized according to a literature procedure.[5] Ethyl acetoacetate (70 mL, 55 mmol) in a 3-neck flask was dissolved in glacial acetic acid (150 mL) and the resulting solution cooled to 0°C with the use of an ice bath. An ice-cold solution of sodium nitrite (42 g, 604 mol) in H_2O (150 mL) was added to the above solution, and the reaction mixture stirred for 24 h at room temperature, using an overhead stirrer, to form the corresponding oxime. After 24 h, the reaction mixture containing the oxime was transferred to a dropping funnel. In another 3-neck

flask, pentane-2,4-dione (56 mL, 0.60 mol) was dissolved in acetic acid (150 mL) with stirring. Anhydrous sodium carbonate (64 g, 0.60 mol) was then added. The dropping funnel containing the oxime was placed on the left-most neck of the 3-neck and its contents (oxime) added dropwise, with stirring via an overhead stirrer placed in the central neck while zinc dust (75 g) was also slowly added via the right-most neck of the flask, making sure that all zinc dust became miscible before the next amount was added. During the addition of the oxime and zinc dust, the reaction was kept below 60 ℃ with an ice bath and exothermicity was further controlled by rate of addition and by adding small amount of acetic acid when needed. The reaction mixture was then stirred at 60 °C for 1 h after complete addition of the oxime and zinc dust. After this time, the mixture was allowed to cool to room temperature and was diluted with excess H_2O and then allowed to stand at room temperature overnight. The following morning, the reaction mixture was filtered, and the isolated white solid was washed with excess water to remove all possible acetic acid, followed by an excess hexane wash to remove all hexane-soluble impurities. The white solid was then dissolved in CH_2Cl_2, and the solution filtered (this removes any remaining zinc dust from the white solid). The filtrate was then dried over Na_2SO_4, and the resulting solution concentrated in vacuo to give the final compound as a white solid (77 g, 67%). ^{1}H NMR (500 MHz; $CDC1_3$) δ 9.37 (br s, 1H), 4.34 (q, *J* = 5 Hz, 2H), 2.64 - 2.42 (m, 9H), 1.37 ppm (t, *J* = 5 Hz, 3H), in accordance with literature.[5]

Ethyl Ester 4-Ethyl-3,5-dimethyl-1H-pyrrole-2-carboxylic acid (B)

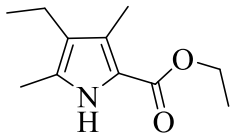

The title compound was synthesized according to a literature procedure.[84] To a stirred solution of ethyl ester 4-acetyl-3,5-dimethy1-1H-pyrrole-2-carboxylic acid (1.00 g, 4.78 mmol) in dry THF (33 mL) under nitrogen at 0 °C was added dropwise BH_3.THF (1M solution in THF, 9.56 mL, 9.56 mmol) via syringe. The resultant reaction mixture was stirred under nitrogen at room temperature

for 18 h. The reaction mixture was then quenched by slowly adding water (5 mL) and 5% aqueous HCl (30 mL), with stirring at room temperature for 30 mins. The reaction mixture was extracted into EtOAc (3 x 30 mL). The combined organic fractions were washed with saturated aqueous $NaHCO_3$ (30 mL) and brine (30 mL), dried over Na_2SO_4, then concentrated in vacuo to give the title product as a white solid (863 mg, 92%). ^{1}H NMR (500 MHz; $CDCl_3$) δ = 8.73 (br s, 1H), 4.32 - 4.27 (m, 2H), 2.41 - 2.35 (m, 2H), 2.28 (s, 3H), 2.20 (s, 3H), 1.37 - 1.32 (m, 3H), 1.07 - 1.01 ppm (m, 3H), in accordance with literature.[84]

3-Ethy1-5-[(4-ethy1-3,5-dimethyl-2H-pyrrol-2-ylidene) methyl]-2,4-dimethyl-1H-pyrrole Monohydrobromide (**C**)

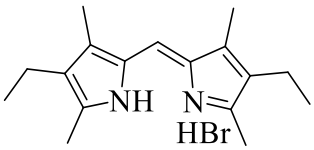

The title compound was synthesized according to a literature procedure.[79] To a solution of ethyl ester 4-ethyl-3,5-dimethyl-1H-pyrrole-2-carboxylic acid (0.86 g, 4.42 mmol) in 90% formic acid (4 mL) stirring at room temperature, was added 48% HBr (0.70 mL, 12 mmol). The mixture was heated at reflux temperature for 1 h. The solution was allowed to cool to room temperature and then refrigerated for 2h. The precipitate was isolated via filtration, washed with ether, and dried at room temperature in air to give the title compound as a dark-red crystalline solid (550 mg, 74%). ^{1}H NMR (500 MHz; $CDCl_3$) δ = 12.95 (br s, 2H), 7.02 (s, 1H), 2.66 (s, 6H), 2.42 (app q, J = 5 Hz, 4H), 2.26 (s, 6H), 1.07 ppm (t, J = 5 Hz, 6H), data in accordance with literature.[79]

3-Ethy1-5-[(4-ethy1-3,5-dimethyl-2H-pyrrol-2-ylidene)methyl]-2,4-dimethyl-1H-pyrrole (C1a)

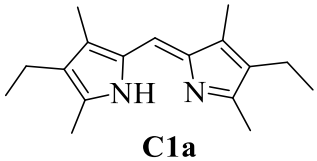

C1a

The bromide salt 3-ethy1-5-[(4-ethy1-3,5-dimethyl-2H-pyrrol-2-ylidene) methyl]-2,4-dimethyl-1H-pyrrole monohydrobromide (1 g, 3 mmol) was dissolved in CH_2C1_2 and washed with aqueous 1M NaOH (10 mL) three times. The organic layer was then dried over anhydrous Na_2SO_4, and the solvent removed to yield dipyrrin **C1a** as a brown, crystalline solid (0.64 g, 84%). ^{1}H NMR (500 MHz; $CDCl_3$) δ 13.56 (br s, 1H), 7.01 (s, 1H), 2.63 (br s, 4H), 2.47 - 2.26 (m, 6H), 2.12 (br s, 3H), 1.07 ppm (s, 8H), data in accordance with literature.[77]

(T-4)-Difluoro-ethy-1-5-[(4-ethy-1-3,5-dimethyl-2H-pyrrol-2-ylidene-KN)methyl]-2,4 dimethyl-1H-pyrrolato-KN] boron

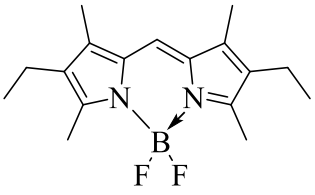

C2a

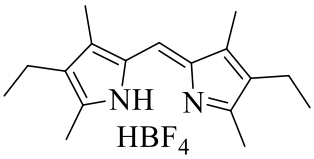

C2b

These compounds were obtained according to GP4. F-BODIPY **C2a** was isolated as a deep red solid (14 mg, 23%). The dipyrrin salt **C2b**, was isolated as a bright orange solid (26 mg, 37%). Data for **C2a**: ^{1}H NMR ($CDC1_3$, 500 MHz) δ = 6.94 (s, 1H, meso-H), 2.49 (s, 6H), 2.38 (q, J = 10 Hz, 4H), 2.16 (s, 6H), 1.06 ppm (t, J = 10 Hz, 6H). Data in accordance with literature.[80]

Data for **C2b**: ^{1}H (500 MHz, $CDC1_3$) δ = 10.78 (br, 2H), 7.06 (s, 1H), 2.55 (s, 6H), 2.44 (q, *J* = 10 Hz, 4H), 2.28 (s, 6H), 1.09 ppm (t, *J* = 10 Hz, 6H). Data in accordance with literature.[75]

Chapter 4 Conclusions

Each chapter in this thesis is individually summarized at the end of each respective chapter. As such, this serves to conclude the thesis by compiling the conclusions from each chapter.

4.1. Chapter 2 Conclusion

This study reports the synthesis of the two new azobispyrroles **B25** and **B26**. These two new azobispyrroles complement the synthesis of **B23** and **B24** reported previously,[68] albeit in trace amounts for **B25**. This achievement demonstrates the reproducibility of the synthetic route to azobispyrrole from 4-nitro butanones. Azobispyrrole **B26** was fully characterized, and **B25** was identified through mass spectrometry supported by characteristic physical properties of polarity and colour.

Future work should focus on obtaining larger amounts of **B23** - **B26** so that a full photochemical evaluation can be completed alongside an evaluation of *E* - *Z* switching behaviors. The synthesis of the methoxy-containing **B25** should be repeated, so that an assessment of the effect of this electron-donating group can be completed alongside potential push-pull effects.

Given that the synthesis of amino diphenylpyrrole (**B7**) was unreliable, future focus should attempt to convert this compound directly into the diazonium salt azobispyrroles using the same synthetic strategy as is used for preparation of many bisarylazo compounds. This route (Scheme 2.2) could potentially afford improved yields and a less challenging purification of the desired azo dye contrary to Scheme 2.5 where challenging purification of the azo dyes was faced (**B23**, **B24** and **B26**).

4.2. Chapter 3 Conclusion

The synthesis of *F*-BODIPY using a continuous flow operation has been investigated in a preliminary manner. The results confirmed that the reaction between a free-base dipyrrin and $BF_3{\cdot}OEt_2$ is rapid, despite the absence of base. However, comparison of results obtained in batch

to those obtained using a crude flow operation shows that there was no significant change in the yields obtained. The results obtained suggest that the continuous flow operation failed to eliminate the interaction between the HF (formally) produced *in situ* with the unreacted $BF_3{\cdot}OEt_2$. Rather, the BF_4^- anion is formed which acts as a counter ion to the protonated dipyrrin and thus leads to the formation of the dipyrrin HBF_4 salt in high amounts. Adding further complexity, and not promoting formation of the desired *F*-BODIPY, the HBF_4 salt of the dipyrrin precipitated upon formation, thus removing both the dipyrrin and the BF_3 from the solution phase. Le Chatelier's Principle would predict such that precipitation significantly reduces success of the desired reaction.

Furthermore, no significant increase was observed with the use of several HF scavengers. In short, there remains the need to develop a methodology which affords better yields of *F*-BODIPY using stoichiometric amounts of $BF_3{\cdot}OEt_2$ and free-base dipyrrin. This may include the use of alternative HF and/or fluoride scavengers.[83] It is important to note that a screen of alternative bases has already been conducted.[80] Another potential solution involves a flow system where mixing and flow rate are increased such as to match the rate of reaction between dipyrrin and $BF_3{\cdot}OEt_2$. Nevertheless, the use of 1 eq, $BF_3{\cdot}OEt_2$ may be used to synthesize up to 50% yield of *F*-BODIPY, where the remaining 50% of the material is readily recovered as the re-useable and recyclable HBF_4 salt.

References

1. Anderson, H. J. Pyrrole: From Dippel to Du Pont. *J. Chem. Educ.* **72**, 875 (1995).
2. Knorr, L. Synthetische Versuche mit dem Acetessigester. II. Mittheilung: Ueberführung des Diacetbernsteinsäureesters und des Acetessigesters in Pyrrolderivate. *Justus Liebigs Ann. Chem.* **236**, 290–332 (1886).
3. Paine, J. B. & Dolphin, D. Pyrrole chemistry. An improved synthesis of ethyl pyrrole-2-carboxylate esters from diethyl aminomalonate. *J. Org. Chem.* **50**, 5598–5604 (1985).
4. Kleinspehn, G. G. A Novel Route to Certain 2-Pyrrolecarboxylic Esters and Nitriles1,2. *J. Am. Chem. Soc.* **77**, 1546–1548 (1955).
5. Knorr, L. Synthese von Pyrrolderivaten. *Berichte Dtsch. Chem. Ges.* **17**, 1635–1642 (1884).
6. Ueber die Derivate des Acetophenonacetessigesters und des Acetonylacetessigesters - Paal - 1884 - Berichte der deutschen chemischen Gesellschaft - Wiley Online Library. https://chemistry-europe.onlinelibrary.wiley.com/doi/10.1002/cber.188401702228.
7. Amarnath, V. *et al.* Intermediates in the Paal-Knorr synthesis of pyrroles. *J. Org. Chem.* **56**, 6924–6931 (1991).
8. Beh, M. H. R. *et al.* Regioselective substituent effects upon the synthesis of dipyrrins from 2-formyl pyrroles. *Can. J. Chem.* **96**, 779–784 (2018).
9. Oldenziel, O. H., Van Leusen, D. & Van Leusen, A. M. Chemistry of sulfonylmethyl isocyanides. 13. A general one-step synthesis of nitriles from ketones using tosylmethyl isocyanide. Introduction of a one-carbon unit. *J. Org. Chem.* **42**, 3114–3118 (1977).
10. Griefs, P. Vorläufige Notiz über die Einwirkung von salpetriger Säure auf Amidinitro- und Aminitrophenylsäure. *Justus Liebigs Ann. Chem.* **106**, 123–125 (1858).

11. Yates, E. & Yates, A. Johann Peter Griess FRS (1829–88): Victorian brewer and synthetic dye chemist. *Notes Rec. R. Soc. J. Hist. Sci.* **70**, 65–81 (2016).
12. Centeno, S. A., Buisan, V. L. & Ropret, P. Raman study of synthetic organic pigments and dyes in early lithographic inks (1890–1920). *J. Raman Spectrosc.* **37**, 1111–1118 (2006).
13. Chemotherapie der bakteriellen Infektionen - Domagk - 1935 - Angewandte Chemie - Wiley Online Library. https://onlinelibrary.wiley.com/doi/abs/10.1002/ange.19350484202.
14. Weissleder, R. & Ntziachristos, V. Shedding light onto live molecular targets. *Nat. Med.* **9**, 123–128 (2003).
15. Khan, Md. N., Parmar, D. K. & Das, D. Recent Applications of Azo Dyes: A Paradigm Shift from Medicinal Chemistry to Biomedical Sciences. *Mini Rev. Med. Chem.* **21**, 1071–1084 (2021).
16. Kirpal, A. & Böhm, W. Über eine neuartige Isomerie in der Pyridin-Reihe (I. Mitteil.). *Berichte Dtsch. Chem. Ges. B Ser.* **65**, 680–682 (1932).
17. Hartley, G. S. The Cis-form of Azobenzene. *Nature* **140**, 281–281 (1937).
18. Fèvre, R. J. W. L. & Worth, C. V. 397. Indications of geometrical isomerism with 2 : 2′-azopyridine. *J. Chem. Soc. Resumed* 1814–1817 (1951).
19. Campbell, N., Henderson, A. W. & Taylor, D. 257. Geometrical isomerism of azo-compounds. *J. Chem. Soc. Resumed* 1281–1285 (1953) .
20. Towns, A. D. Developments in azo disperse dyes derived from heterocyclic diazo components. *Dyes Pigments* **42**, 3–28 (1999).
21. Benkhaya, S. *et al.* Synthesis of a New Asymmetric Composite Membrane with Bi-Component Collodion: Application in the Ultra filtration of Baths of Reagent Dyes of Fabric Rinsing/Padding. *J. Mater. Environ. Sci.* **7**, 4556–4569 (2016).

22. Collier, S. W., Storm, J. E. & Bronaugh, R. L. Reduction of Azo Dyes During in Vitro Percutaneous Absorption. *Toxicol. Appl. Pharmacol.* **118**, 73–79 (1993).
23. Al-Rubaie, L. A.-A. R. & Mhessn, R. J. Synthesis and Characterization of Azo Dye Para Red and New Derivatives. *E-J. Chem.* **9**, 465–470 (2012).
24. Gürses, A., Açıkyıldız, M., Güneş, K. & Gürses, M. S. Classification of Dye and Pigments. in *Dyes and Pigments* (eds. Gürses, A., Açıkyıldız, M., Güneş, K. & Gürses, M. S.) 31–45 (Springer International Publishing, 2016).
25. McLaren, K. *The colour science of dyes and pigments*.
26. Sandhya, S. Biodegradation of Azo Dyes Under Anaerobic Condition: Role of Azoreductase. in *Biodegradation of Azo Dyes* (ed. Atacag Erkurt, H.) 39–57 (Springer, 2010).
27. Benkhaya, S., M'rabet, S. & El Harfi, A. Classifications, properties, recent synthesis and applications of azo dyes. *Heliyon* **6**, e03271 (2020).
28. Bandala, E. R. *et al.* Application of azo dyes as dosimetric indicators for enhanced photocatalytic solar disinfection (ENPHOSODIS). *J. Photochem. Photobiol. Chem.* **218**, 185–191 (2011).
29. Yousefi, H., Yahyazadeh, A., Rufchahi, E. O. M. & Rassa, M. Synthesis, spectral properties, biological activity and application of new 4-(benzyloxy)phenol derived azo dyes for polyester fiber dyeing. *J. Mol. Liq.* **180**, 51–58 (2013).
30. Roldo, M. *et al.* Azo compounds in colon-specific drug delivery. *Expert Opin. Drug Deliv.* **4**, 547–560 (2007).
31. Beer, P. D. & Gale, P. A. Anion Recognition and Sensing: The State of the Art and Future Perspectives. *Angew. Chem. Int. Ed.* **40**, 486–516 (2001).

32. Loudet, A. & Burgess, K. BODIPY Dyes and Their Derivatives: Syntheses and Spectroscopic Properties. *Chem. Rev.* **107**, 4891–4932 (2007).

33. Kwon, Y.-D., Byun, Y. & Kim, H.-K. 18F-labelled BODIPY dye as a dual imaging agent: Radiofluorination and applications in PET and optical imaging. *Nucl. Med. Biol.* **93**, 22–36 (2021).

34. Ziessel, R., Ulrich, G. & Harriman, A. The chemistry of Bodipy: A new El Dorado for fluorescence tools. *New J. Chem.* **31**, 496 (2007).

35. Baruah, M., Qin, W., Basarić, N., De Borggraeve, W. M. & Boens, N. BODIPY-Based Hydroxyaryl Derivatives as Fluorescent pH Probes. *J. Org. Chem.* **70**, 4152–4157 (2005).

36. Ulrich, G., Goze, C., Guardigli, M., Roda, A. & Ziessel, R. Pyrromethene dialkynyl borane complexes for 'cascatelle' energy transfer and protein labeling. *Angew. Chem. Int. Ed Engl.* **44**, 3694–3698 (2005).

37. Ametamey, S. M., Honer, M. & Schubiger, P. A. Molecular Imaging with PET. *Chem. Rev.* **108**, 1501–1516 (2008).

38. Pike, V. W. PET radiotracers: crossing the blood–brain barrier and surviving metabolism. *Trends Pharmacol. Sci.* **30**, 431–440 (2009).

39. Jacobson, O., Kiesewetter, D. O. & Chen, X. Fluorine-18 Radiochemistry, Labeling Strategies and Synthetic Routes. *Bioconjug. Chem.* **26**, 1–18 (2015).

40. Pogue, B. W., M.d, E. L. R., Achilefu, S. & Dam, G. M. van. Perspective review of what is needed for molecular-specific fluorescence-guided surgery. *J. Biomed. Opt.* **23**, 100601 (2018).

41. Pogue, B. W., M.d, E. L. R., Achilefu, S. & Dam, G. M. van. Perspective review of what is needed for molecular-specific fluorescence-guided surgery. *J. Biomed. Opt.* **23**, 100601 (2018).

42. Veys, I. *et al.* ICG-fluorescence imaging for detection of peritoneal metastases and residual tumoral scars in locally advanced ovarian cancer: A pilot study. *J. Surg. Oncol.* **117**, 228–235 (2018).

43. Lu, H., Mack, J., Yang, Y. & Shen, Z. Structural modification strategies for the rational design of red/NIR region BODIPYs. *Chem. Soc. Rev.* **43**, 4778–4823 (2014).

44. Kaur, P. & Singh, K. Recent advances in the application of BODIPY in bioimaging and chemosensing. *J. Mater. Chem. C* **7**, 11361–11405 (2019).

45. Lv, H., Zhang, X., Wang, S. & Xing, G. Assembly of BODIPY-carbazole dyes with liposomes to fabricate fluorescent nanoparticles for lysosomal bioimaging in living cells. *Analyst* **142**, 603–607 (2017).

46. Griefs, P. Vorläufige Notiz über die Einwirkung von salpetriger Säure auf Amidinitro- und Aminitrophenylsäure. *Ann. Chem. Pharm.* **106**, 123–125 (1858).

47. Herbst, W. & Hunger, K. *Industrial Organic Pigments: Production, Properties, Applications*. (John Wiley & Sons, 2006).

48. Kucharska, M. & Grabka, J. A review of chromatographic methods for determination of synthetic food dyes. *Talanta* **80**, 1045–1051 (2010).

49. Domagk, G. Chemotherapie der bakteriellen Infektionen. *Angew. Chem.* **48**, 657–667 (1935).

50. Garcia-Amorós, J., Sánchez-Ferrer, A., Massad, W. A., Nonell, S. & Velasco, D. Kinetic study of the fast thermal cis-to-trans isomerisation of para-, ortho- and polyhydroxyazobenzenes. *Phys. Chem. Chem. Phys.* **12**, 13238–13242 (2010).

51. Kirpal, A. & Böhm, W. Über eine neuartige Isomerie in der Pyridin-Reihe (I. Mitteil.). *Berichte Dtsch. Chem. Ges. B Ser.* **65**, 680–682 (1932).

52. Weston, C. E., Richardson, R. D., Haycock, P. R., White, A. J. P. & Fuchter, M. J. Arylazopyrazoles: Azoheteroarene Photoswitches Offering Quantitative Isomerization and Long Thermal Half-Lives. *J. Am. Chem. Soc.* **136**, 11878–11881 (2014).

53. Siewertsen, R. *et al.* Highly Efficient Reversible Z−E Photoisomerization of a Bridged Azobenzene with Visible Light through Resolved S1(nπ*) Absorption Bands. *J. Am. Chem. Soc.* **131**, 15594–15595 (2009).

54. Bléger, D. & Hecht, S. Visible-Light-Activated Molecular Switches. *Angew. Chem. Int. Ed.* **54**, 11338–11349 (2015).

55. Crespi, S., Simeth, N. A. & König, B. Heteroaryl azo dyes as molecular photoswitches. *Nat. Rev. Chem.* **3**, 133–146 (2019).

56. Dokić, J. *et al.* Quantum Chemical Investigation of Thermal Cis-to-Trans Isomerization of Azobenzene Derivatives: Substituent Effects, Solvent Effects, and Comparison to Experimental Data. *J. Phys. Chem. A* **113**, 6763–6773 (2009).

57. Bandara, D. & Burdette, S. Photoisomerization in Different Classes of Azobenzene. *Chem. Soc. Rev.* **41**, 1809–25 (2012).

58. Wei-Guang Diau, E. A New Trans-to-Cis Photoisomerization Mechanism of Azobenzene on the S_1 (n,π*) Surface. *J. Phys. Chem. A* **108**, 950–956 (2004).

59. Yu, L., Xu, C. & Zhu, C. Probing the π → π* photoisomerization mechanism of cis-azobenzene by multi-state ab initio on-the-fly trajectory dynamics simulation. *Phys. Chem. Chem. Phys.* **17**, 17646–17660 (2015).

60. Bandara, H. M. D. & Burdette, S. C. Photoisomerization in different classes of azobenzene. *Chem. Soc. Rev.* **41**, 1809–1825 (2012).

61. Calbo, J. *et al.* Tuning Azoheteroarene Photoswitch Performance through Heteroaryl Design. *J. Am. Chem. Soc.* **139**, 1261–1274 (2017).

62. Garcia-Amorós, J., Díaz-Lobo, M., Nonell, S. & Velasco, D. Fastest Thermal Isomerization of an Azobenzene for Nanosecond Photoswitching Applications under Physiological Conditions. *Angew. Chem. Int. Ed.* **51**, 12820–12823 (2012).

63. Diaz-Rodriquez, R. Some Aspects of Inorganic and Organometallic Chemistry of Dipyrrins. (Dalhousie University, 2021).

64. Grossi, M. *et al.* Mechanistic Insight into the Formation of Tetraarylazadipyrromethenes. *J. Org. Chem.* **77**, 9304–9312 (2012).

65. Jiao, L. *et al.* Conformationally Restricted Aza-Dipyrromethene Boron Difluorides (Aza-BODIPYs) with High Fluorescent Quantum Yields. *Chem. – Asian J.* **9**, 805–810 (2014).

67. Chang, K.-C. *et al.* Photoisomerization of electroactive polyimide/multiwalled carbon nanotube composites on the effect of electrochemical sensing for ascorbic acid. *Polym. Int.* **64**, 373–382 (2015).

68. Antina, E. V., Bumagina, N. A., V'yugin, A. I. & Solomonov, A. V. Fluorescent indicators of metal ions based on dipyrromethene platform. *Dyes Pigments* **136**, 368–381 (2017).

69. Wood, T. E. & Thompson, A. Advances in the Chemistry of Dipyrrins and Their Complexes. *Chem. Rev.* **107**, 1831–1861 (2007).

70. Lu, H., Mack, J., Yang, Y. & Shen, Z. Structural modification strategies for the rational design of red/NIR region BODIPYs. *Chem. Soc. Rev.* **43**, 4778–4823 (2014).

71. Mula, S. *et al.* Design and Development of a New Pyrromethene Dye with Improved Photostability and Lasing Efficiency: Theoretical Rationalization of Photophysical and Photochemical Properties. *J. Org. Chem.* **73**, 2146–2154 (2008).

72. Lu, P. *et al.* Boron dipyrromethene (BODIPY) in polymer chemistry. *Polym. Chem.* **12**, 327–348 (2021).

73. Treibs, A. & Kreuzer, F.-H. Difluorboryl-Komplexe von Di- und Tripyrrylmethenen. *Justus Liebigs Ann. Chem.* **718**, 208–223 (1968).

74. Loudet, A. & Burgess, K. BODIPY Dyes and Their Derivatives: Syntheses and Spectroscopic Properties. *Chem. Rev.* **107**, 4891–4932 (2007).

75. Lundrigan, T., Cameron, T. S. & Thompson, A. Activation and deprotection of F-BODIPYs using boron trihalides. *Chem. Commun.* **50**, 7028–7031 (2014).

76. Wagner, R. W. & Lindsey, J. S. Boron-dipyrromethene dyes for incorporation in synthetic multi-pigment light-harvesting arrays. *Pure Appl. Chem.* **68**, 1373–1380 (1996).

77. Groves, B. R., Cameron, T. S. & Thompson, A. Deuteration and tautomeric reactivity of the 1-methyl functionality of free-base dipyrrins. *Org. Biomol. Chem.* **15**, 7925–7935 (2017).

78. Baumann, M., Moody, T. S., Smyth, M. & Wharry, S. A Perspective on Continuous Flow Chemistry in the Pharmaceutical Industry. *Org. Process Res. Dev.* **24**, 1802–1813 (2020).

79. Bumagina, N., Berezin, M., Semeikin, A. & Antina, E. Difluoroborates of phenyl-substituted aza-dipyrromethenes: Preparation, spectral properties, and stability in solution. *Russ. J. Gen. Chem.* **85**, 2739–2742 (2015).

80. Lundrigan, T. *et al.* An improved method for the synthesis of F-BODIPYs from dipyrrins and bis(dipyrrin)s. *Org. Lett.* **14**, 2158–2161 (2012).

81. Michael, B. Study and Development of Synthetic Methodology Towards Pyrrolic Frameworks. (Dalhousie University, 2019) Thesis PhD.

82. Beh, M. H. R. *et al.* Robust synthesis of F-BODIPYs. *Org. Biomol. Chem.* **14**, 11473–11479 (2016).

83. Li, X. & Russell, R. K. Using Potassium Carbonate to Scavenge Hydrogen Fluoride: A Scale-Up Process for Quantitative Production of (1-Cyclopropyl-6,7-difluoro-1,4-dihydro-8-methoxy-4-(oxo-κO)-3-quinolinecarboxylato-κO3)difluoro−Boron. *Org. Process Res. Dev.* **12**, 464–466 (2008).

84. Rastogi, S. *et al.* Synthetic prodigiosenes and the influence of C-ring substitution on DNA cleavage, transmembrane chloride transport and basicity. *Org. Biomol. Chem.* **11**, 3834–3845 (2013).

Appendix A. Synthesis of azo dye

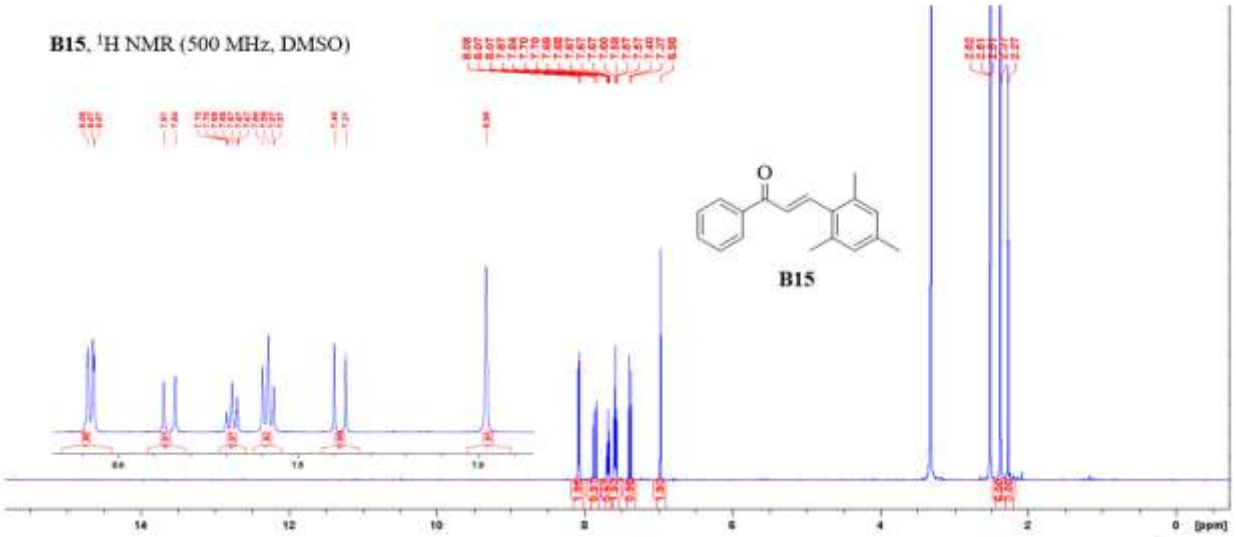

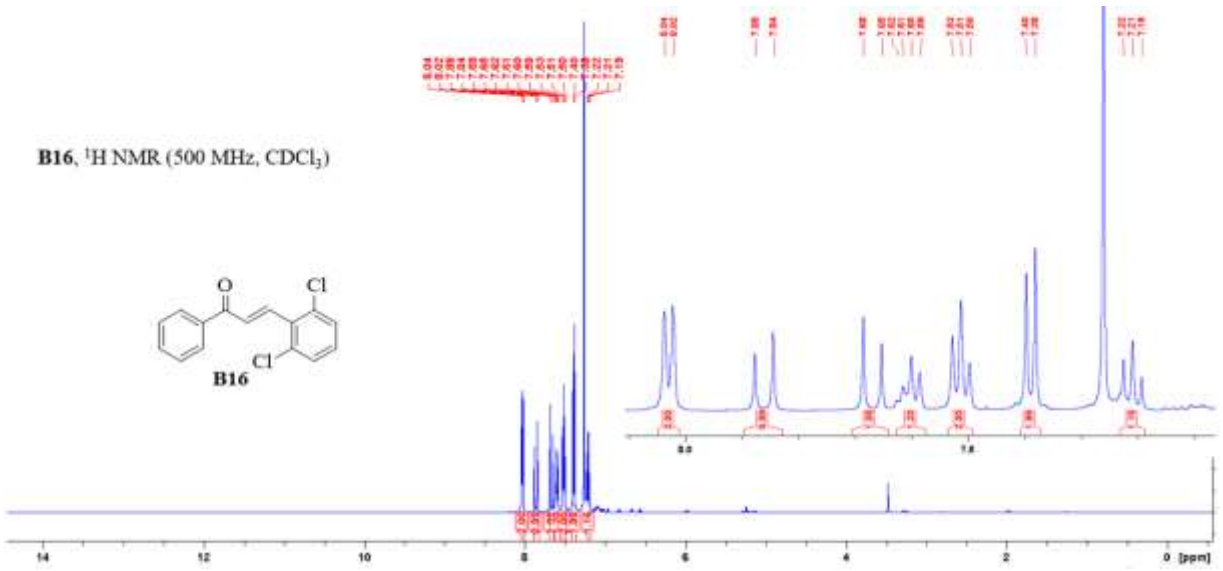

B17, ^{1}H NMR (500 MHz, $CDCl_3$)

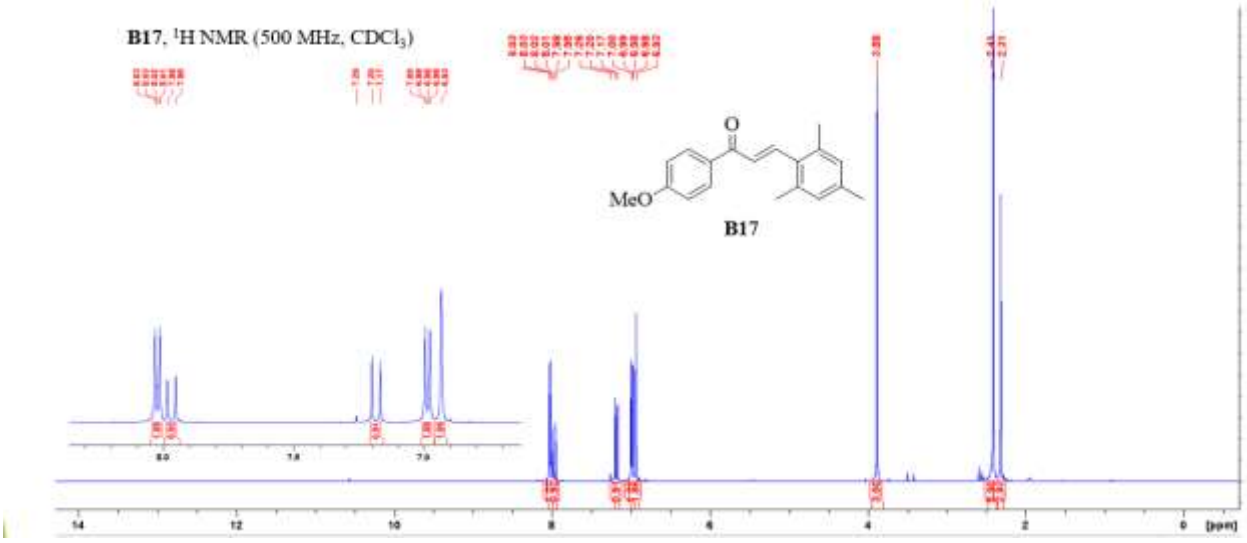

B17

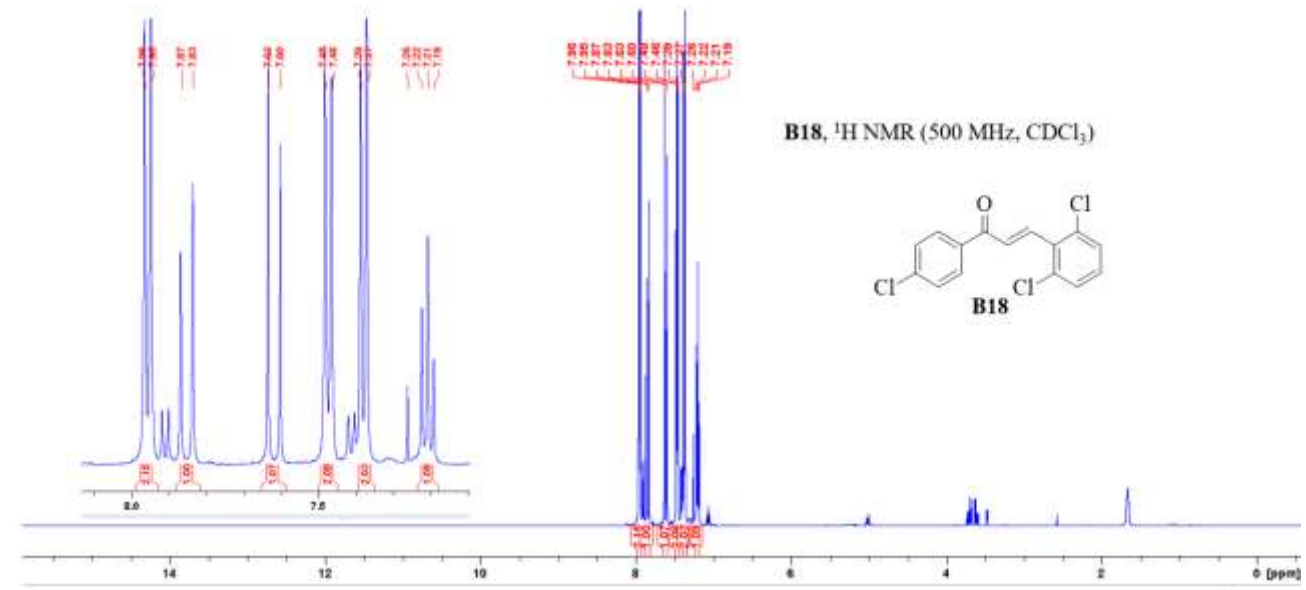

B18, ^{1}H NMR (500 MHz, $CDCl_3$)

B18

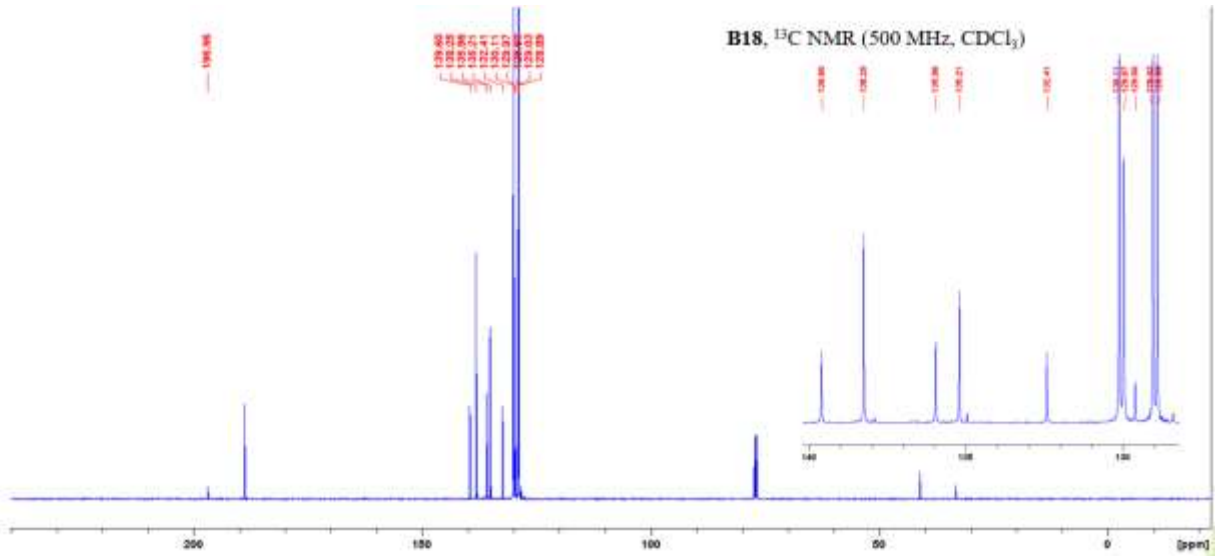
B18, ^{13}C NMR (500 MHz, $CDCl_3$)
200
150
100
50
0
[ppm]

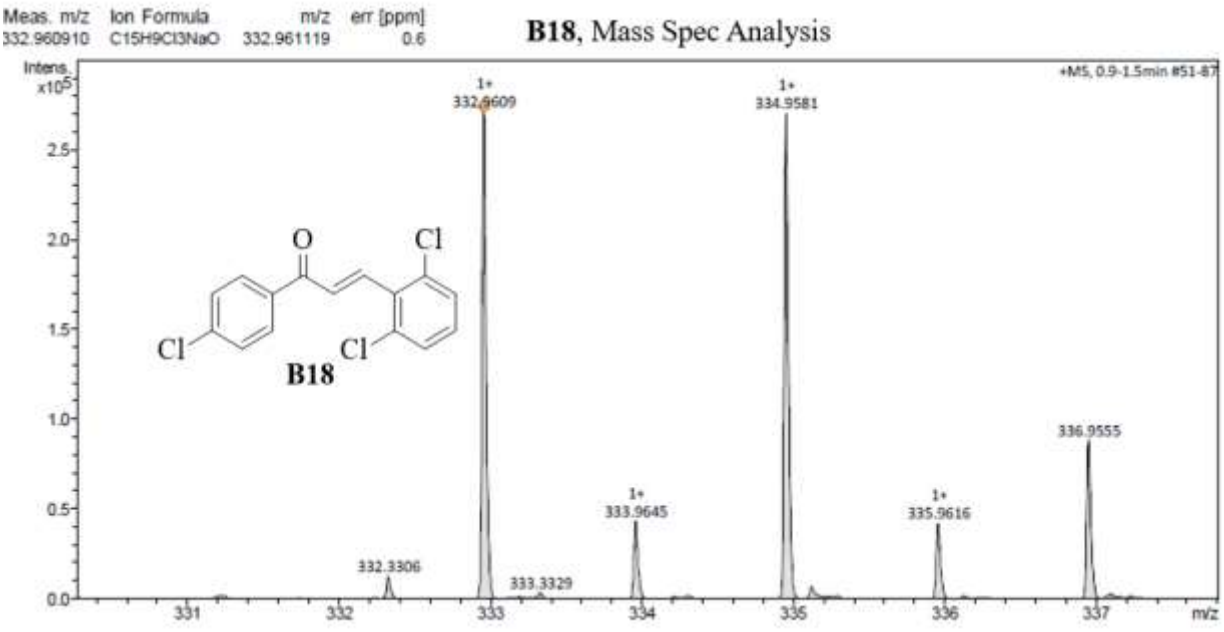
Meas. m/z Ion Formula m/z err [ppm]
332.960910 C15H9Cl3NaO 332.961119 0.6
B18, Mass Spec Analysis
Intens.
x10^5
+MS, 0.9-1.5min #51-87
1+
332.9609
1+
334.9581
1+
333.9645
1+
335.9616
336.9555
332.3306
333.3329
O
Cl
Cl
Cl
B18
331
332
333
334
335
336
337
m/z

B19, ^{1}H NMR (300 MHz, $CDCl_3$)

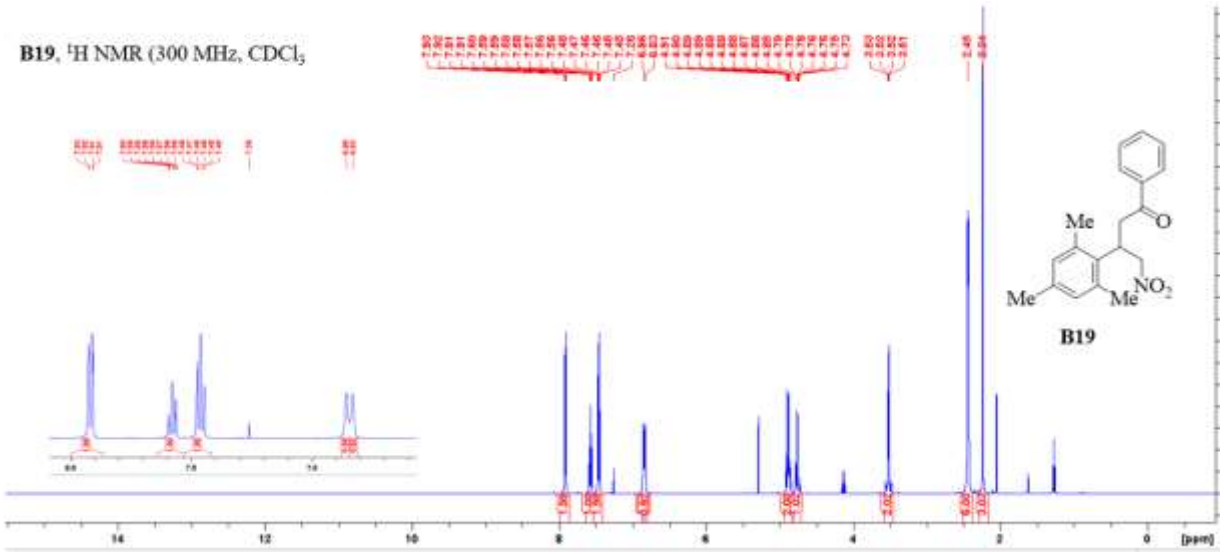

B20, ^{1}H NMR (500 MHz, $CDCl_3$)

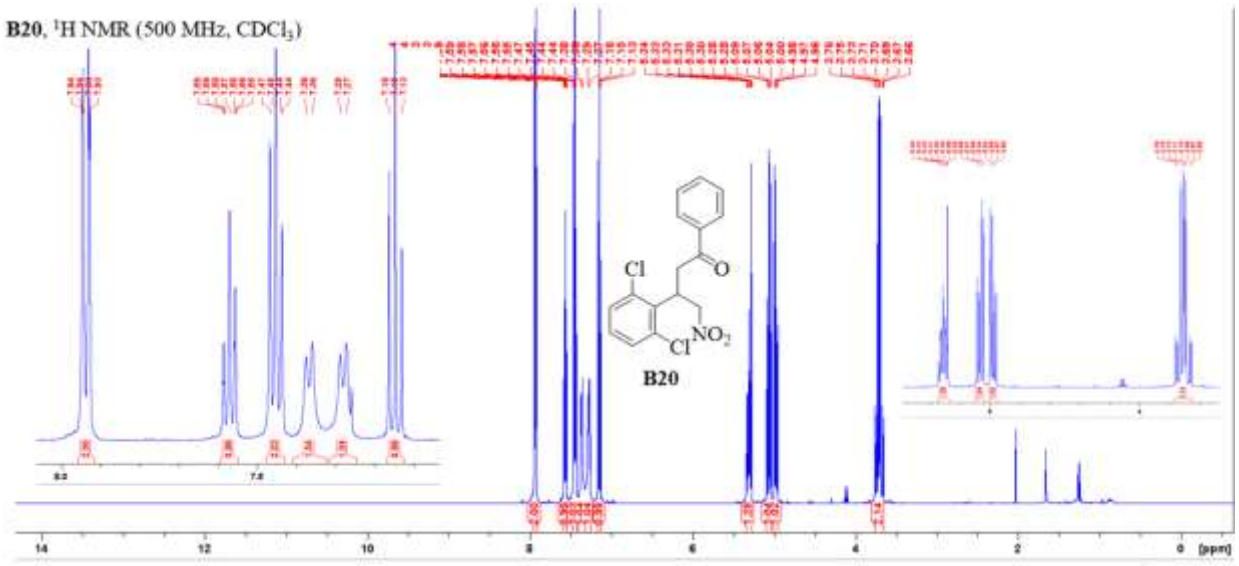

B21, ^{1}H NMR (300 MHz, $CDCl_3$)

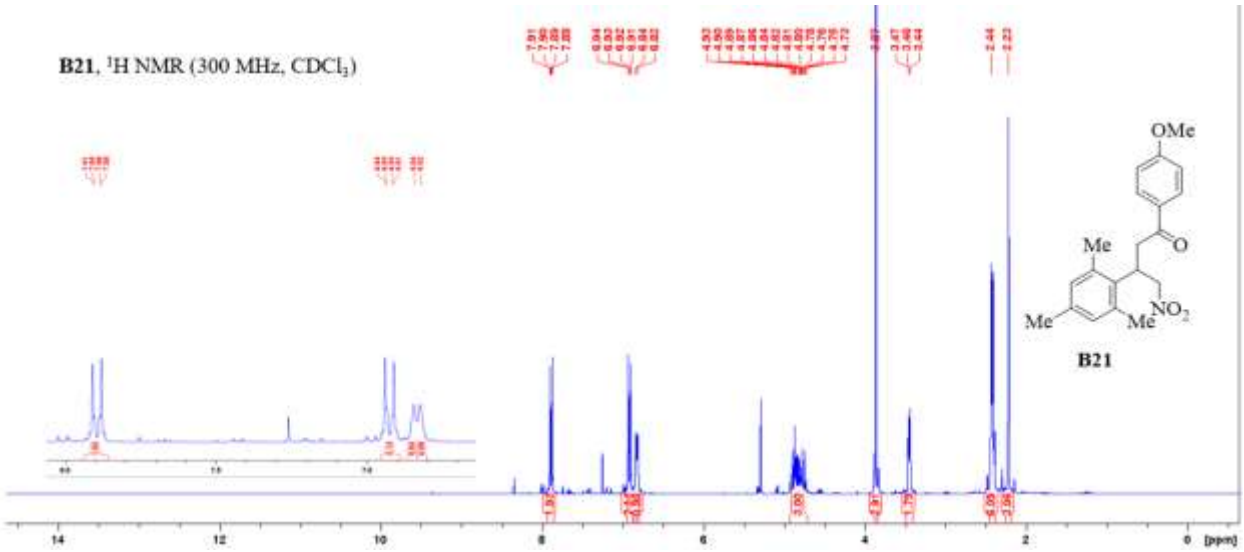

B22, ^{1}H NMR (300 MHz, $CDCl_3$)

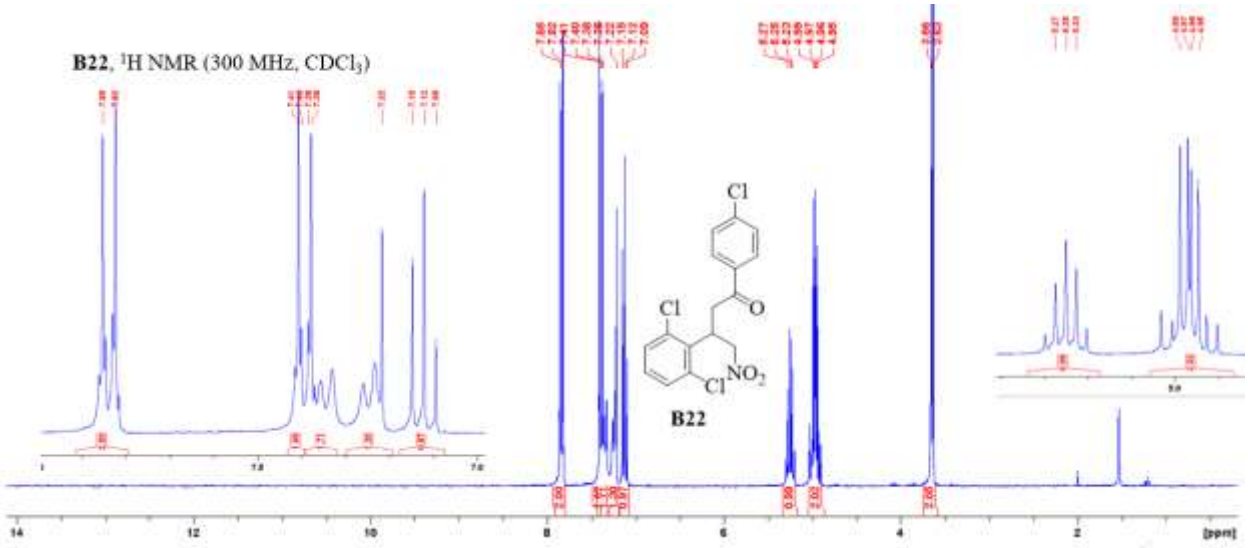

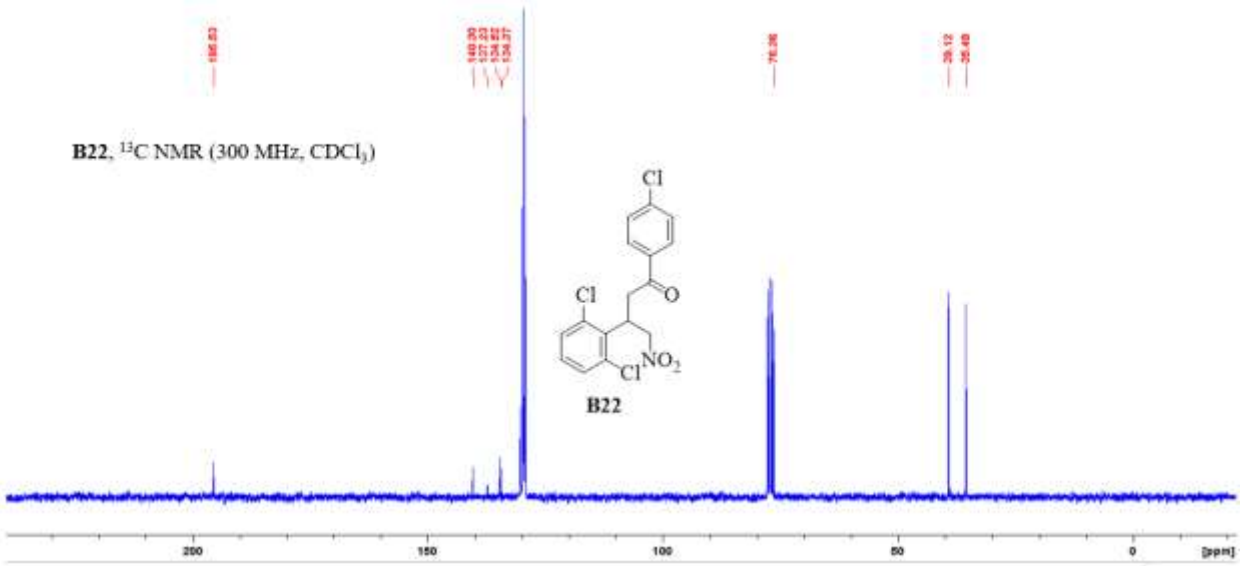

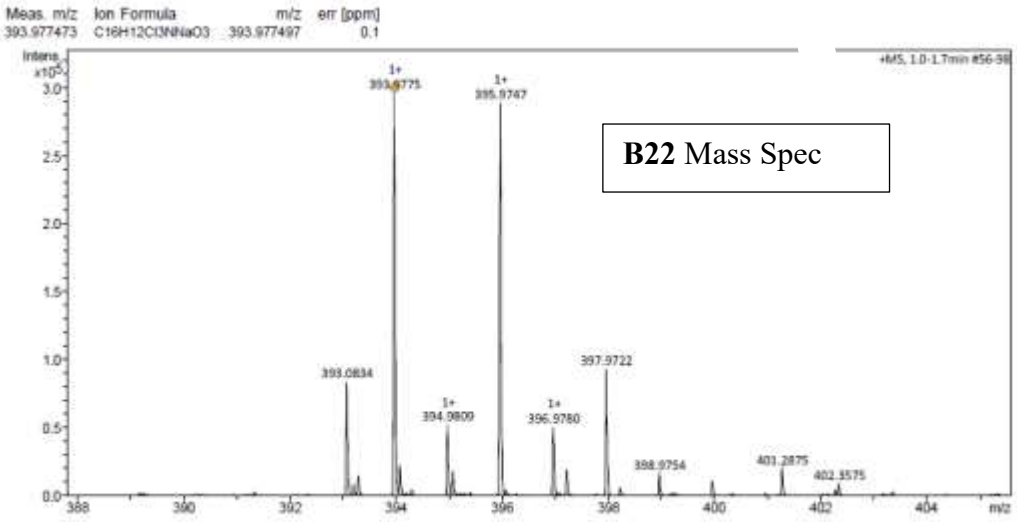

B22 Mass Spec

B23, ^{1}H NMR (500 MHz, $CDCl_3$)

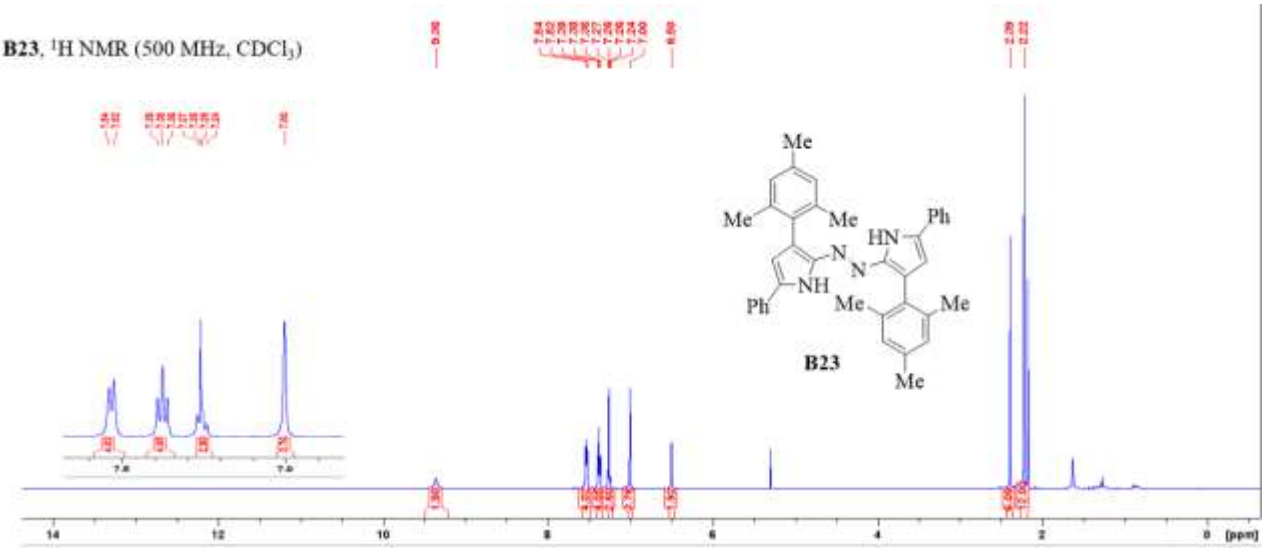

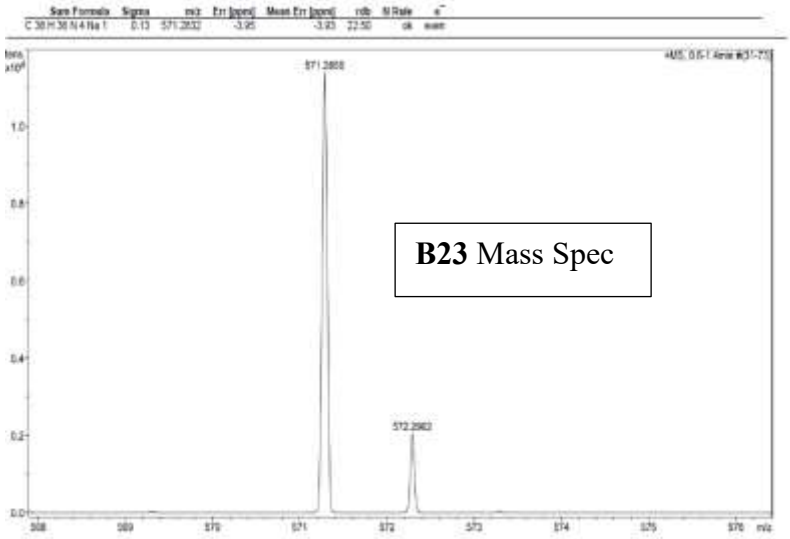

B23 Mass Spec

B23, ^{13}C NMR (500 MHz, $CDCl_3$)

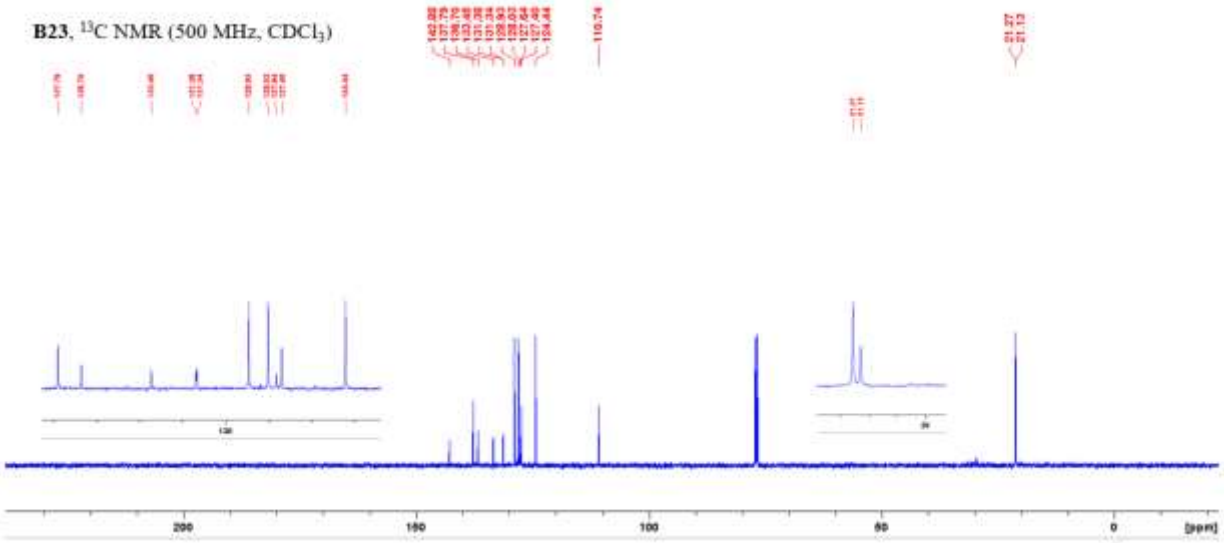

B24, ^{1}H NMR (500 MHz, $CDCl_3$)

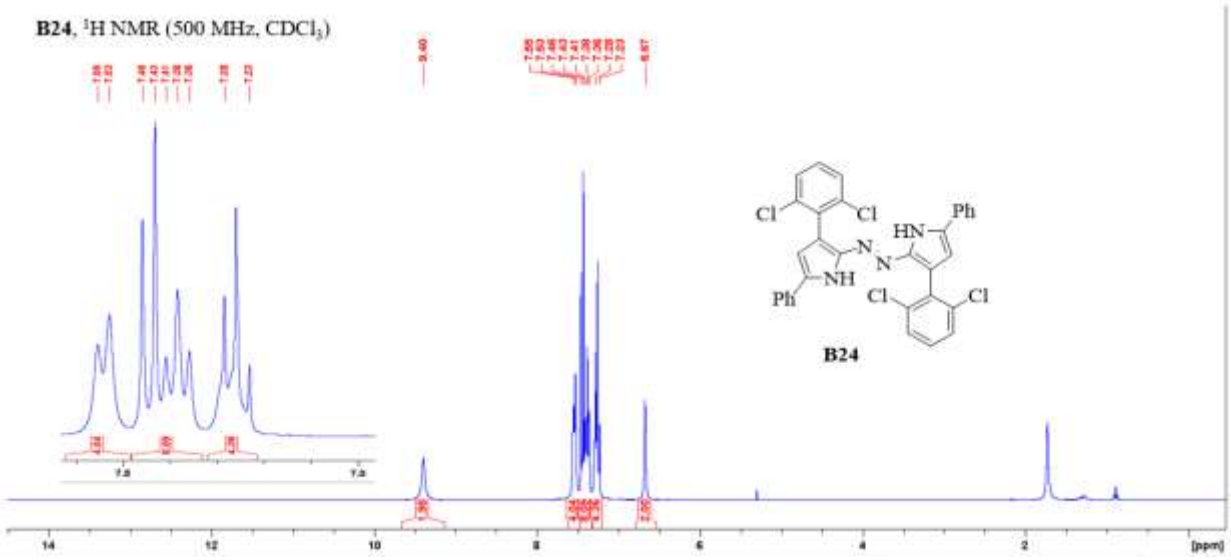

B24

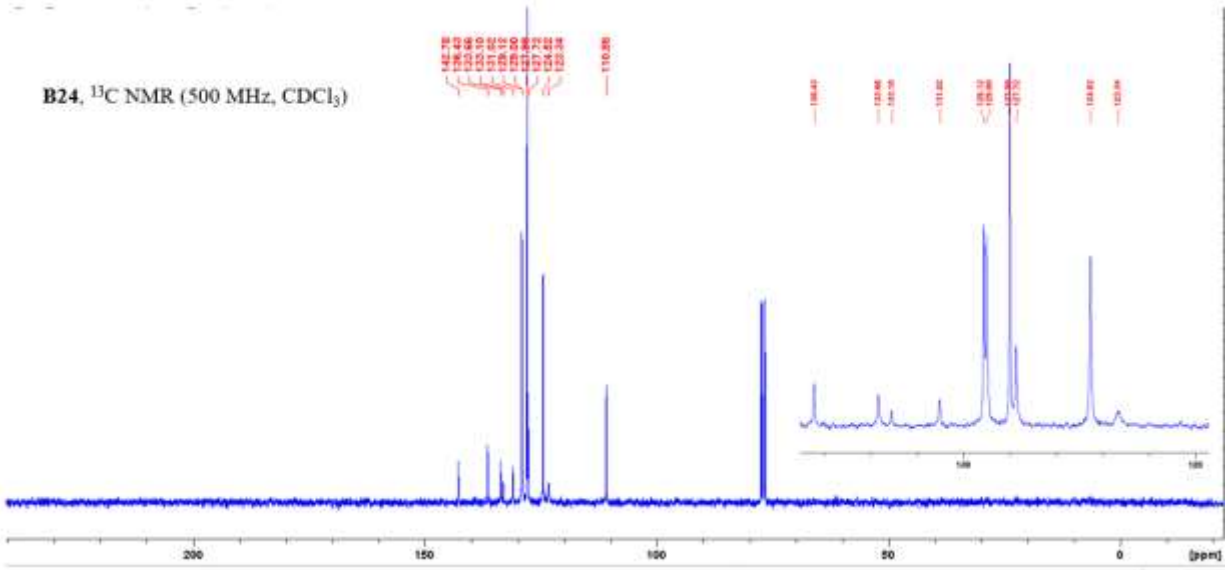
B24, ^{13}C NMR (500 MHz, $CDCl_3$)
200
150
100
50
0
[ppm]

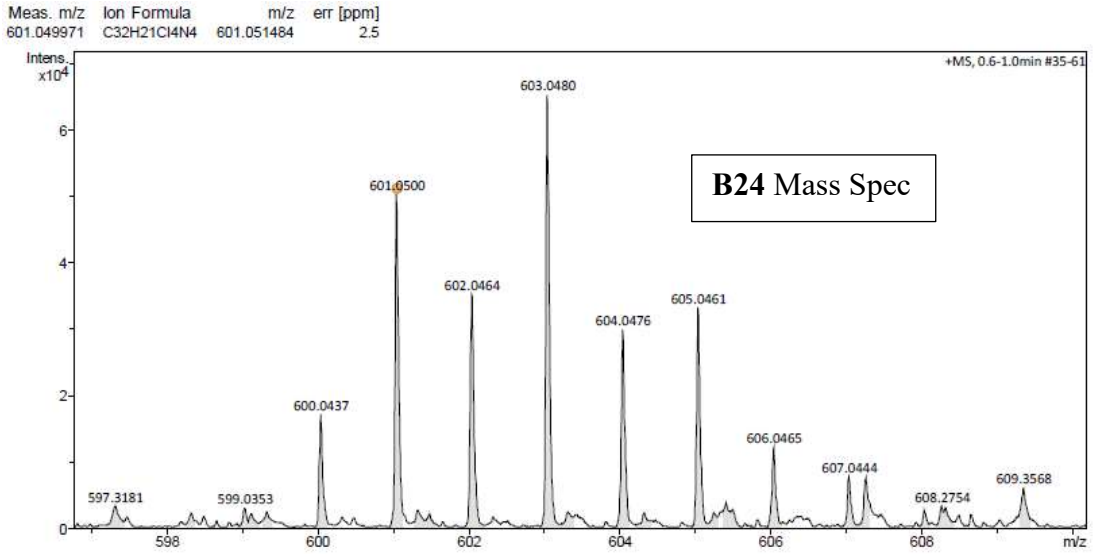
Meas. m/z Ion Formula m/z err [ppm]
601.049971 C32H21Cl4N4 601.051484 2.5
Intens.
x10^4
+MS, 0.6-1.0min #35-61
603.0480
601.0500
602.0464
604.0476
605.0461
600.0437
606.0465
607.0444
609.3568
597.3181
599.0353
608.2754
B24 Mass Spec
m/z

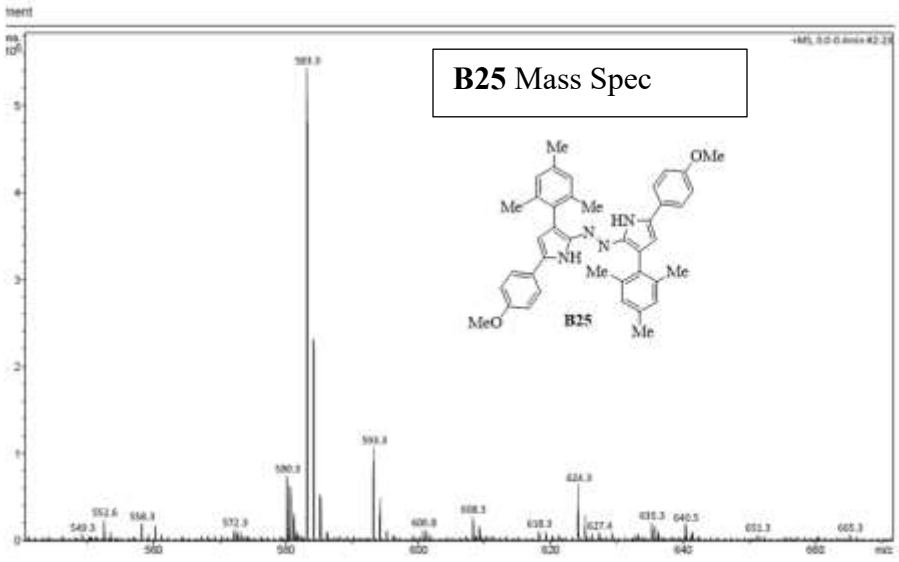
B25 Mass Spec
Me
OMe
Me
Me
HN
N
N
NH
Me
Me
MeO
Me
B25

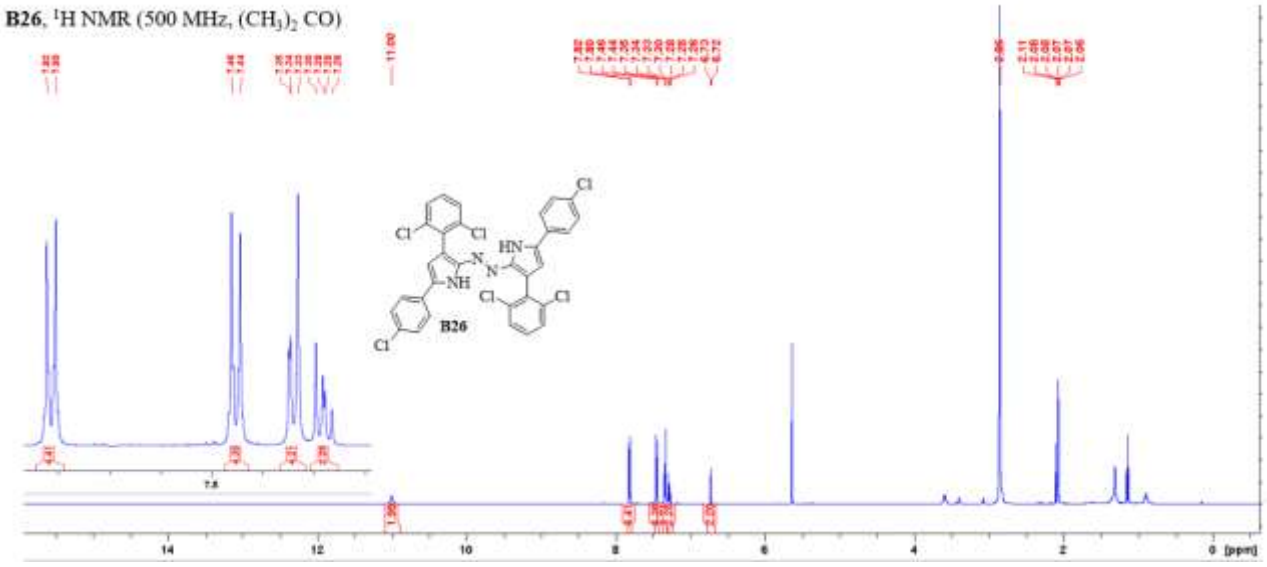
B26, ^{1}H NMR (500 MHz, $(CH_3)_2$ CO)
Cl
Cl
HN
N
N
NH
Cl
Cl
Cl
B26
14
12
10
8
6
4
2
0 (ppm)

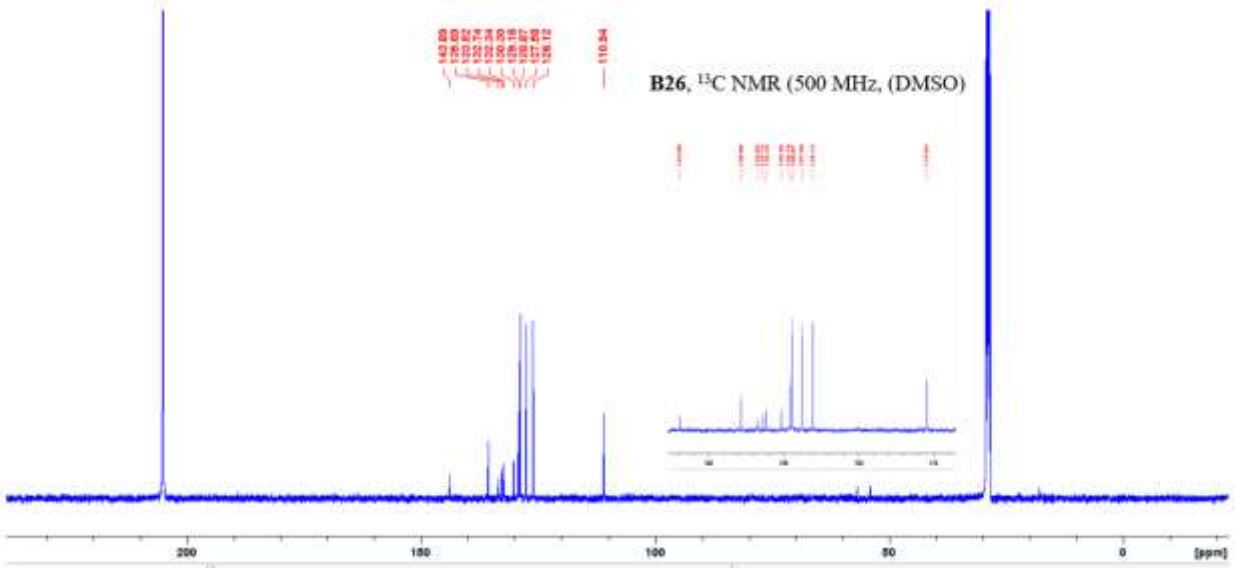
B26, ^{13}C NMR (500 MHz, (DMSO)
200
150
100
50
0
[ppm]

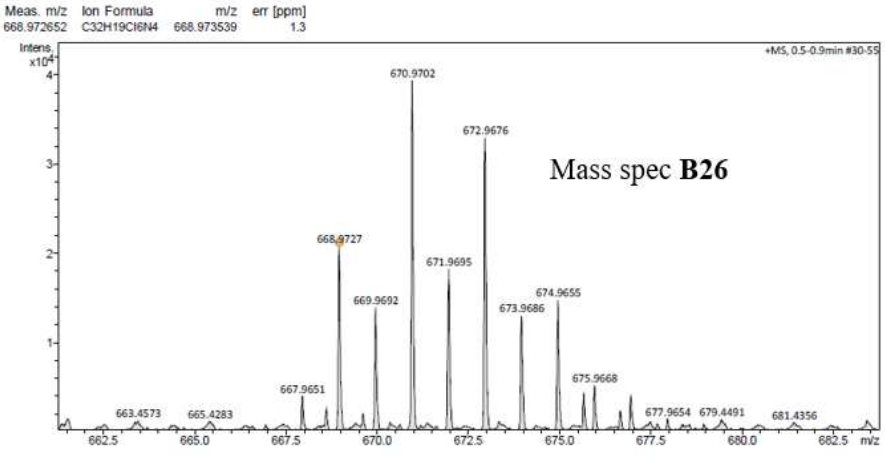
Meas. m/z Ion Formula m/z err [ppm]
668.972652 C32H19Cl6N4 668.973539 1.3
Intens.
x10^4
+MS, 0.5-0.9min #30-55
670.9702
672.9676
Mass spec B26
668.9727
671.9695
669.9692
674.9655
673.9686
675.9668
667.9651
663.4573
665.4283
677.9654
679.4491
681.4356
662.5
665.0
667.5
670.0
672.5
675.0
677.5
680.0
682.5
m/z

B5, ^{1}H NMR (500 MHz, $CDCl_3$)

B5

B6, ^{1}H NMR (500 MHz, $CDCl_3$)

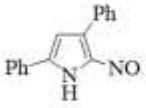

B6

B7, ^{1}H NMR (500 MHz, $CDCl_3$)

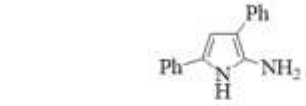

B7

B13, ^{1}H NMR (500 MHz, $CDCl_2$)

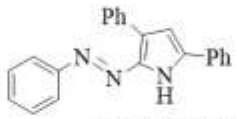

B13 (*E* isomer)

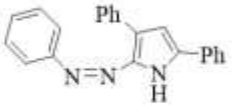

B13 (*Z* isomer)

B13 Mass Spec

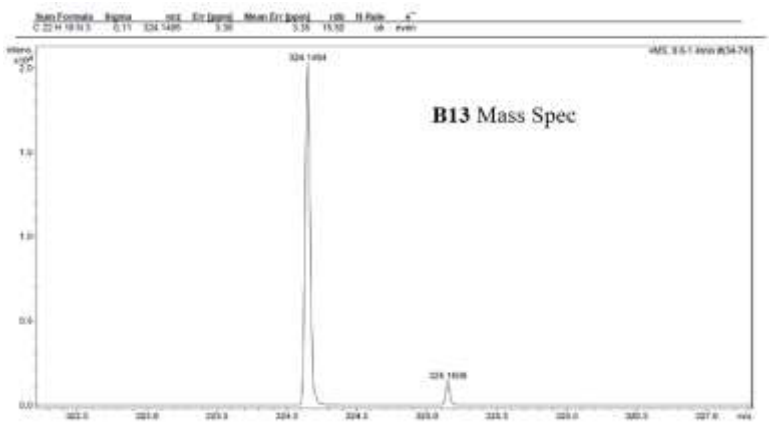

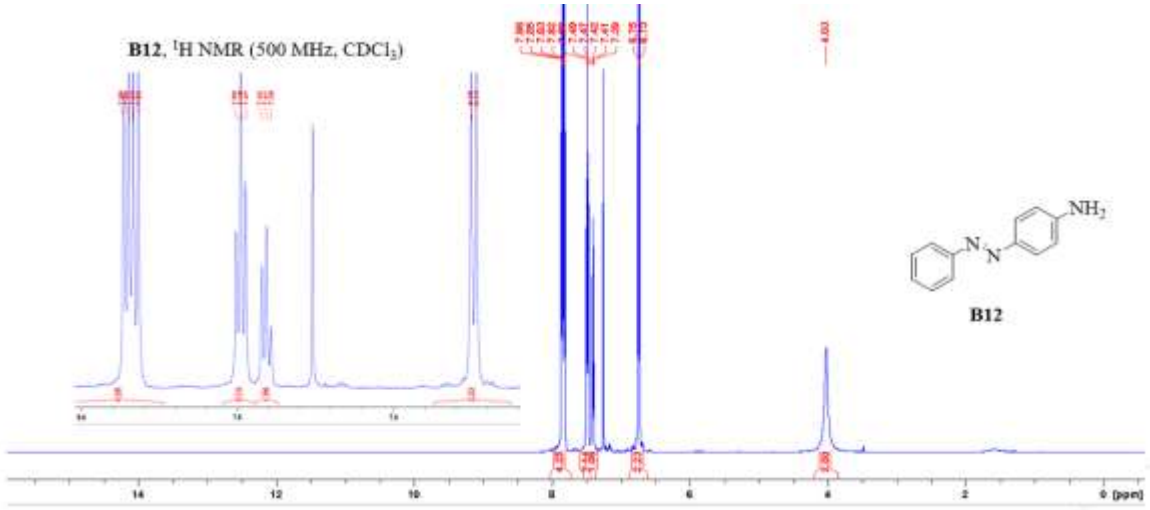
B12, ^{1}H NMR (500 MHz, $CDCl_3$)
NH_2
B12

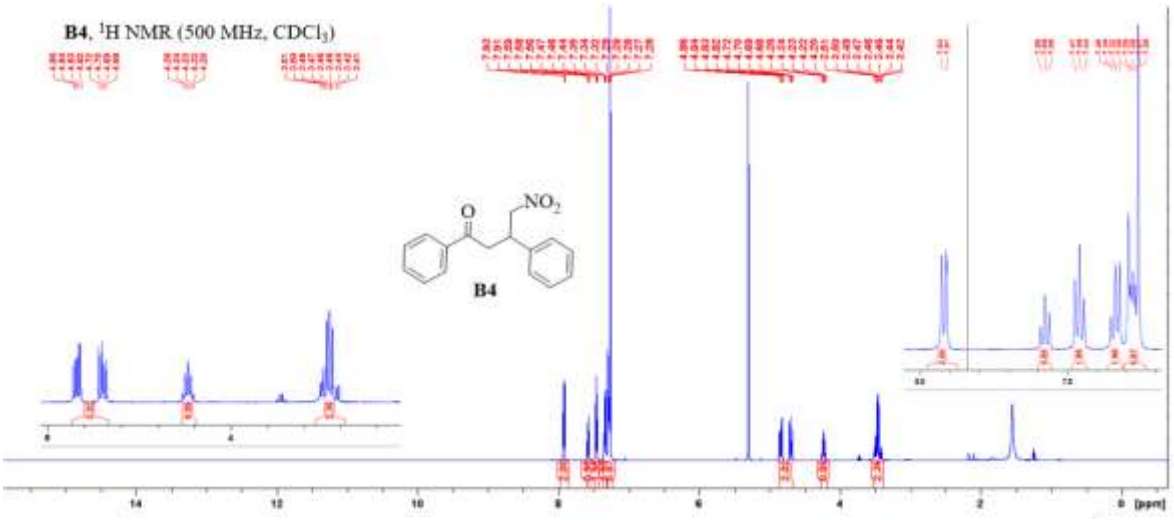
B4, ^{1}H NMR (500 MHz, $CDCl_3$)
O
NO_2
B4

Appendix B. Attempts towards the synthesis of *F*-BODIPYs using a stoichiometric amount of dipyrrin and $BF_3 \cdot OEt_2$ in a continuous flow operation.

NMR spectra for Optimization of the continuous flow process with a flow reactor coil of 30 cm and 0.05 cm internal diameter tubing (Table 3.1)

Entry 1

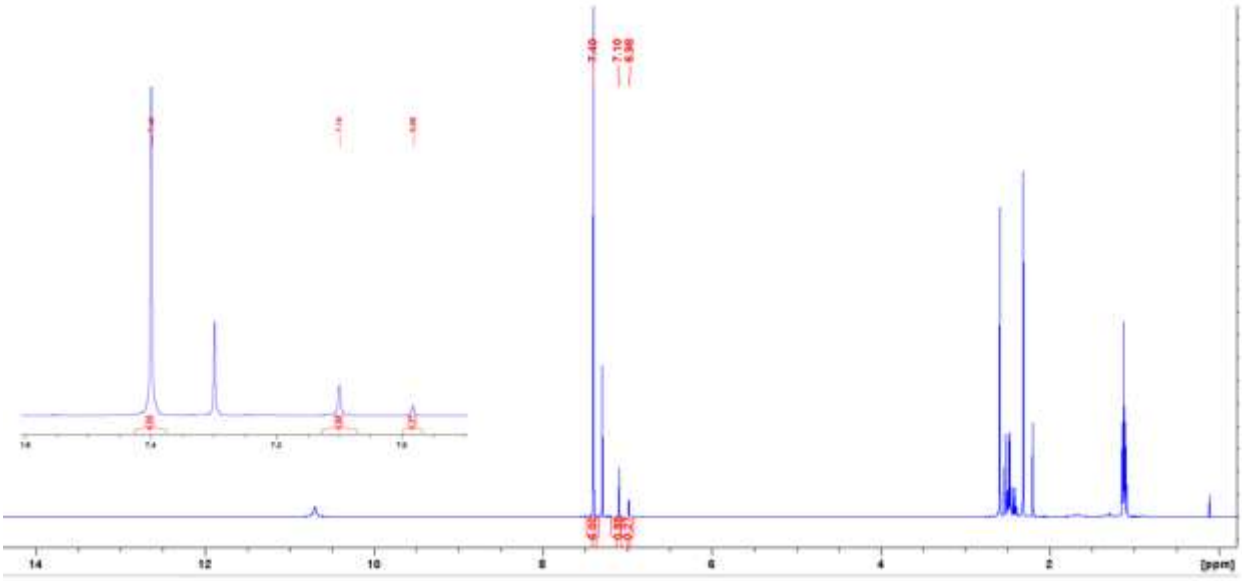

Entry 2

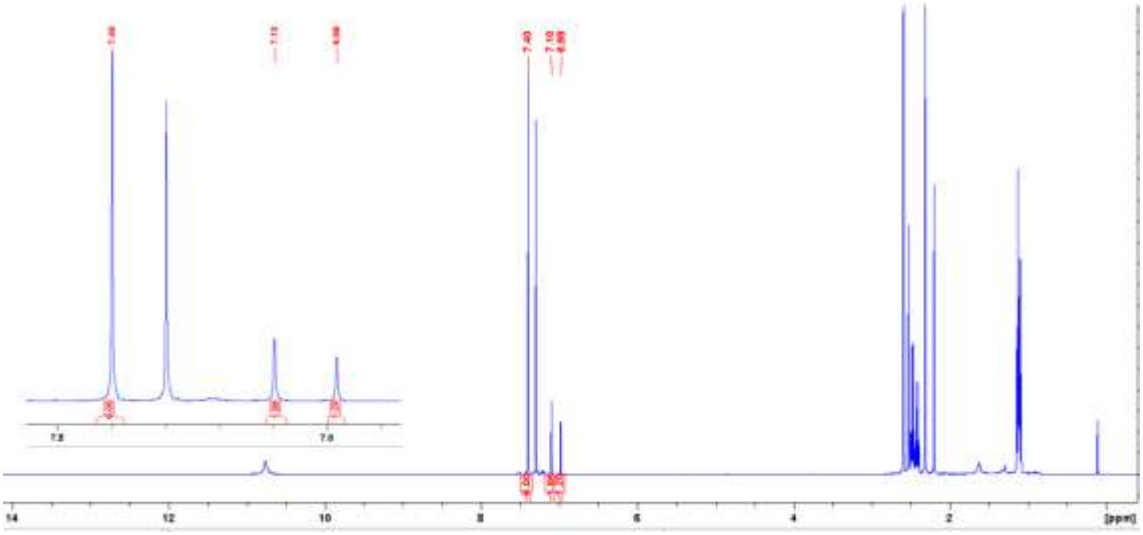

Entry 3

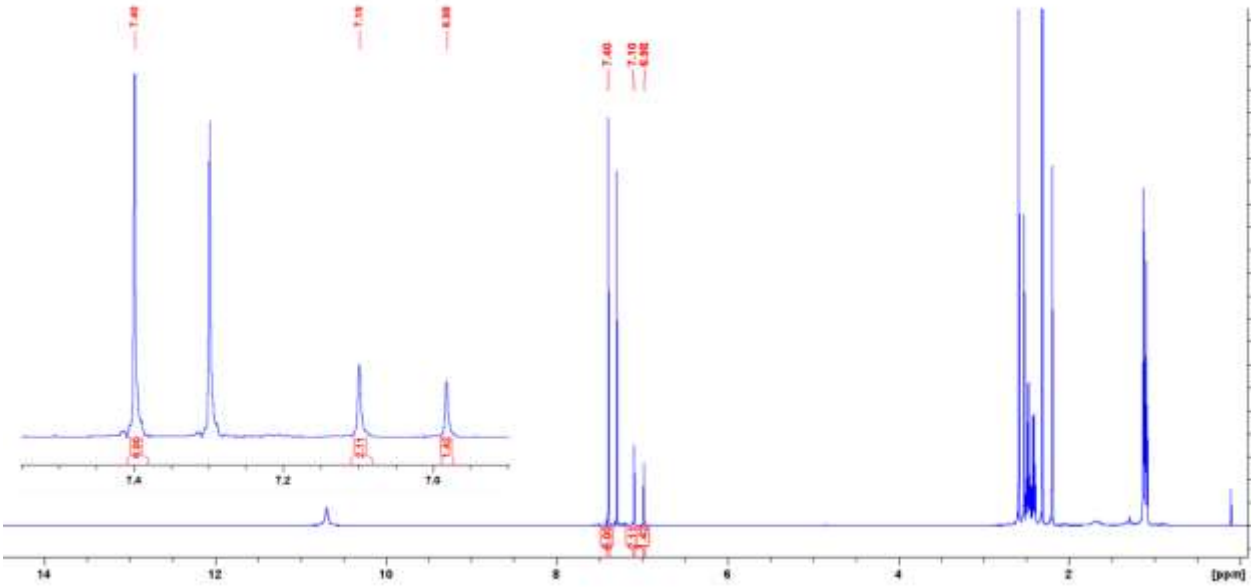

NMR spectra for Effect of 1.5 eq. of scavengers on dipyrrin C1a via stoichiometry addition of $BF_3{\cdot}OEt_2$ for the synthesis of *F*-BODIPY (Table 3.3)

In THF

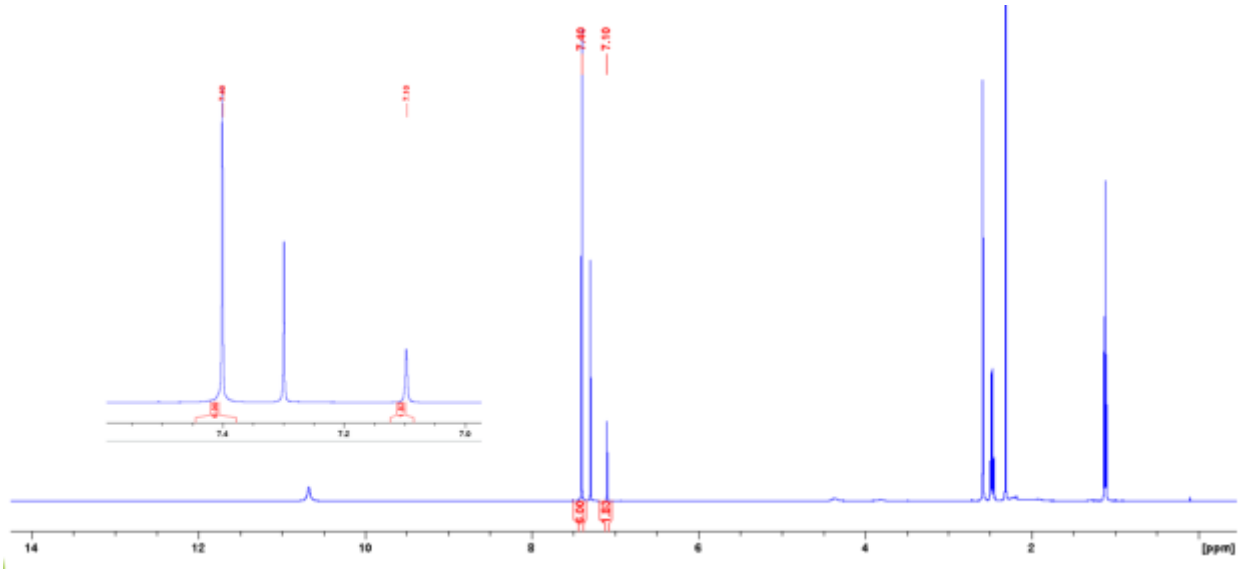

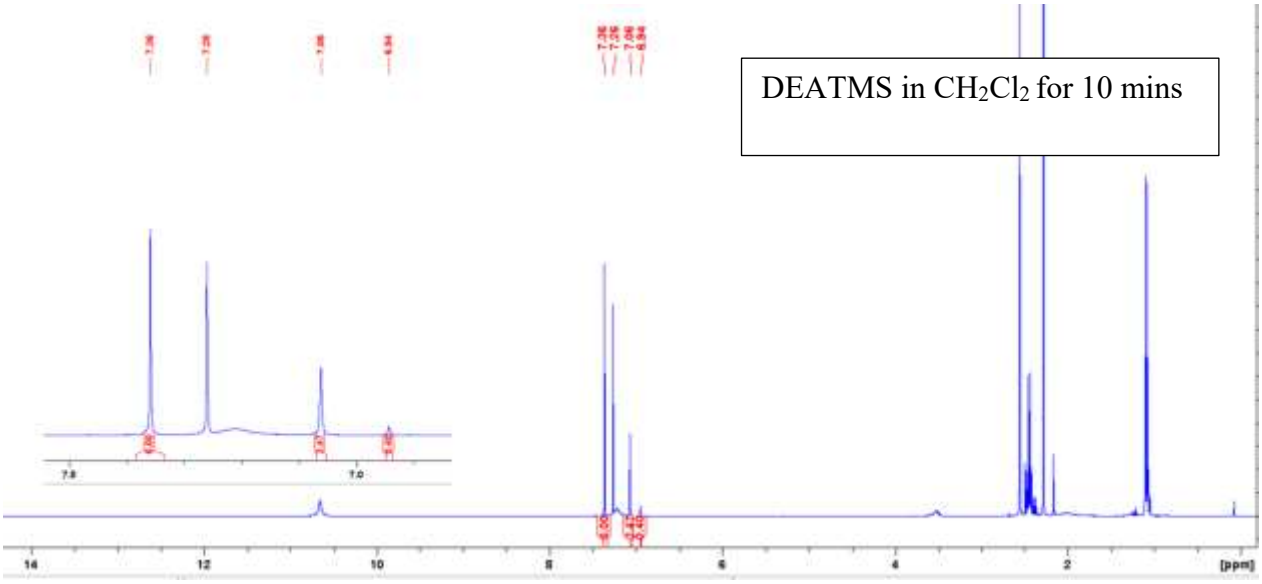
DEATMS in CH_2Cl_2 for 10 mins

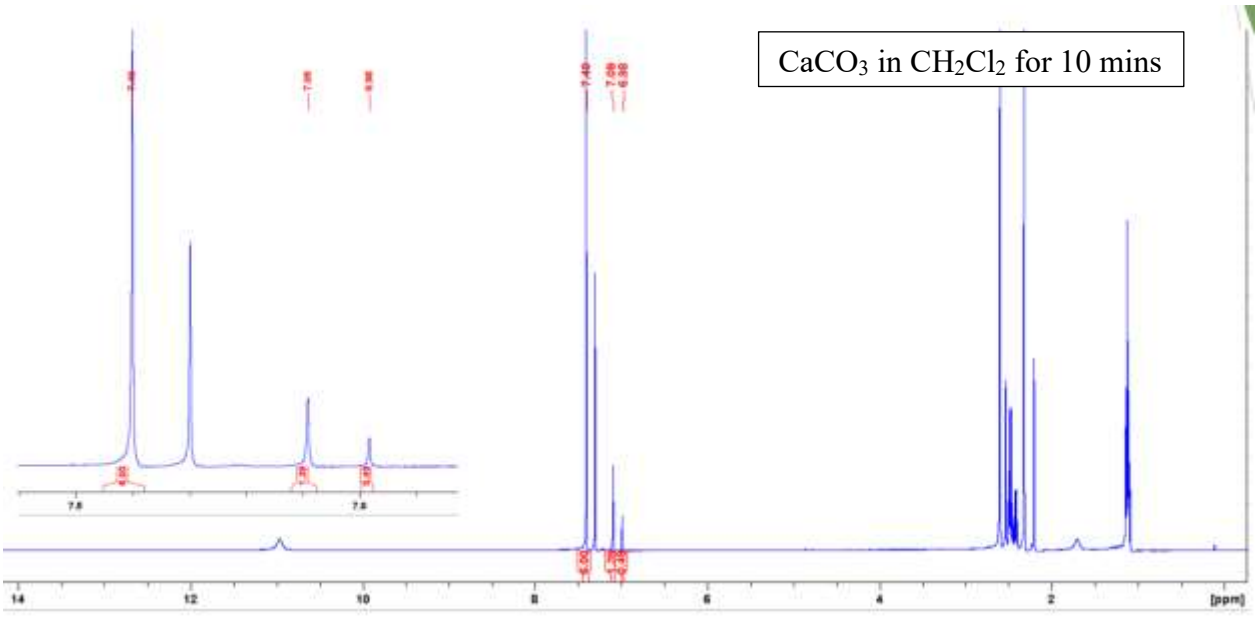
$CaCO_3$ in CH_2Cl_2 for 10 mins

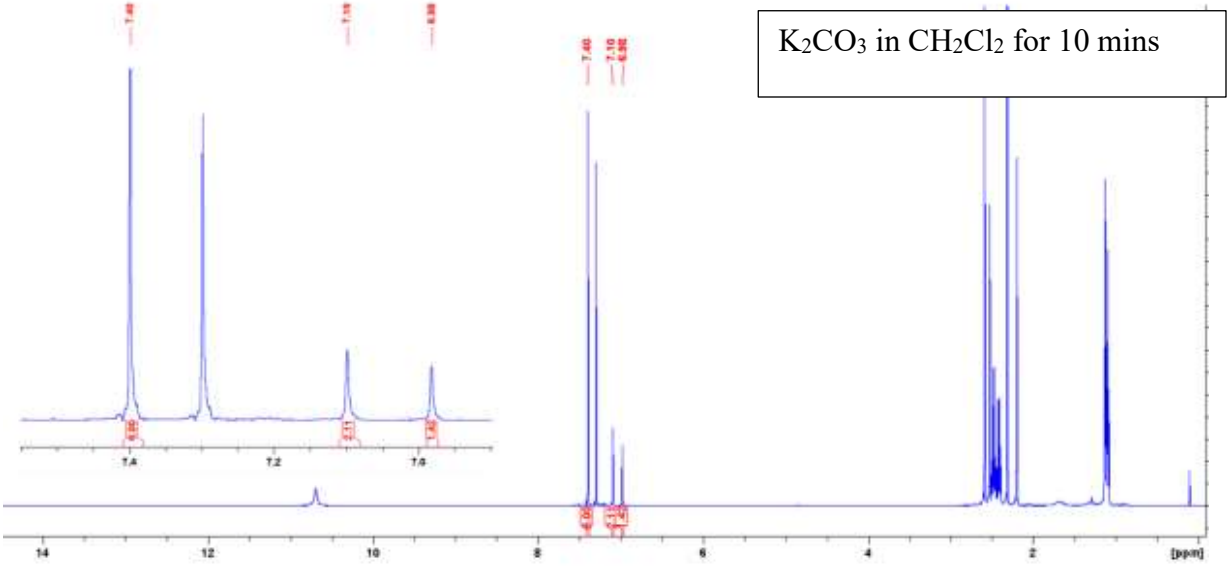
K2CO3 in CH2Cl2 for 10 mins

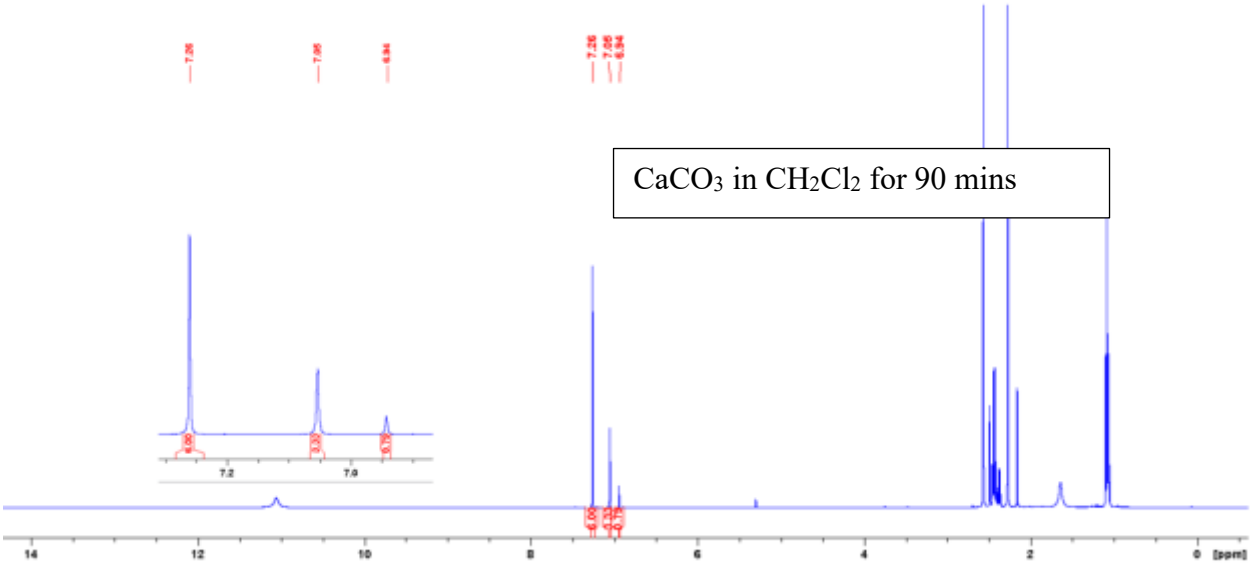
CaCO3 in CH2Cl2 for 90 mins

Results from the addition of $BF_3 \cdot OEt_2$ (1 eq.) to free-base **C1a** in toluene batch method (using ^1H NMR spectroscopy analytical method) (Table 3.1)

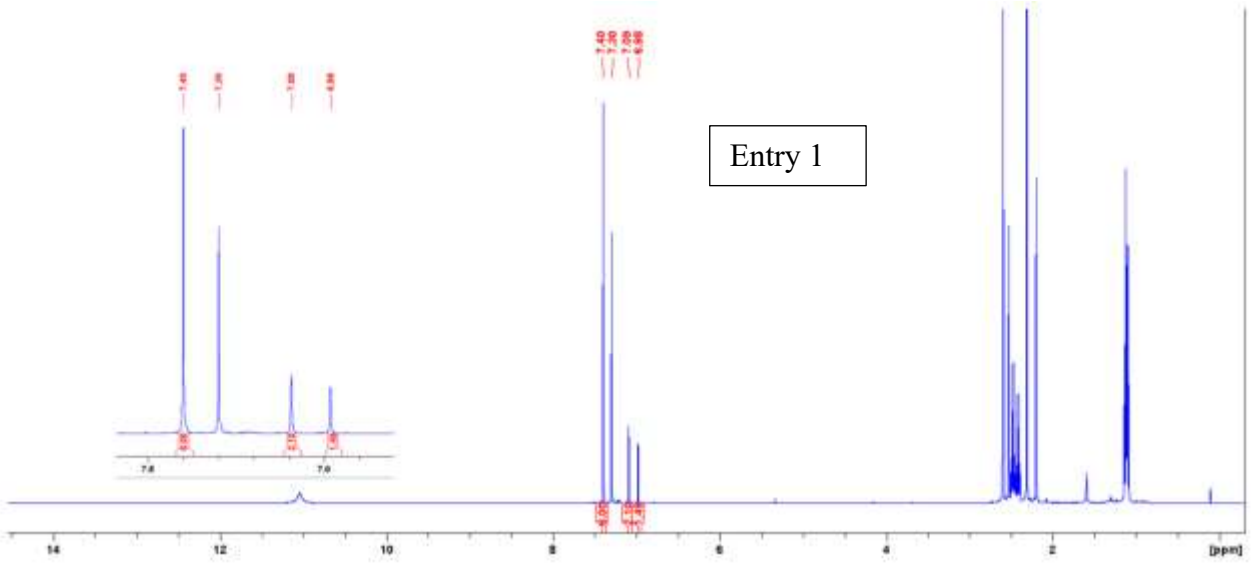

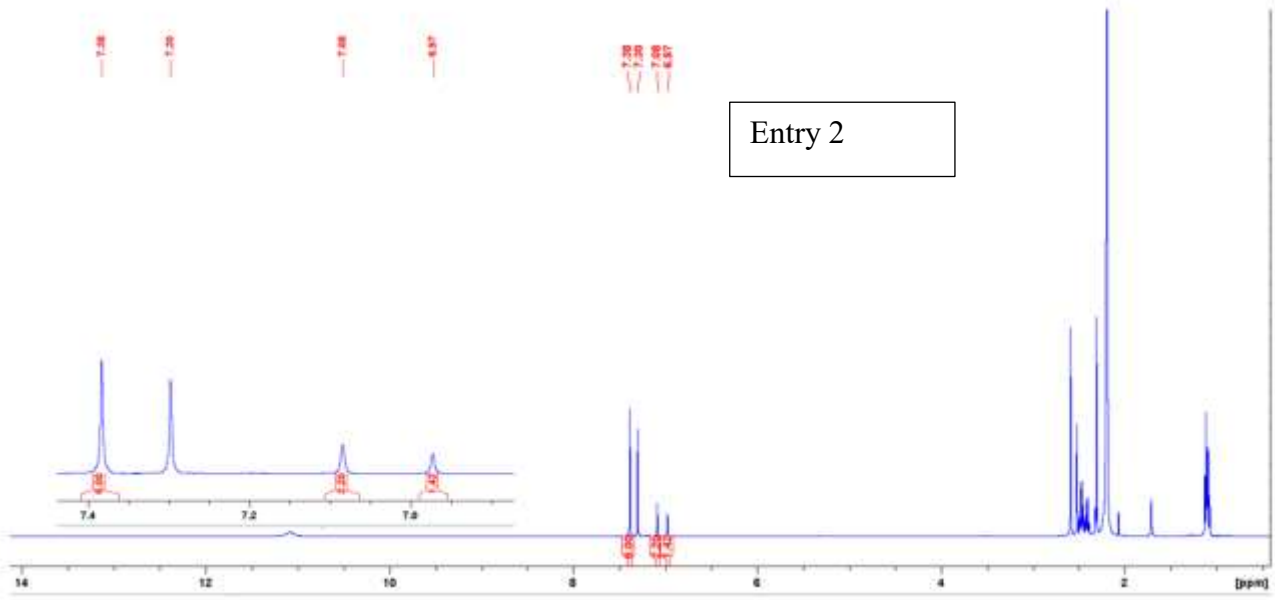

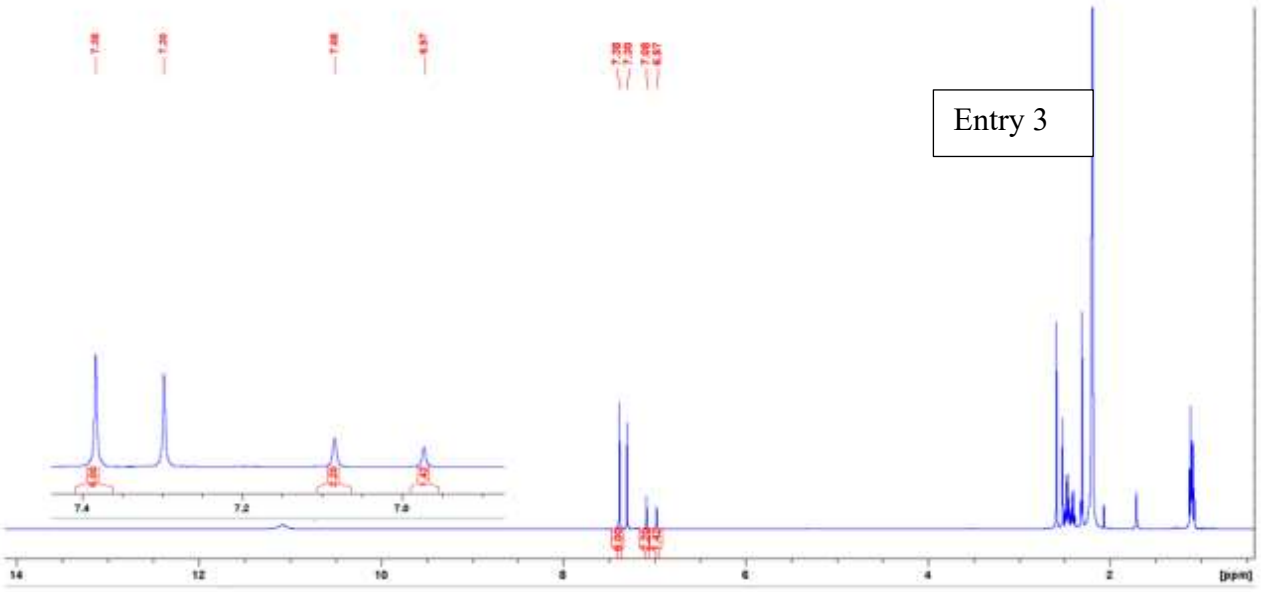
Entry 3

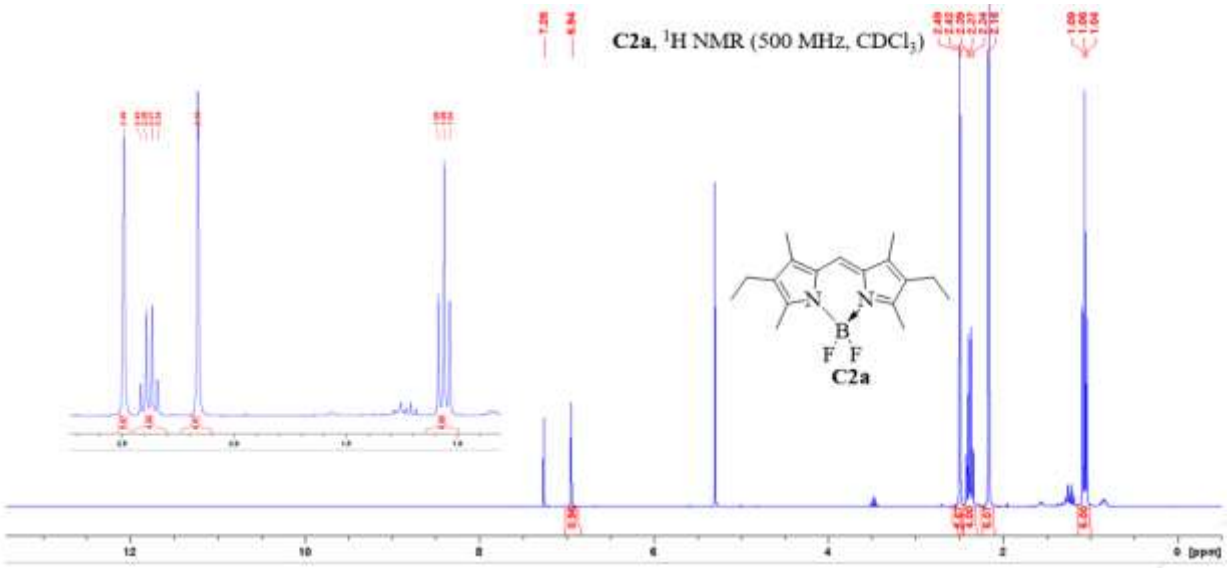
C2a, ^{1}H NMR (500 MHz, $CDCl_3$)
C2a

C2b, ^{1}H NMR (500 MHz, $CDCl_3$)

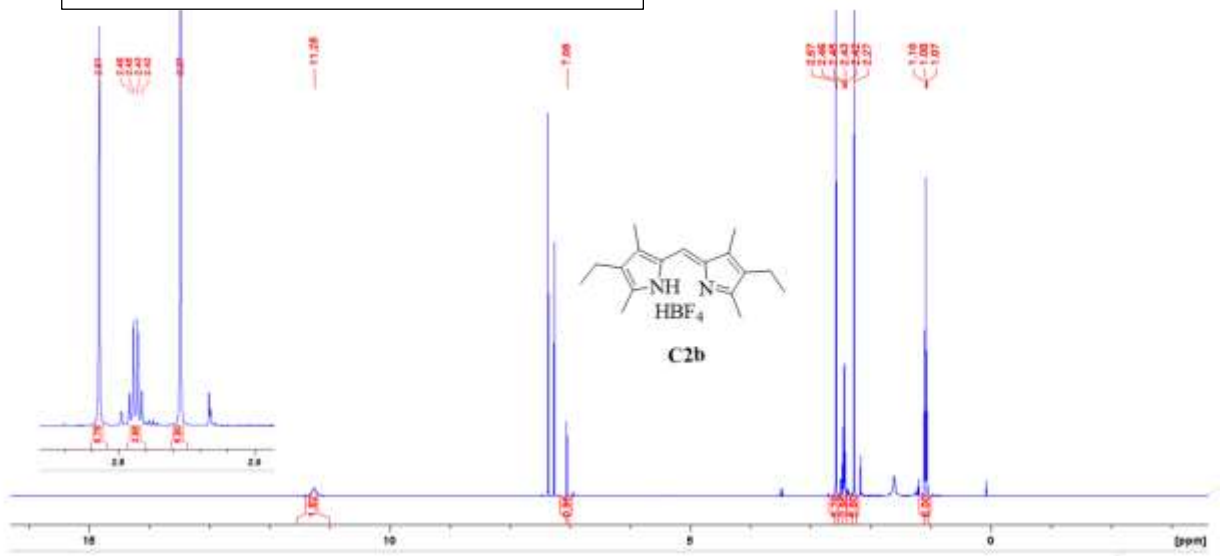

A, ^{1}H NMR (500 MHz, $CDCl_3$)

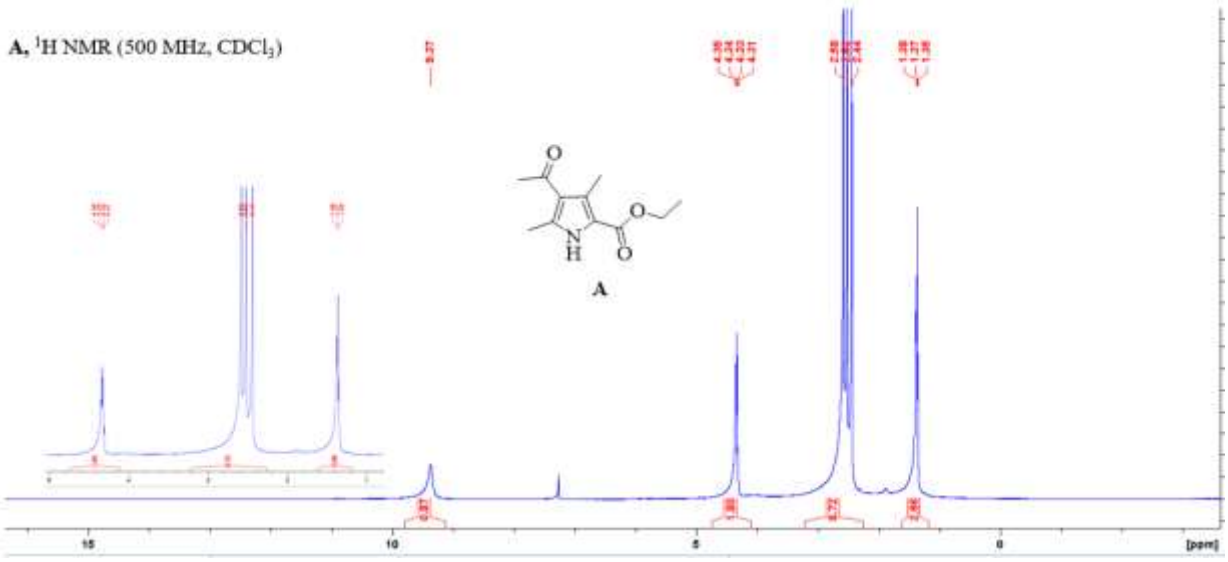

B, ^{1}H NMR (500 MHz, $CDCl_3$)

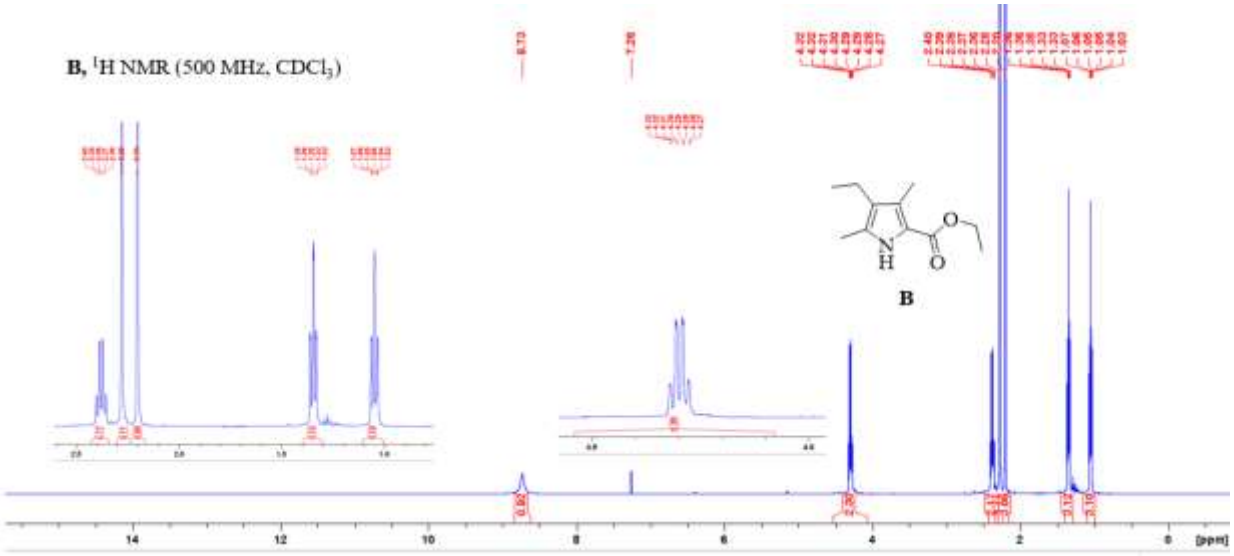

B

C, ^{1}H NMR (500 MHz, $CDCl_3$)

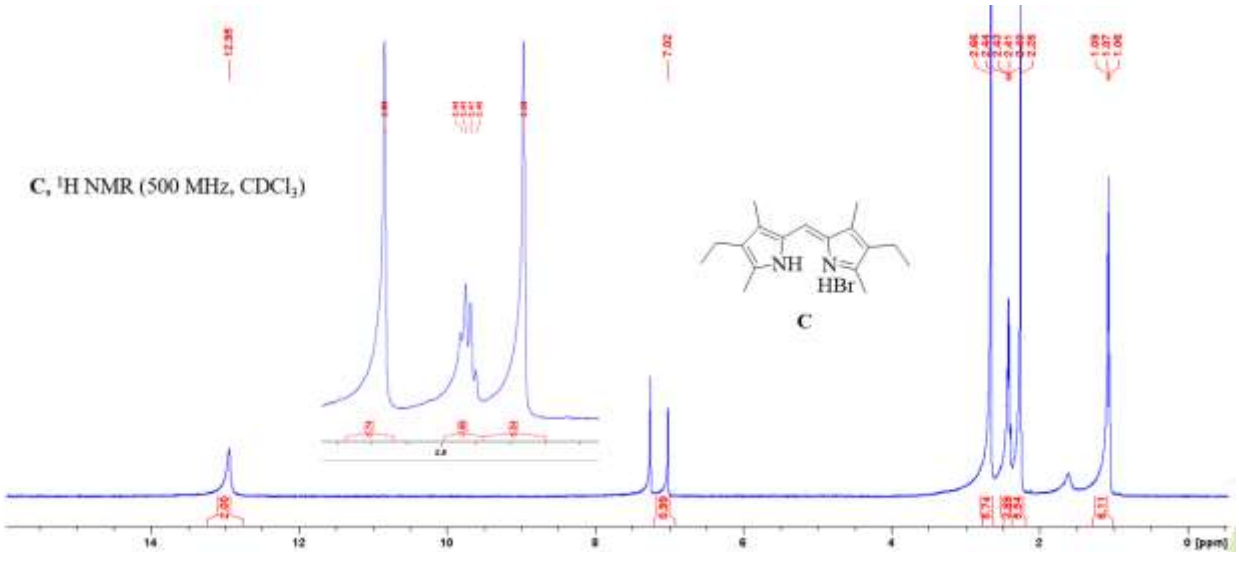

C

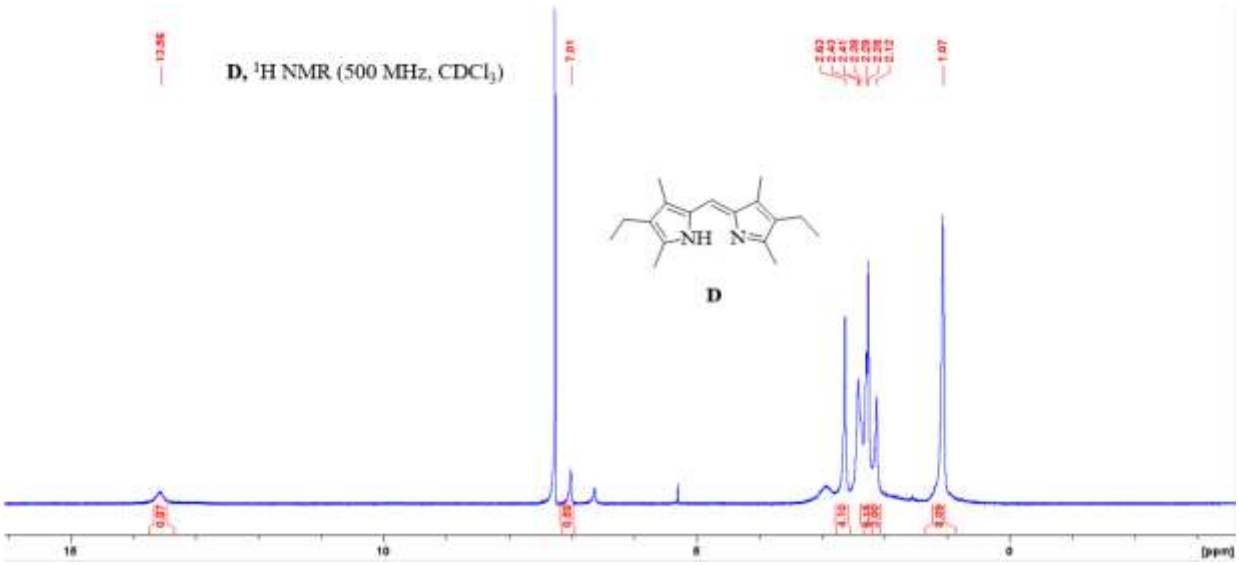
D, ^{1}H NMR (500 MHz, $CDCl_3$)
NH
N
D
10
8
0
(ppm)